SYNTHESIS AND CHARACTERIZATION OF COST-EFFECTIVE CHABAZITE (CHA) ZEOLITE CATALYSTS FOR THE CONVERSION OF METHANOL TO LIGHT OLEFINS (MTO) PROCESS

BY

GALAL ATEF AHMED NASSER

A Thesis Presented to the
DEANSHIP OF GRADUATE STUDIES

KING FAHD UNIVERSITY OF PETROLEUM & MINERALS

DHAHRAN, SAUDI ARABIA

In Partial Fulfillment of the
Requirements for the Degree of

MASTER OF SCIENCE

In

CHEMICAL ENGINEERING

December, 2017

KING FAHD UNIVERSITY OF PETROLEUM & MINERALS

DHAHRAN- 31261, SAUDI ARABIA

DEANSHIP OF GRADUATE STUDIES

This thesis, written by **GALAL ATEF AHMED NASSER** under the direction of his thesis advisor and approved by his thesis committee, has been presented and accepted by the Dean of Graduate Studies, in partial fulfillment of the requirements for the degree of **MASTER OF SCIENCE IN CHEMICAL ENGINEERING**

Dr. Zuhair Omer Malaibari
(Advisor)

Dr. Mohammed Ba-Shammakh
Department Chairman

Dr. Oki Muraza
(Co-Advisor)

Prof. Salam A. Zummo
Dean of Graduate Studies

Dr. Mohammad M. Hossain
(Member)

2/1/18
Date

Dr. Adnan M. Al-Amer
(Member)

Dr. Sagheer onaizi
(Member)

This work is dedicated to my parents, brothers, sisters, wife and father-in-law

ACKNOWLEDGMENTS

All praise and thanks to Almighty Allah for giving me health, strength, patience and knowledge. I would like to express my great thanks to King Fahd University of Petroleum and Minerals (KFUPM), namely, the Chemical Engineering Department (CHE) for hosting me since 2009 when I started doing the bachelor degree. In particular, I am very thankful to all CHE faculties.

My special thanks to my advisor Dr. Zuhair Omer Malaibari for his support, guidance and valuable comments. Also my special thanks go to Dr. Oki Muraza for his always support, encouragement and guidance since I was doing the COOP program and up to today. I am very thankful to my committee member Dr. Adnan Al-Amer, Dr. Mohammed Mozaher and Dr. Sagheer Onaizi for their valuable contribution to this research.

I would like to express my deep thanks to the Center of Research Excellence in Nanotechnology (CENT) for allowing me to use all CENT's facilities during this research. I am very thankful to the CENT director Dr. Zain Yamani for his always support and encouragement. I would like also to thank Dr. Abbas Hakeem for teaching me how to handle many equipment. My thanks also goes to all CENT affiliates; Mr. Idris, Mr. Sanhoop, Dr. Qasem Drmosh, Mr. Anas Karrar, Mr. Mohammed Hassan, Mr. Saheed, Mr. Ibrar and Mr. Qamer.

I am very grateful to my parents, my brothers (Maged, Maher, Fawaz & Safwan), my sisters (Sonia, Ashgan, and Julia), my wife, my cousin Aref, my uncles (Saleh and Mohammad), my father in law, my grandmother and whole family for their prayers and supports.

Last but not least, I would like to thanks my friends and colleagues Mr. GALAL Aqeel, Mr. Madyn, Mr. Saleem, Mr. Ammar, Mr. Mohammad Al-ezzi, Mr. Magd Nadeem, Mr. Abullah Al-madani, Mr. Mohmmad Ameen, Mr. Yahya Al-buri, Mr. Abdullrashid And Mr. Hassan Saleh for their friendness and kindness.

TABLE OF CONTENTS

LIST OF TABLES

LIST OF FIGURES

LIST OF ABBREVIATIONS

MTO	:	Methanol to olefins
CHA	:	Chabazite
MAHyS	:	microwave-assisted hydrothermal synthesis
TOS	:	Time on stream
OSDA	:	Organic structure directing agent
XRD	:	X-ray diffraction
NMR	:	Nuclear Magnetic Resonance
XRF	:	X-ray fluorescence
FE-SEM	:	Field-emission scanning electron microscopy
TOS	:	Time on stream
ST	:	Steam cracking
tpd	:	tone per day

ABSTRACT

Full Name : [Galal Atef Ahmed Nasser]

Thesis Title : [Synthesis and characterization of cost-effective Chabazite (CHA) zeolite catalysts for the conversion of methanol to olefins (MTO) process]

Major Field : [Chemical Engineering]

Date of Degree : [December, 2017]

Light olefins ($C^{=}_{2}$-$C^{=}_{4}$) are very important intermediates for many processes in the petrochemical industry. Conventionally, they are produced from steam cracking units, alongside other products. Nowadays, the prices of lower olefins are increasing. Other processes which are very selective towards light olefins and depend on sustainable resources are highly required to increase olefins production. The methanol to olefins (MTO) process which is very selective towards ethylene and propylene is a very promising process.

Currently, the MTO process is commercialized and ZSM-5 and SAPO-34 catalysts are known to have excellent activity with different selectivities and deactivation rates. However, the synthesis of these two catalysts requires the use of an organic structure directing agent (OSDA) which makes their preparation methods challenging economically. Thus, this research was devoted to find a cost-effective method to synthesize a novel Chabazite (CHA) catalyst for the MTO reaction.

Two approaches with different molar gel compositions have been followed to fabricate a cost-effective and selective CHA zeolite catalyst. The first approach was the synthesis of an OSDA-free CHA zeolite in the presence of a fluoride ion. While in the second approach, SSZ-13 seed was used to assist the CHA synthesis by utilizing microwave-

assisted hydrothermal synthesis (MAHyS). Several experiments have been conducted to investigate different conditions under which the CHA catalyst was formed. After the successful fabrication of CHA zeolite catalysts, we used different characterization techniques to characterize the prepared catalyst. XRD, NMR and XRF were used to investigate the structure and to measure the elemental compositions. The textural properties, the morphology and the acidity were characterized using nitrogen physisorption, FE-SEM and NH_3-TPD, accordingly.

For the first approach: A series of cost-effective aluminum-rich chabazite (Al-rich CHA) zeolite with improved textural properties was synthesized without using templates. Herein, we report a detail synthesis method for CHA zeolite without using an organic structure directing agent (OSDA-free). Pure CHA zeolites were successfully synthesized under different gel compositions.. The BET results showed that ion-exchange enhanced the surface area from around 1 m^2/g to around 485 m^2/g. Aging time had a significant influence on the crystallization rate, particles' size and shape. The synthesized CHA zeolite was evaluated in the methanol-to-olefin (MTO) reaction at different reaction temperatures. The conversion was maintained at 100% for 4 h at 350 °C and for 2 h at 400 and 450 °C. The selectivity to lower olefins was correlated to the reaction temperature and time on stream (TOS). The highest olefins selectivity was ca. 93.8 at 180 min TOS and reaction temperature of 350 °C.

In the Second approach: Cost-effective aluminum rich (Al-rich) CHA zeolite was synthesized by seed-assisted hydrothermal synthesis under microwave irradiation to shorten the crystallization time. Al-rich CHA zeolite was successfully synthesized within 6 h. The Al CHA was synthesized under different stirring rates and evaluated for the

methanol-to-olefins reaction at three different temperatures in a fixed bed reactor. Boron was incorporated by in-situ synthesis. The XRD pattern revealed that the synthesized CHA was crystalline. The performance evaluation revealed that reaction temperature and TOS affected both the catalyst's stability and selectivity to light olefins. At a lower temperature (350 °C), the Al-rich CHA was more stable and less selective to light olefins at the beginning of the reaction. The selectivity was increased from 41.8% at TOS of 10 min up to 85.0% at TOS of 120 min. In contrast, the selectivities of olefins at TOS of 10 min were 55.0 and ca. 79.6% when the reaction temperatures were 400 °C and 450 °C, respectively. Incorporation of boron only enhanced the olefins selectivity at the initial stages of the reaction. The total olefins' selectivity over the parent CHA was ca. 41.8% and then increased to ca. 71.5% when the CHA was incorporated with boron (Si/B = 13).

ملخص الرسالة

الأسم الكامل: جلال عاطف أحمد ناصر

عنوان الرسالة: تصنيع وتخصيص مادة الزيوليت من نوع كابازيت والتي أُستخدمت كمادة محفزة لعملية تحويل الميثانول الى اوليفينات صغيرة.

التخصص: الهندسة الكيميائية

تاريخ الدرجة العلمية: ديسمبر 2017

تعتبر الأوليفينات الخفيفة من أهم المركبات التي تستخدم لإنتاج العديد من المواد في المصانع البتروكيميائية. إن الطريقة الإعتيادية لإنتاج هذه المركبات هي عن طريق تكسير المركبات الهيدروكاربونية في المصفآة في ظل وجود البخار. وبالنظر الى سعر المركبات الأوليفينية، سنجد أن سعرها في تزايد مستمر، لذلك لابد من وجود عملية بديلة تعتمد على مصادر متجددة وذات إنتقائية عالية لإنتاج الأوليفينات لسد حاجة السوق. وتعتبر عملية تحويل "الميثانول إلى أوليفينات" من أهم العمليات الواعدة التي تعتمد على مصادر متجددة، وتمتاز بانتقائية عالية نحو إنتاج الاوليفينات الخفيفة.

حالياً تم تطبيق عملية تحويل الميثانول الى أوليفينات واقعياً، حيث تستخدم مادتي الـ (ZSM-5) و (SAPO-34) كمواد محفزة لسير العملية. كلا المادتين أثبتت نشاطهما التفاعلي بنسب انتقائية مختلفة، ولكن يدخل في آلية تحضيرهما مركب عضوي يرمز له بـ (OSDA) الذي يجعل طريقة التحضير مكلفة وغير مرغوبة اقتصادياً. لذلك كُرّس هذا البحث لإيجاد طريقة اقتصادية ومجدية لتحضير مادة محفزة تدعى كابازيت (Chabazite) والتي ستستخدم في تحويل الميثانول الى اوليفينات خفيفة.

ولتحقيق هدف البحث، عملنا على تصنيع مادة الــكابازيت بطريقيتين مختلفتين؛ الطريقة الأولى قمنا بتصنيع مادة الكابازيت منخفضة التكلفة في وجود أيون الفلور وغياب OSDA أثناء التصنيع. أما الطريقة الثانية فقمنا بتصنيع الكابازيت بمساعدة كابازيت تم تصنيعه مسبقاً مستغلين اشعاعات الميكرويف أثناء عملية التصنيع. وقمنا باجراء العديد من التجارب لغرض معرفة تحت أي ظروف يمكن تحضير الكابازيت. بعد ان حضرنا الكابازيت ذو النقاية العالية قمنا بدراسة خصائصه مستخدمين عدة أجهزة؛ حيث تم إستخدام جهاز الاشعة السينية (XRD) وجهاز NMR

وجهاز XRF لتحليل البنية التركيبة وقياس نسبة العناصرالمكونة للكابازيت، كذلك تم استخدام المجهر الإلكتروني وأدمصاص الأمونيا لمعرفة الخصائص التكوينية ودرجة حموضة الكابازيت.

الطريقة الأولى: تم تصنيع سلسلة من الزيوليت من نوع كابازيت الغني بالألمنيوم مع تحسن في الخصائص التكوينية دون الحاجة الى استخدام OSDA. حيث أظهرت دراسة الـ BET ان عملية تبادل الايونات قد عززت مساحة السطح من حوالي 1 م^2 / جم الى 485 م^2/ جم. ان عامل الوقت أثناء عملية التحضير كان له دوراً مهم بالتأثير على معدل التبلور وحجم وشكل الجسيمات. وتم اختبار كفائة المادة في تفاعل تحويل الميثانول الى أوليفينات عند درجة حرارة 350 و400 و 450 درجة مئوية، حيث أظهرت نتائج التفاعل تحول كامل للميثانول لمدة 4 ساعات عند درجة حرارة 350 و لمدة ساعتين عند درجتي حرارة 400 و 450 درجة مئوية. أما بالنسبة للانتقائية، فقد وجد أنها مرتبطة بكل من درجة الحرارة ووقت التفاعل، فقد لحظ أعلى نسبة إنتقائية حول 93.8 % بعد مرور 180 دقيقة من بدء التفاعل عند 350 درجة مئوية.

الطريقة الثانية: تم تصنيع كابازيت رخيص التكلفة في ظل وجود كابازيت مسبق التحضير وذلك باستغلال إشعاعات الميكروويف لتقليل وقت التصنيع، حيث تم الحصول على كابازيت نقي خلال 6 ساعات. الكابازيت المصنع والغني بالألمنيوم تم تحضيره عند معدل تحريك ديناميكلي مختلف، ومن ثم تم اختباره في تفاعل تحويل الميثانول الى أوليفينات عند ثلاث درجات حرارية مختلفة. إضافة الى تصنيع كابازيت نقي، تم اضافة عنصر البورون خلال عملية التصنيع لدراسة مدى تأثيره على التفاعل. ولقد أظهرت دراسة الاشعة السينية بإن الكابازيت المصنع كان متبلوراً بشكل جيد و مطابقاً تماماً للمرجع. كذلك أظهرت نتائج دراسة التفاعل أن درجة حرارة التفاعل وزمن التفعاعل كان لهما تأثيراً كبيراً من حيث الانتقائية والكفائة، فعندما كانت درجة الحرارة منخفضة (350 درجة مئوية) كان الكابازيت أكثر استقراراً لكن أقل إنتقائية، وبالمقابل، عند درجة حرارة أعلى كان الكابازيت أكثر انتقائية لكن أقل استقراراً، حيث زادت الانتقائية من 41.8 % الى 85% عندما زاد وقت التفاعل من 10 دقيقة الى 120 دقيقة، وبعد 10 دقائق من التفاعل كانت الانتقائية للاوليفينات 55% عند درجة حرارة 400 مقارنة بـ 79.6% عندما ارتفعت درجة حرارة التفاعل الى 450 درجة مئوية. الجدير بالذكر ان إضافة عنصر البورون عمل فقط على تحسين الانتقائية في بداية التفاعل.

CHAPTER 1

INTRODUCTION

Olefins or alkenes are unsaturated and very active hydrocarbons with a general chemical formula of C_nH_{2n}. Among these alkenes are light olefins (such as ethylene, propylene and butene), which are very important building blocks for the petrochemical industries as starting materials for manufacturing of polyolefin and for reactions such as oxidation, halogenation and oligomerizations [1]. Additionally, light olefins are used to manufacture fibers, plastic and large number of chemicals such as benzene, isopropyl benzene, styrene, and propylene oxide and epoxy ethane [2, 3]. Thus light olefins are main resources for many derivatives that we daily use in our life [4].

As the world population is keeping in increase and as our life comfort involves the use of more olefins derivatives, the demand for light olefins will grow vastly. In 2013, the demand for ethylene and propylene was 133 and 83 million metric tons, respectively, while the expected demand in 2023 will be 194 million metric tons for ethylene and 126 million metric tons for propylene. With the increasing demand of ethylene and propylene, their price will also keep increasing. **Figure 1** shows the increase in price for ethylene and propylene in the United States for the period of 2007-2014. From **Figure 1**, it's clear that the increase in propylene price is more than of ethylene. This increase is caused by the ethane cracking which produces more ethylene leading to lower supply of propylene.[5]

There are a number of technologies dedicated to produce olefins, however steam cracking (SC) technology is the primarily technology for the production of light olefins. In the SC, naphtha and ethane, which are oil-based derivatives, are cracked in the presence of steam to olefins and other products [1, 6]. Other technologies such as the conversion of methanol to olefins (MTO), the Fischer-Tropsch synthesis, oxidative coupling of methane and catalytic dehydrogenation of light alkane produce olefins with lower capacities [4]. The advantage, disadvantage and the way of each technology works is discussed briefly in chapter 2.

In this section, it is worthy to mention that production of lower olefins using the SC process requires high temperature which consumes huge amount of energy [2]. Also, the amount produced from steam cracking does not meet the world demand of olefins. Thus, alternative routes for the production of light olefins with higher selectivity toward ethylene and propylene are required to meet their growing demand and to ensure sustainable resources. Methanol to olefins (MTO) route is one of the promising processes to increase the production of light olefins with controllable selectivity to either propylene or ethylene, low emission of carbon dioxide and less energy consumption [1, 7]. **Figure 2** shows the amount of methanol used for the production of light olefins. Moreover, MTO process, which is now commercialized, is an excellent alternative process for olefins production because: (I) it is economically favored, (II) it is favored in term of simplicity, (III) environment friendly and (VI) its feedstock is sustainable and does not rely on oil. Hence, MTO process development met a great attention. Thus, our focus in this study is to develop and efficient and cost-effective catalyst for the production of olefins from MTO process.

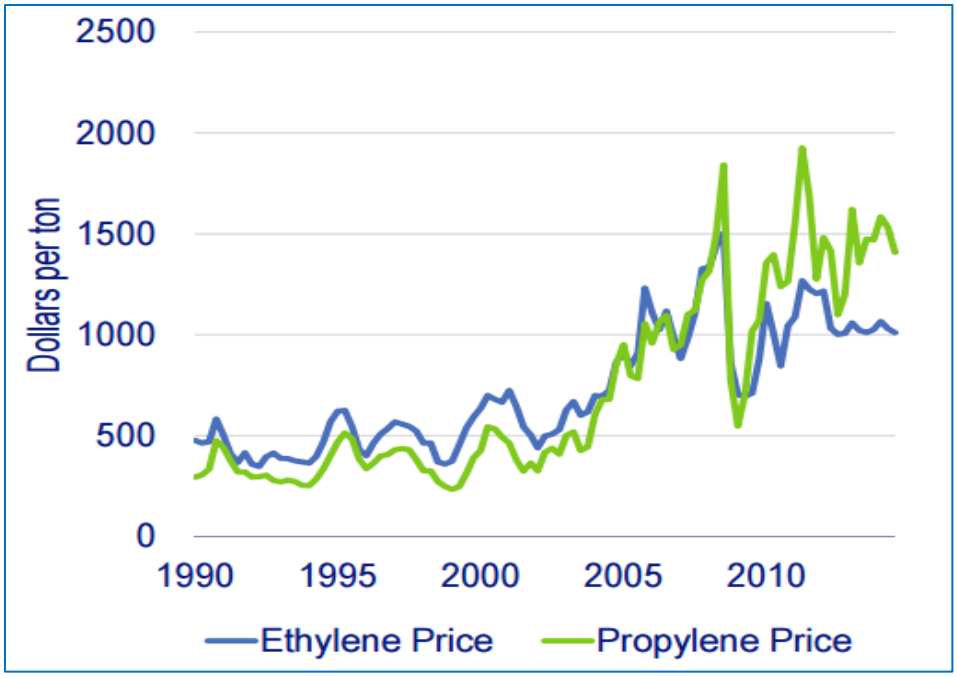

Figure 1. Ethylene and Propylene Price in United States since 1990 up to 2010. (Vienna/OPEC presentation, 2014)

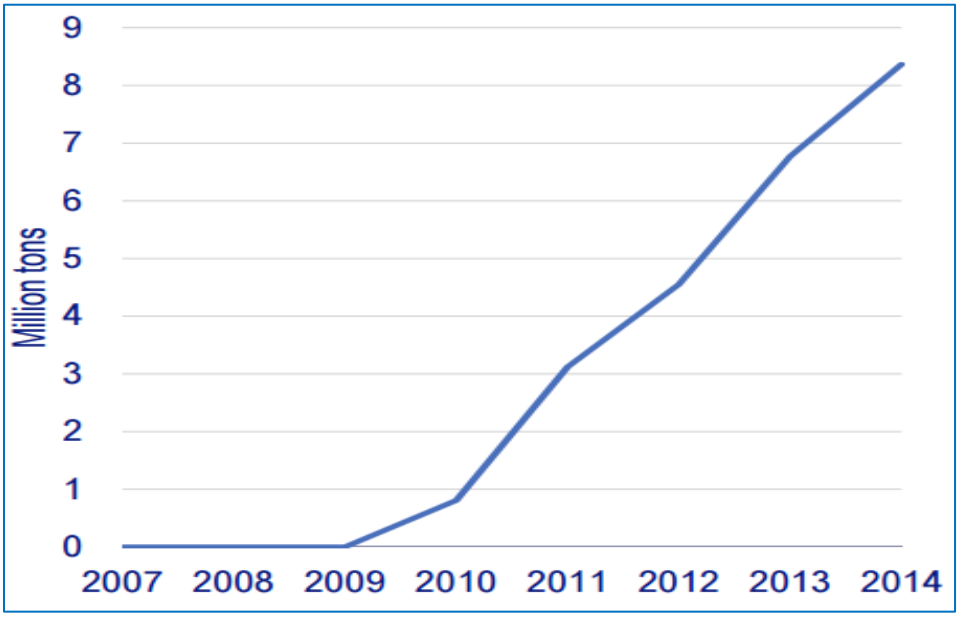

Figure 2. Methanol consumption for the production of olefins in China[5]

Many type of acidic zeolites framework have been utilized in the literature for the MTO reaction. Among these catalysts are ZSM-5 and SAPO-34 which show excellent performance in the MTO reaction. However, the two catalysts showing different selectivities to olefins and different deactivation rate because they have different topologies and physical properties. ZSM-5, for example, which has a MFI topology is very stable in the MTO reaction but it is not selective as SAPO-34. In contrast, SAPO-34 with CHA topology is more selective to lower olefins but it suffers from the fast deactivation.

The preparation of these catalysts involves the use of templates which are expensive and have negative effect on the environment. This work focuses on the production of light olefins from methanol with high stable and selectivity to lower olefins using cost-effective catalysts. Hence, our attention will be to the zeolite catalysts with the CHA topology. To have cost-effective CHA zeolites, we will focus on the preparation of OSDA-Free CHA.

1.1 Objective

The general objective of this research is to fabricate a stable and selective cost-effective CHA zeolite catalyst for the conversion of methanol to light olefins. To achieve that objective, two approaches have been examined for the catalyst fabrication

First approach:

The objective of this approach is to investigate and evaluate the preparation of an OSDA-Free CHA zeolite in the presence of Fluoride ion. In more details:

1. Hydrothermally synthesize CHA zeolite without using any organic structure directing agent (OSDA).
2. Investigate the effect of altering gel composition on the catalysts crystallinity, morphology, Si /Al ratio and particles' size and shape.
3. Study the effect of metal incorporation on the CHA performance in the MTO reaction.
4. Characterize the synthesized catalysts using different characterization techniques.
5. Test the prepared catalysts in a fixed bed reactor to study their activity, selectivity and stability in the conversion of MTO process

Second approach:

In this approach, microwave irradiation was used to synthesize an OSDA-free CHA zeolites from an amorphous aluminosilicate gel in the presence of a seed. In more details

1. Synthesize of pure CHA zeolite without using templates.
2. Optimize the synthesis time.
3. Investigate the effect of B incorporation.
4. Characterize the synthesized catalysts using different characterization techniques.
5. Evaluate the performance of the prepared zeolite in MTO reaction at different temperatures.

1.2 Methodology

The plan set for achieving the objective of this work is summarized in **Figure 3**. As mentioned in the objective section of this document, there will be two approaches for the synthesis of cost-effective catalysts without using any templates. In the first approach, the CHA zeolite catalyst was synthesized from basic chemicals following a cost-effective method that excludes the use of an OSDA. In the synthesis of the catalysts, large numbers of experiments were conducted to explore the effect of different compositions of the gel on the crystallinity and physical properties of CHA zeolite. Finally, the catalyst activity was evaluated in a fixed bed reactor for conversion of methanol to olefins.

The second approach was dedicated to synthesize CHA zeolite using microwave heating and SSZ-13 seed to assist the formation of CHA phase. In this method, the preparation method of CHA zeolite was adapted form literature but with shorter crystallization time.

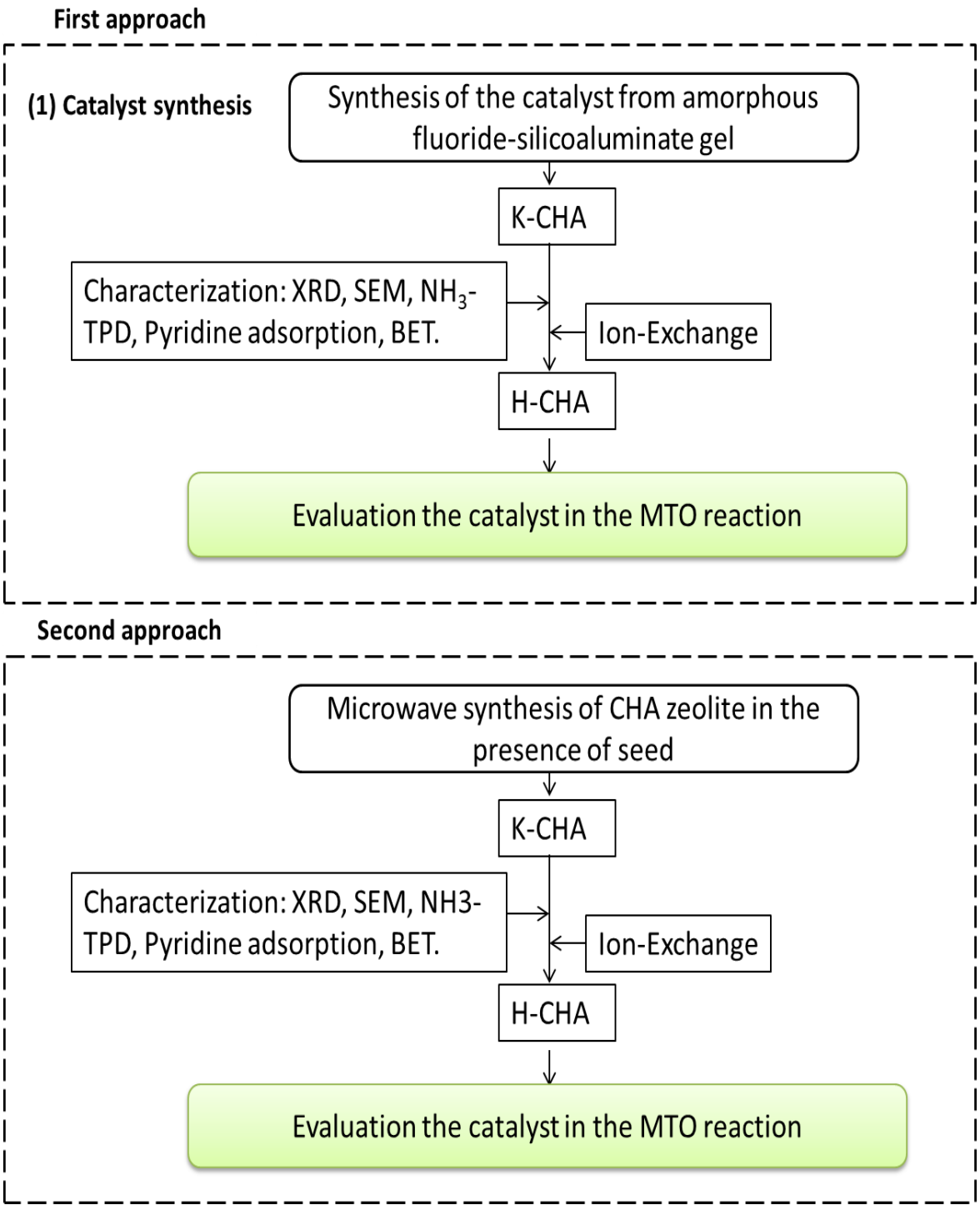

Figure 3. A summary for the methodology followed to achieve the work

CHAPTER 2

LITERATURE REVIEW

2.1 MTO process

The process of methanol to olefins is a very important process for the production of light olefins from non-oil routes such as coal and natural gas through the conversion of methanol [8]. Even the feedstock to the MTO process can be obtained from oil, MTO process works as a bridge between modern industries and coal, biomass and natural gas [9, 10]. The potential importance of MTO process is that two or more carbons are formed from a single carbon which can be derived from different resources [1]. Historically, the first report for methanol conversion to hydrocarbons and ether as side products is dating back to 1880 [11]. However, the importance of methanol conversion to the industry was appeared in the early of 1970s by the discovery of Mobiles researchers.

Prior to MTO process, methanol is firstly derived from syngas (a mixture of carbon dioxide and hydrogen) which is produced from the gasification of coal or from the steam reforming of natural gas [12]. **Figure 4** shows how methanol is produced from non-oil resources. Then the methanol is transformed to an equilibrium mixture of dimethyl ether (DME), methanol and water. Finally, the equilibrium mixture is converted to hydrocarbons (gasoline or light olefins) depending on the type of catalysts used and the process conditions [12]. For example, at around 400 °C and an optimum partial pressure of methanol, the methanol to gasoline (MTG) reaction at the presence of ZSM-5 catalyst takes place. These conditions are optimum for the transformations of olefins to aromatics

and paraffins. Altering the reaction temperature and changing the type of catalyst favors MTO or methanol to propylene (MTP) processes. A detail description of the MTO reaction mechanism is given in section 2.5 of this document.

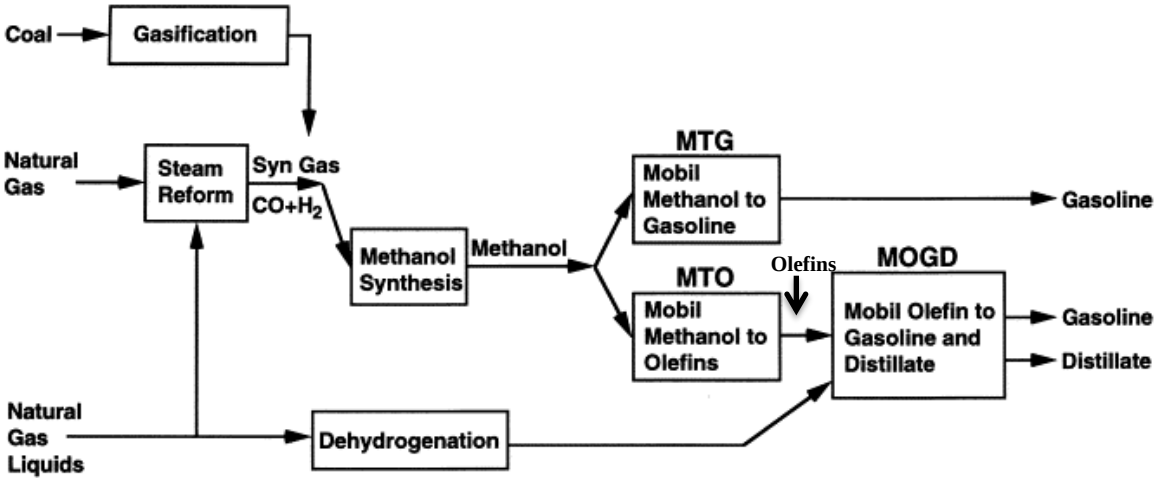

Figure 4. Hydrocarbons production through methanol.

2.1.1 MTO History

During the first and the second oil crises, mobile increased its effort in the development of methanol conversion to gasoline (MTG) process. As a result of this, MTO process was discovered by chance when Mobile researchers in 1970s were trying to find new routes to produce gasoline with high octane-number over HZSM-5 [13-15]. In their strategy, they were feeding methanol and isobutene hoping that a methyl carbine or methyl cation will form and actively react with the alkane to form longer chain of alkanes. However, they noticed that the products were a liquid consisting of gasoline and a gas containing aromatics and paraffins. The researcher found that the products were formed by the conversion of methanol. This was proofed by mass balance on isobutene which was not consumed during the reaction. Additionally, when the pure methanol was feeded alone,

they found the same products. This led to the discovery of the conversion of methanol to hydrocarbons (MTG) process [14, 15].

Since MTO process has been firstly proposed by Mobile Oil in 1970s, many studies have been conducted to develop the process by studying the kinetic of the process, catalysts synthesis and establishing research and development centers[9]. Studying or fabricating catalysts with higher efficiency, which will decrease the operating cost of the MTO process, is another important point in the development of MTO process [15]. The type of the catalysts used in the MTO process is solid acidic catalysts. Many types of zeolites have been evaluated in the MTO process; however, ZSM-5 and SAPO-34 were proven to have excellent activities in the MTO process.

2.2 Technologies of olefins production from methanol

The attention to methanol conversions was initiated after the first and second oil crises in 1973 and 1979 for the purpose of gasoline production, methanol-to-gasoline (MTG) [16]. In the MTG process, olefins were as intermediate products in the production of gasoline. Later, Mobile produced olefins as primary products while gasoline as secondary products. Then, this process has been extended to olefins oligomerization to produce combined products of gasoline and diesel as shown in **Figure 5**.

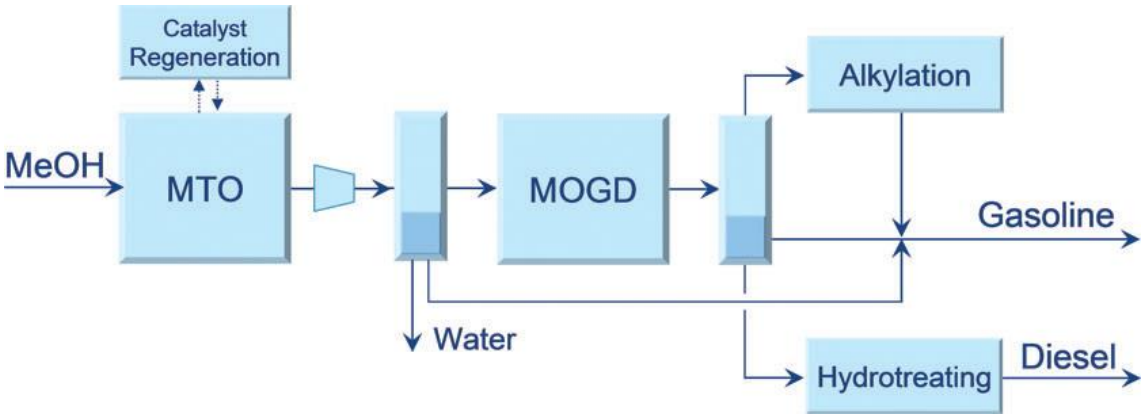

Figure 5. The conversion of olefins to gasoline and diesel, the process called Mobile olefins to gasoline and distillate process (MOGD)[16].

After that, a number of processes have been developed. Herein, we will give a brief summary of technologies used to produce light olefins from methanol.

2.2.1 INEOS or UOP/Hydro MTO process

In 1995, UOP and Norsk Hydro (now INEOS) developed the MTO process over SAP-34 catalyst [16-18]. They developed a pilot plant with a capacity of 0.75 [18] or 0.9 [17]ton per a day of methanol feed using fluidized bed reactor at Hydro in Norway. Later in 2009, this process was combined with a process from TOTAl called olefin cracking process (OCP) for further enhancement of propylene and ethylene selectivity as shown in **Figure 6**. The capacity of this combined process was around 10 tpd of methanol feed. In 2013, a first commercial MTO plant which produces 295 kt/y of lower olefins was built in Nanjing, China.

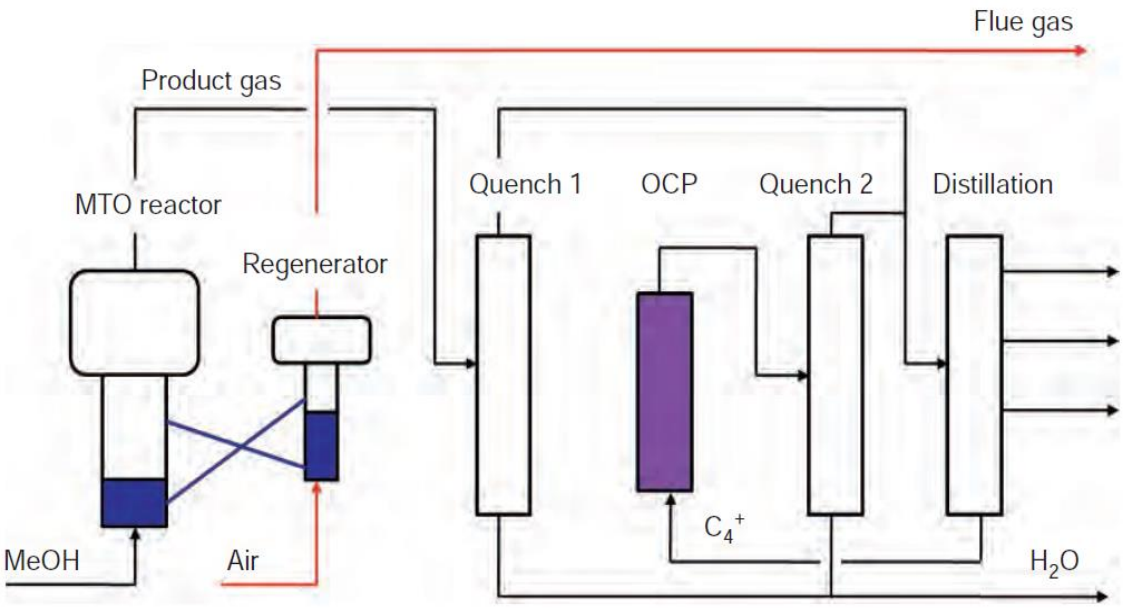

Figure 6. Schematic diagram of the combined INEOS and OCP process[18].

2.2.2 Lurgi MTP process

The Lurgi MTP process is the same as the UOP's MTO process, except a special attention was paid to propylene selectivity by using ZSM-5 catalysts. The reaction temperature is ranging between 450 and 500 °C using a fixed bed reactor. For the purpose of maximizing the propene selectivity, C_2 and C_4 olefins were recycled back to the reactor as shown in **Figure 7**. The process was designed in such a way that the fixed-bed reactors are in parallel to allow regeneration from time to time. This process has been commercialized in China in 2010 with a capacity ca. 500 kt per year of propene and 185 kt per year gasoline. [16-18]

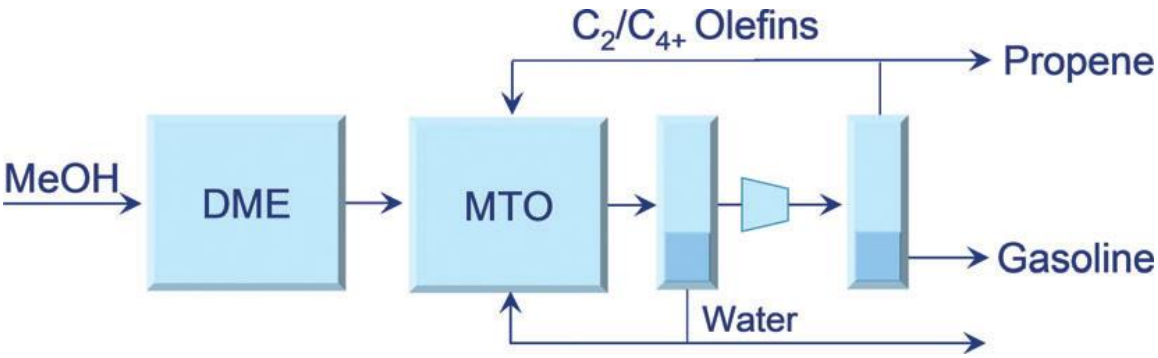

Figure 7. The Lari MTP process[16].

2.2.3 JGC/Mitsubishi DTP process

In 2007, the Japan Gasoline company (JGC) and the Mitsubishi, together, have developed another process for propylene production called Dominant Technology for Propylene (DTP).The catalyst used in this process is ZSM-5 modified with calcium. DME or a mixture of DME and methanol is feeded to a series of fixed-bed reactors operating at 500 °C and 1 atm [17].

2.3 Zeolites

Zeolites, which were discovered in 1756 by the Swedish scientist Axel Fredrik, are microporous inorganic crystalline solid materials. Zeolites were discovered when Fredrik was heating unknown minerals and he noticed a generation of steam from these minerals [19]. After this accident, Fredrik named these materials as "Zeolites" which has been derived from two Greek words; "ζέω (zéō) mean to boil" and "λίθος (líthos) means stone". Thus, a basic definition of zeolites and based on translation is "the stones that boil" [20].

Zeolites are basically formed from the tetrahedral of TO_4, where T can be Al, Si, P, B, Ge, Zn etc. [20]. In most cases the T is Si and Al, thus an explanation of zeolites framework will be given based on the Si and Al. **Figure 8** shows the AlO_4 and SiO_4 tetrahedral and how they are connected to form the basic network of zeolite framework. Aluminum (Al) has a 3 valance electron and appears in its cationic form as Al^{+3} while Silicon has 4 valance electrons and appears as Si^{+4}. Oxygen which works as a bridge between alumina and silica has two valance electrons and its anion form is O^{-2}. Thus, oxygen will bond with two atoms, Si and Al, to form a structural as shown in **Figure 8 a**. This binding will lead to the appearance of a negative charge on the Al (**Figure 6 a**) but this anion tends to forms on the oxygen atom as shown in **Figure 8 b**. To have the structure to be neutral, a cation must compensate the negative charge. The cation could be Ca^{+1}, Na^{+1}, H^{+1}, K^{+1} etc.

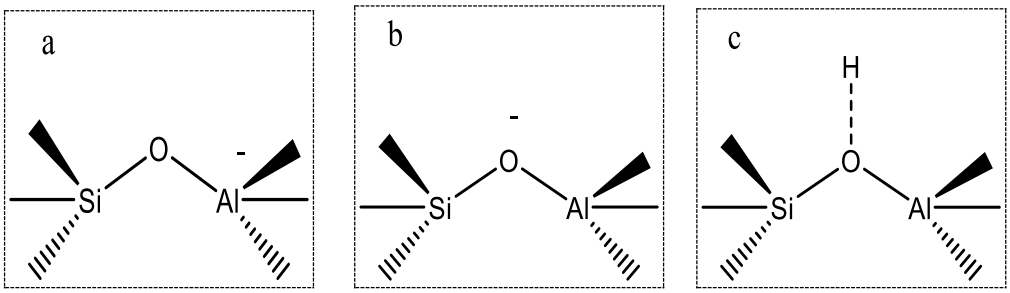

Figure 8. Basic structure of zeolites, tetrahedral of AlO_4 and SiO_4

2.3.1 History of zeolite

The history of zeolite is back to the discovery date of the natural zeolite in 1756 [21]. Since that time, extensive application of natural zeolites led to the further discovery of their intrinsic properties such as the reversible water adsorption capacity. Later, in 19th century, scientists found that zeolites possessing the ion-exchanged property with metallic cations under similar properties. At that time, scientist recognized that zeolites can adsorb ethanol, formic acid vapor, water and methanol, and cannot easily adsorb benzene, diethyl ether and acetone. This property made scientist to recognize the importance of the zeolites in adsorption applications.

In nature, zeolites firstly were found in cavities and vugs of basalts. A time later, namely in the 19th century, zeolites were found in the sedimentary rocks. The formation of zeolites is recognized by a certain genetic forms, mentioned somewhere else [21]. The intense investigation to minerals resulted in the discovery of more zeolites; more than 40 types of natural zeolites up to now have been discovered. Chabazite, Clinoptiloite Mordenite, Heulandite and Stilbite, to name but a few, are examples of natural zeolites.

Nowadays, natural zeolites are used for water and gas separation, softening of water, drying …etc [21].

2.3.2 Structural building units of zeolites

The structure of zeolites is consisting of several building units. The primary building unit of zeolites is the tetrahedra of AlO_4, SiO_4 (aluminosilicate zeolites) and PO_4 (in the case of aluminophosphate or silicoaluminophosphate) [22]. More complex building units of zeolites are formed by the combination of the primary building units. The 4-corner sharing of the tetrahedra results in a microporous and low framework density. The framework density is defined as the number of T atoms per 1000 Å [20, 23]. For understanding the structure of zeolites, it can be viewed as composite of rings which are formed by a number of tetrahedra. The name of the ring is given based on the number of tetrahedral it contains. For example, the four ring (4-ring) is consisting of 4 tetrahedra. Other tetrahedral n-rings are exists, where n can be 4, 6, 6, 10 or 12 tetrahedra as shown **Figure 9**.

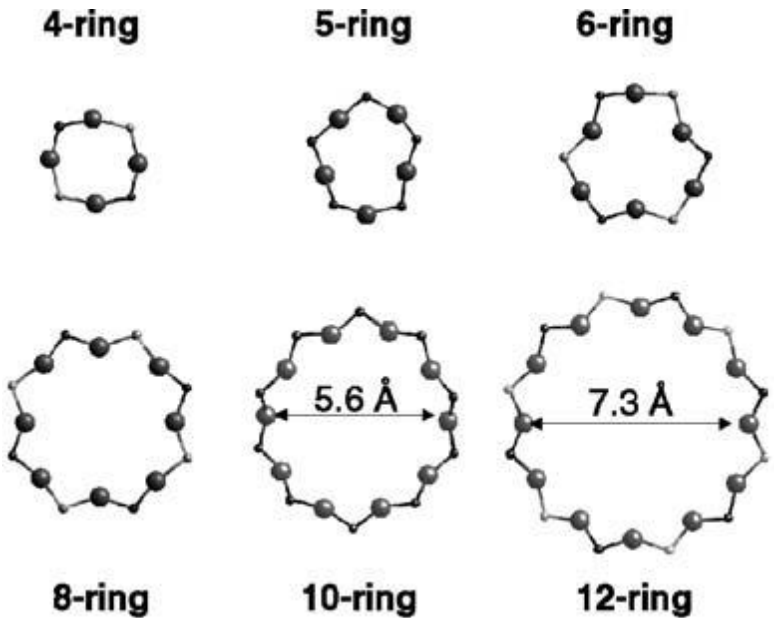

Figure 9. Secondary building units of zeolites [21].

2.3.3 Composition of zeolites framework

After a brief discussion about zeolites building units in which the basic building units consisting of the TO_4 tetrahedra, someone may ask how the tetrahedra and ions are arranged in the zeolites framework? In silicoauluminate zeolites, bonding of the Al and Si tetrahedral follow the criterion depicted in **Figure 10**. Arrangement in **Figure 10 A, b, c, d, e** and **f** is possible, while the arrangement in **Figure 10 a** is unlikely to occur due to Lowenstein's rule constraint [22]. This means that Al-O-Al is impossible [24].

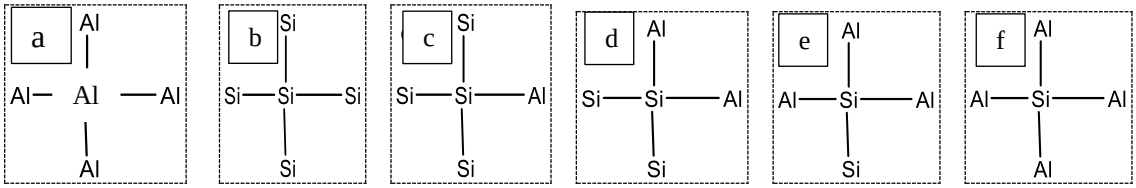

Figure 10. Possible arrangement of SiO_4 and AlO_4 tetrahedra; the oxygen atom that connect between Si and Si or Si and Al is not shown.

2.3.4 Acidity of zeolites

Zeolites are very acidic solid catalysts which have been utilized in the reactions that require acidity such as cracking and MTO process. The source of acidity in zeolite is raised from the orientation of their structure. The basic building unit of zeolites is the tetrahedral of alumina $(AlO_4)^{-5}$ and silica $(SiO_4)^{-4}$. These tetrahedral are joined together to form Si-O-Si or Si-O-Al bond. The Si-O-Al is missing a positive charge, a cation, to make it neutral. The cation can be any type of cations (such as K^{1+}, Ca^{2+}, Mg^{1+}, Na^{1+}, NH_4^{1+}) which can be exchanged by a desired one [25]. When the cation is a proton H^+, the proton will attach to the oxygen to form hydroxyl group bridge between Si and Al (Si-OH-Al). This hydroxyl group is the responsible for the Brønsted acid sites which are used for cracking and conversion of methanol to hydrocarbons [26, 27]. Another hydroxyl groups are do exist in the zeolites structure. The Si-OH which called as the silanol group is found at the termination or defects in the zeolite framework. The Al-OH group is found in the case of extra framework of aluminum [25]. In fact, there are different forms of Al which can be present as extra framework in zeolites such as Al_2O_3, AlOOH, $AL(OH)^{2+}$, $Al(OH)^{2+}$ [28].

2.3.5 CHA frameworks

The frameworks of CHA zeolite is consisting of four rings (4R), six rings (6R) and eight rings (8R). In CHA framework, a series of double six rings (D6R) is linked by a series of 4R that are skewed to form a cage with a pore opening of 8R as shown in **Figure 11**. The cations present in the framework of CHA zeolite can be located at different positions. They can be in the center of the D6R, in the center of the cage or near to the moth opening of the 8R [29]. The location of the ions, usually after ion-exchange the proton

ion, can be determined using infrared and NMR analysis. It has been found that the stretching and chemical shift of the OH bridge differ by the size of the pore where the ion presents [29].

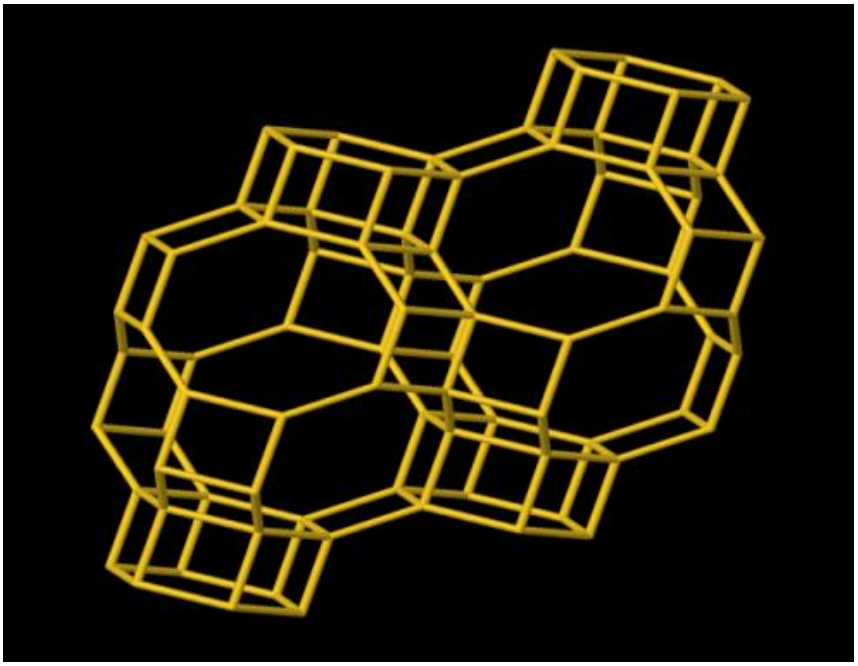

Figure 11. Arangement of 4R and 6R to form of CHA cavity (IZA).

2.3.6 Synthesis of zeolites

As mentioned earlier, zeolites can be found in nature or can be synthesize in the lab. Zeolites which are found in nature are called natural zeolites and tend to have impurities that limit their application as catalysts in many reactions [30-32]. However, pure zeolites with desired properties can be synthesized in the lab. The first batch of zeolite synthesis is dated back to 1950s [33]. There are different methods for the synthesis of zeolites; hydrothermal method, vapor phase transport and steam assisted conversion method. The hydrothermal method involves three main steps; (i) the mixing of amorphous reactants such as alumina, silica, and a cation at room temperature , (ii) heating the mixture at a

temperature ranging from 70 up to 200 °C in a Teflon-lined stainless steel, this process called crystallization, (iii) separation and washing the crystallized zeolites [33]. Although, the steps seem to be easy to follow, a number of factors strongly affect the formation of zeolites framework, morphology, crystal size and composition. For example, the presence of structure directing agent (an organic chemical used to direct the structure formation), type of alkaline metals and source of alumina and silica all have strong influences on the synthesis. For more detail regarding zeolite synthesis, a reader is recommended to read other sources [33, 34].

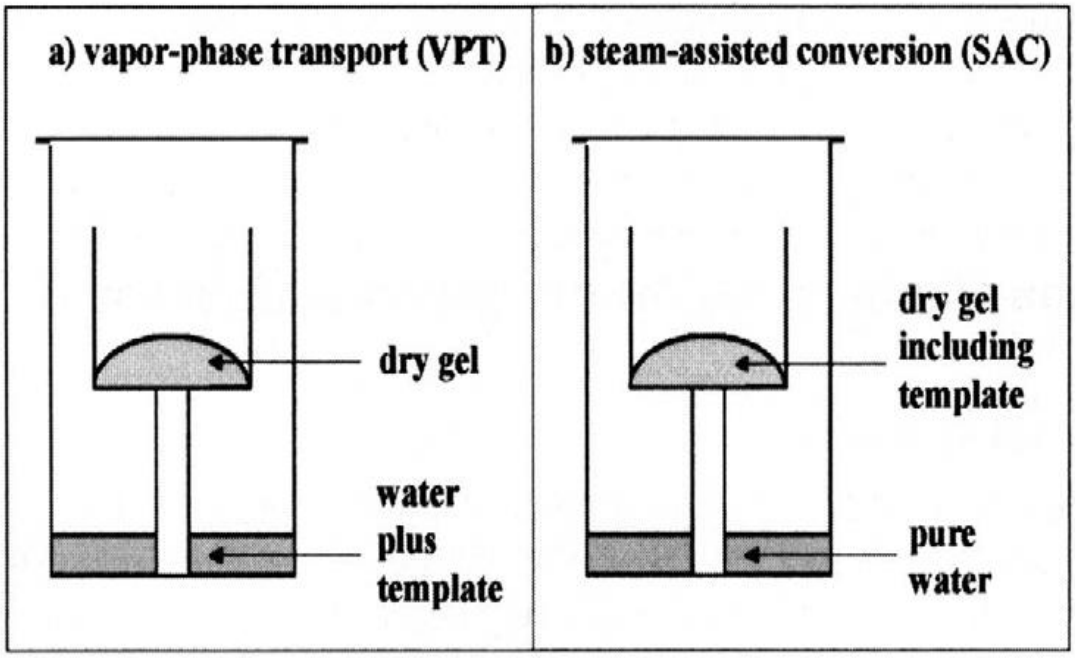

Figure 12. Vapor phase transport (a) and steam-assisted conversion (b) methods of zeolites synthesis [35].

2.3.7 Characterization of zeolites

There is a number of sophisticated equipment uses to characterize different properties of zeolites. For example, the structure of zeolites can be investigated using X-ray diffraction (XRD), Nuclear Magnetic Resonance (NMR) spectroscopy and X-ray fluorescence (XRF). Field-emission scanning electron microscopy (Fe-SEM) and energy dispersive X-ray (EDX) are used for the morphology analysis. The acidity, surface area and pore volume distribution are measured by the Ammonia-Temperature Program Desorption (NH_3-TPD), the pyridine adsorption in the Fourier transform infrared spectroscopy (FT-IR) and N_2 adsorption/desorption isotherm, accordingly.

In this section, a brief background about the equipment will be presented, and the experimental procedure for each equipment will be explained when it is used throughout the work.

Surface area analysis

Brunauer–Emmett–Teller (BET) theory is one of the most popular methods used for surface area measurement of solid materials. The Langmuir isotherm is the starting point of the BET theory. Calculation of the surface area is based on adsorption a gas (usually nitrogen) at liquefied temperature. Prior the analysis, the samples are degassed at an appropriate temperature in order to remove any adsorbed gasses or impurities.

The following equation is called BET equation:

$$\frac{1}{v[(\mathrm{po}/p)-1]} = \frac{c-1}{v_m c}\left(\frac{p}{\mathrm{po}}\right) + \frac{1}{v_m c} \qquad \textbf{Eq. 1}$$

Where: *v* is the amount of adsorbed gas, *po* the equilibrium pressure of the adsorbate gas, *p* the saturation pressure, po/p the relative pressure, v_m is the quantity of gas adsorbed by one layer and *c* the BET constant

From above equation, the term $\frac{1}{v[(\mathrm{po}/p)-1]}$ can be plotted against $\frac{p}{\mathrm{po}}$ to give a straight line with a slope (*A*) = $\frac{c-1}{v_m c}$ and intercept (*I*) =$\frac{1}{v_m c}$. From the slope and intercept, the adsorbed gas quantity and BET constant can be calculated.

The total surface area is calculated from:

$S_{\mathrm{total}} = \frac{(v_m N s)}{V}$ where N is Avogadro's number, s the cross section of the gas and *V* molar volume of the adsorbate gas .

While the specific surface area is calculated from:

$S_{\mathrm{BET}} = \frac{S_{\mathrm{total}}}{a}$ where *a* is the mass of the adsorbent .

Nuclear Magnetic Resonance (NMR) spectroscopy

The Nuclear Magnetic Resonance (NMR) spectroscopy is the technique used to investigate the structure of zeolites. It determines the orientation of the compounds in the structure; the distribution of aluminum, silicon, phosphorous and any other elements incorporated in the zeolites framework [24]. But, what is the concept behind NMR?

The concept behind NMR is that a magnetic field is applied to the nuclei of a certain element and then measure the amount of energy required to put different nuclei in

resonance. Resonance is a phenomenon in which an external object or a vibrating object makes another object to oscillate; matching of frequencies. The amount of energy required to put an object in resonance is effect by the nuclei environment, shielded or de-shielded environment. Then the NMR provides a signal indicating the amount of energy to put nuclei in resonance. Each nuclei will have a unique signal.

For zeolites, mainly ^{27}Al, and ^{29}Si solid state NMR are used to study the coordination of aluminum and silicon tetrahedral. For ^{29}Si NMR, 5 peaks can beaks, which are corresponding to the five coordination of Si as shown in **Figure 13**, can be detected [24, 36].

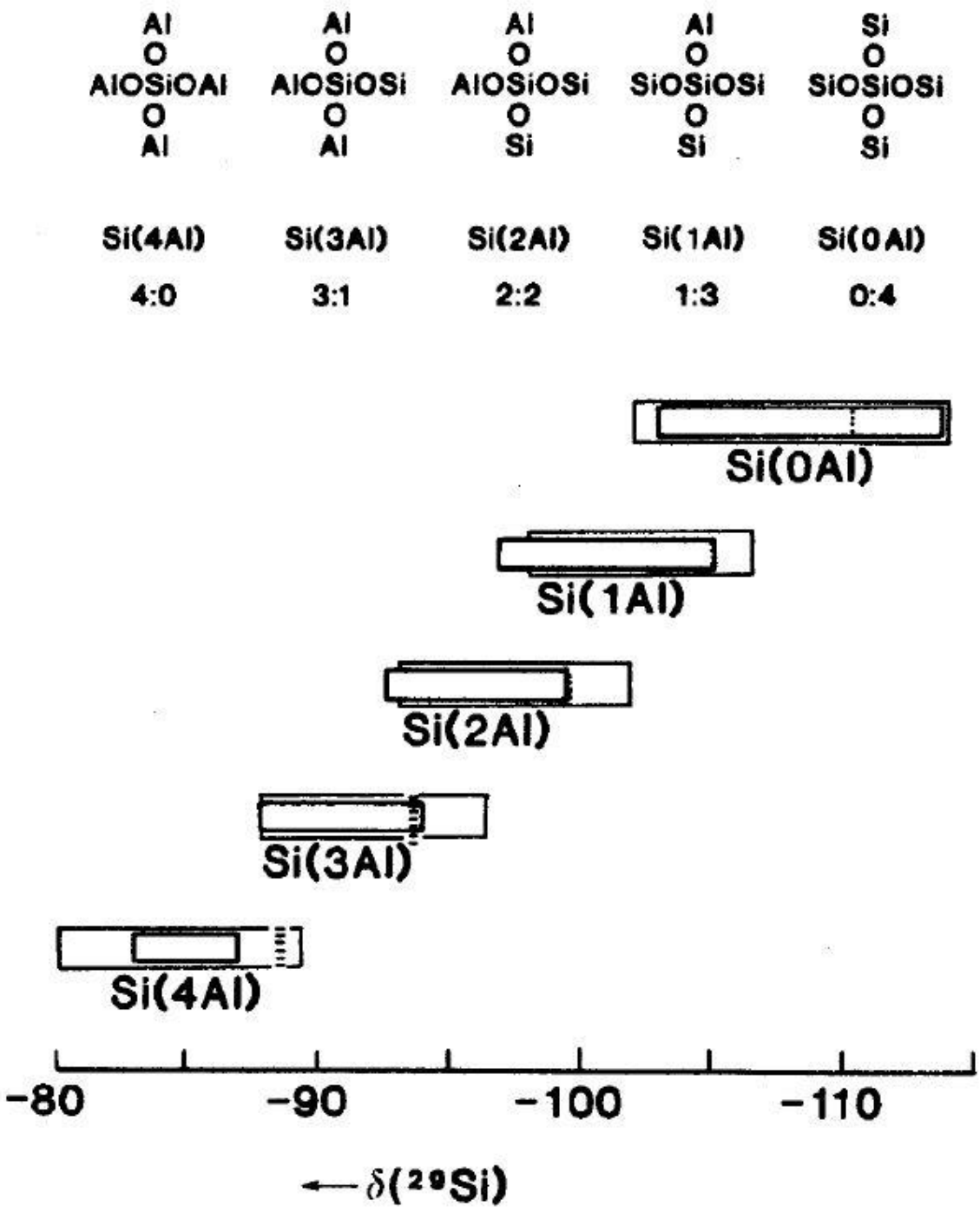

Figure 13. NMR peaks positions corresponding to different arrangement of Si orientation[36].

Fourier series –infrared (FT-IR) and Pyridine adsorption

To understand the IR spectroscopy, it's preferable to have some key points about functional group and frequencies. Different Functional groups wag, bend and stretch at different frequencies. Thus, the functional group will adsorb light frequencies that match the frequencies of lagging, stretching and bending. For well understanding, let us assume molecule A having this functional group (O=C), the double bond will stretch at a frequency of , say, 3 Hz while it lag at 5 Hz. If a source of light is passed through this molecule at a frequency of 2 Hz, then the detector will detect the same frequency. Therefore, we will have 100% transmission of the light. Then, if the frequency of the light is changed to 3 or 5 Hz which is the same as the stretching and lagging frequency, the transmission of light will be close to zero. Thereafter, a graph representing the transmission versus the frequencies can be generated and adsorption bands can be seen, **Figure 14**.

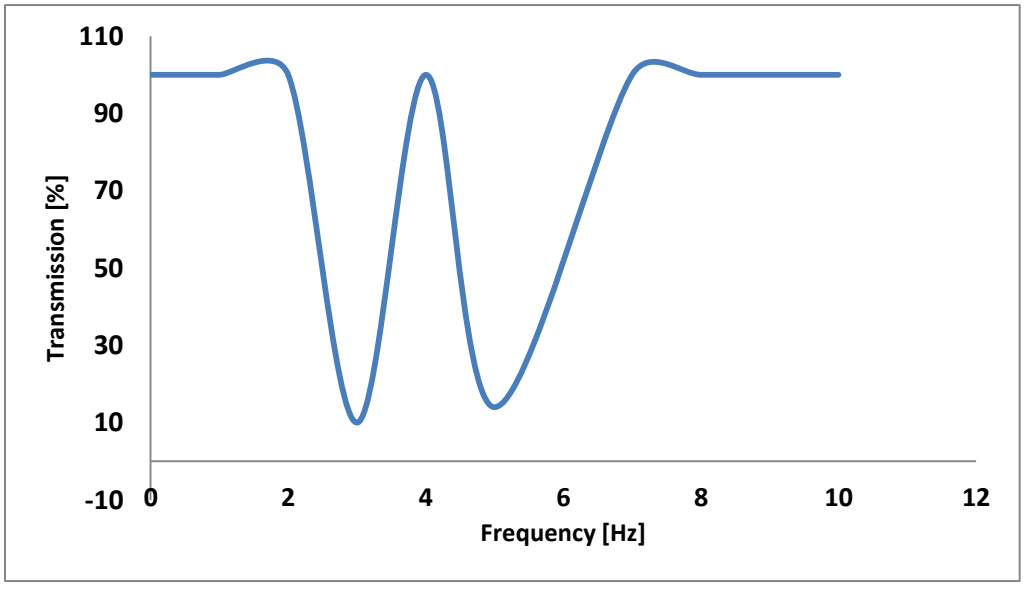

Figure 14. Generated figure to explain the concept of IR

X-ray diffraction

XRD is an analytical technique used to identify a crystalline material. But what is x-ray and what are the benefits of it in characterizing solid materials? X-ray is an electromagnetic radiation with a wavelength of ca. 10 nm to 10^{-1} nm. The XRD provide information about the phase, grain size, strain and crystal defects. The XRD consists of the x-ray tube, sample holder and x-ray detector. The x-ray is generated in a cathode tube where a filament is being heated to generate electrons, which are accelerated by a applying a voltage difference. The produced electrons hit a sample and causes a dislodge to electrons in the inner shell so that an x-ray which is a characteristic of the sample is being produced and recorded by a detector. [37]

The crystallite size of a material can be estimated using Scherre equation, Eq. 2.

$$t = \frac{0.9\lambda}{\beta cos\theta} \qquad \text{Eq. 2}$$

Where λ is the wavelength, β is the width of the peak at the middle of the peak intensity and θ is the diffraction angle.

Gas Chromatography (GC)

Chromatography is a wide topic; however a brief introduction on GC will be given. Generally, the GC is used for materials that are volatile and hydrophobic. The system of GC is consisting of three main parts; the injector, column, and detector. The injector is a place where a sample is injected and got mixed with the carrier gas (the mobile phase). Column is a very thin long narrow tube that is coiled to form cylinder shape like. The

column is placed inside an oven to ensure that the analytes (desired samples to be separated) in a vapor form. The analyte are then mounted by the end of the column to a detector. Detector is a device used to sense the elutes (the outlet of the column). There are many types of detectors; some detectors are used for one purpose, ex. to calculate retention time, and some other for multifunction. Usually, GCs are equipped with more than one detector which is ordered in series.

Field-Emission scanning electronic microscope (FE-SEM)

The electron microscope is a sophisticated type of microscopes in which a beam of electrons are used to give an image about a sample. The electronic microscope gives better magnification and resolution than light microscope. **Figure 15** shows the main components of the SEM. In SEM, beam of electrons, which pass through a condenser lens to make a narrow beam, is scanned over a sample. Beam of electrons bombard the sample emit secondary electrons which are then detected by a detector to give an image bout the sample.

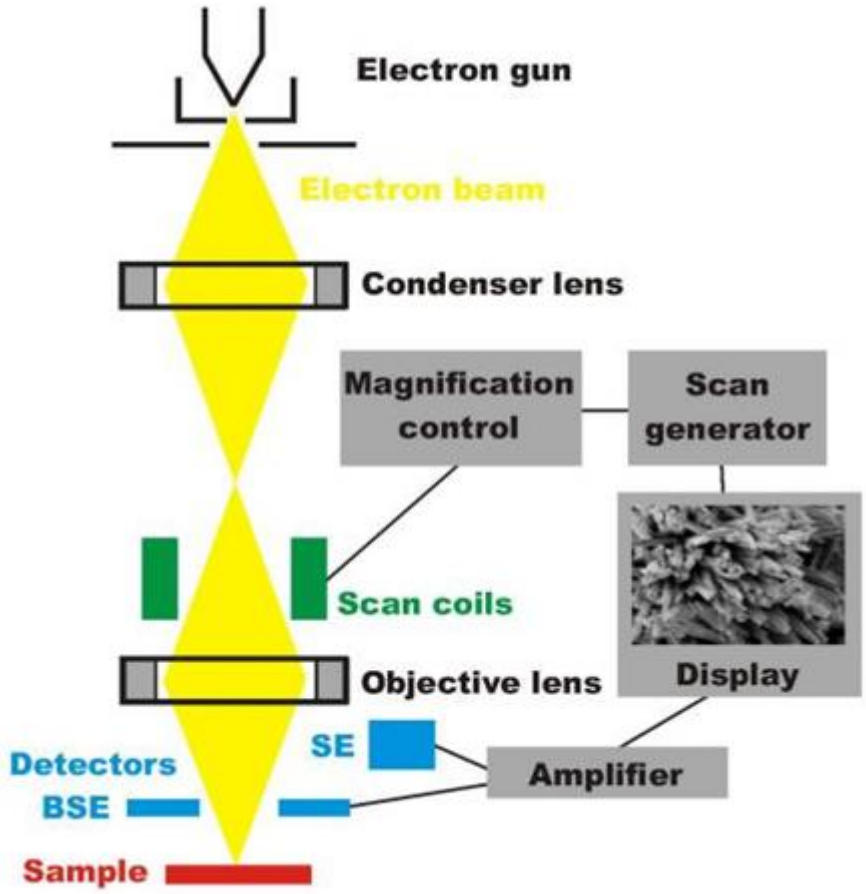

Figure 15. Main component of SEM [38]

Energy Dispersive X-ray (EDX)

The EDX is provided with the FE-SEM with different detector to detects the x-ray emitted from the sample.

2.4 MTO catalysts

Methanol is easily converted into hydrocarbons over solid acidic catalysts. Thus, several types of acidic zeolites in the literature with different topology such as DDR [7, 39], ERI, LTA, UFI, [40] MFI and CHA have been studied in the MTO reaction. Chabazite zeolites are exhibiting an excellent activity in the MTO reaction. However, the solid acidic zeolites SAPO-34 and ZSM-5 are the two catalysts that have been applied in the industry. ZSM-5 with MFI topology is very well known and active catalyst in many reactions, MTO reaction is an example. However, ZSM-5 is less selective towards light olefins and gives wide range of hydrocarbons due to the relative large pore size and small cage size. On the other han, SAPO-34 with the CHA topology is very active and has higher selectivity to lower olefins.

OSDA free synthesis of CHA zeolite have been reported by the conversion of FAU zeolite [41-43] or using seed assisted hydrothermal synthesis [44]. Fabricating of CHA zeolite without using OSDA resulted in low Si/Al ration (Si/Al less than 3). The low silica zeolite decreases the activity of the CHA zeolites. However, the low silica CHA can be post-treated to reduce the alumina content. Ji et al prepared CHA zeolite by hydrothermal conversion of Y-zeolite and the post treated using steam and acid to remove the alumina from the CHA framework [41]. In their work, they steamed the as-synthesized CHA (Si/Al =2.4) at different temperature to get CHA with different Si/Al ration. The dealuminated CHA showed better activity in the MTO reaction than the parent CHA; an increase in the conversion and selectivity to olefins.

Topology of the catalysts (pore and cage size and cage opening) and acidity have strong influence on the selectivity of lower olefins. Reaction temperature also affects the the

selectivity of lower olefins and methanol conversion. In the following section, we will investigate how acidity, topology and temperature influence the conversion, lifetime of the catalysts and selectivity to light olefins.

Table 1. Different templates used for the synthesis of SSZ-13 CHA zeolites

Template Name	Type of framework	Preparation method*	Applications	Crystallization time	Crys. T(°C)	Ref.
Cupper complex (Cu2+ and tetraethylenepentamine, Cu-TEPA)	Cu-SSZ-13	A	SCR	3-6 d	140	[45, 46]
choline chloride	SSZ-13	B	SCR	5	140	[47]
Conversion of FAU zeolite	CHA	C	ETO	7-21 d	125	[48]
OSDA Free +Seed	CHA	D	MTO	1-3	170	[44]
(TEAOH) + FAU zeolite (CBV-720)	CHA	E	SCR	3 d	160 or140	[49]
Conversion of FAU zeolites	CHA	F	MTO	5	100	[50]
dual-template (TMAdOH) and (TMAdOH + C22-4-4Br2).	SSZ-13	G	MTO	4-6 d	150	[51]
TMADA iodide	SSZ-13	H	-	6 d	140	[52]
OSDA Free using fluoride route	CHA	I	-	3-7	160-180	[53]
Seed +benzyl trimethylammonium	SSZ-13	J	-	2,4	160	[54]
Cu-TEPA	SSZ-13	K	SCR	4	140	[55]

*: See the appendix for the preparation detail.

2.4.1 Effect of reaction temperature on MTO catalyst activity

The effect of temperature on the conversion and selectivity to lower olefins is summarized in **Table 2**. The effect of reaction temperature is linked to the type of framework. Frameworks with larger pores and cages size such as ZSM-5 shows higher stability at higher temperatures, while small pores zeolites deactivate quickly as the reaction temperature increases.

Table 2. Selectivity to light olefins and conversion of methanol at different temperatures over different type of catalysts

catalysts	Rxn. Temperature (°C)	Pressure (atm)	Time on Stream (minutes)	WHSV (h^{-})	Conversion (%)	Selectivity to olefins	Selectivity to propylene	Selectivity to ethylene	Ref.
CHA	400	1	0-200		100	-	-	-	[44]
CHA	350	1	30	0.93	100	-	34-36	18-31.9	[33]
CHA, SSZ-13	350	-	60	0.8	100	91.3	44.9	46.4	[37]
SAPO-34	300	1	20, 30, 50	6	50, 8, 0	-	-	-	[45]
H-SSZ-13					100, 10, 8				
SAPO-34	325	1	10, 30,70	6	90,40, 0	-	-	-	
H-SSZ-13					100, 85,20				
SAPO-34	350	1	30, 45,90	6	97, 92, 5	-	-	-	
H-SSZ-13					100, 100, 90				
SAPO-34	375	1	30, 60, 150	6	100.100,65	-	-	-	
H-SSZ-13					100, 100, 40				
SAPO-34	400	1	60, 120, 180	6	100, 98, 75	-	-	-	
H-SSZ-13					100, 50, 22				
SAPO-34	425	1	60, 90, 150	6	100, 92, 19	-	-	-	
H-CHA (2.4)	325	1	30, 90, 150	0.5	85,90, 30	79.7, 76, 73.2	38.8,45.2,46.6	40.9,30.8,27.1	[41]
H-CHA (14)	325	1	30, 90, 210	0.5	100,100,35	72.5, 84.2, 77.6	39.4, 40.6, 49.7	33.1, 43.6, 27.9	
H-CAH (24)	325	1	30, 90, 210	0.5	100,100,94	48.4, 53.8, 77.3	29.9, 31.1, 46.4	18.5, 22.7, 30.9	
H-CHA (38)	325	1	30, 90, 270	0.5	100,100,94	78.8, 78.8, 84.2	41.3, 42.5, 44.2	37.5, 36.3, 40.0	
H-CHA (67)	325	1	30, 90, 270	0.5	100,100,100	74.4, 81.8, 87.7	39.1, 42.8, 48.8	35.3, 39.0, 38.9	
H-CHA (2.4)	275	1	30	0.5	2	-			[41]
H-CHA (14)	275	1	30,60, 120	0.5	100,100, 75				
H-CAH (24)	275	1	30, 90,180	0.5	95, 95, 50				
H-CHA (38)	275	1	30, 90, 150	0.5	88, 90, 78				
H-CHA (67)	275	1	30, 90, 150	0.5	75, 91, 78				

2.4.2 Effect of topology on MTO reaction

In general, the reactions that use heterogeneous catalysts are affected by the surface area, pore entrance size, acidity, and particle size. For example zeolites such as LTA, ERI, UFI and CHA with 8 member-ring pore entrance show excellent selectivity toward light olefins in the MTO reaction. The small pore entrance in zeolites prevents the transfer of larger molecules (ex. Branched aliphatic and aromatic hydrocarbons) and thus increases the olefins selectivity. However, these types of zeolites framework differ in activity as a result of the difference in their cage size. Large molecules such as poly-methyl benzene are formed inside the cages and work as active intermediates in the formation of the light olefins. But the extra condensation of these intermediate to cyclic hydrocarbons cause catalyst deactivation as a results of the blockage of acid sites, reduction the active intermediates and limiting the diffusion of the products by the cyclic hydrocarbons.

Figure 16 shows the cage size of different zeolites framework while **Figure 17** shows the products distribution of different zeolites framework at the same reaction conditions. It is very obvious from the two figures that the deactivation is related to the cage size, for example CHA which has the smallest cage size showed lower products distribution because the small cage hinder the further condensation of poly methylbenzene.[40, 56]

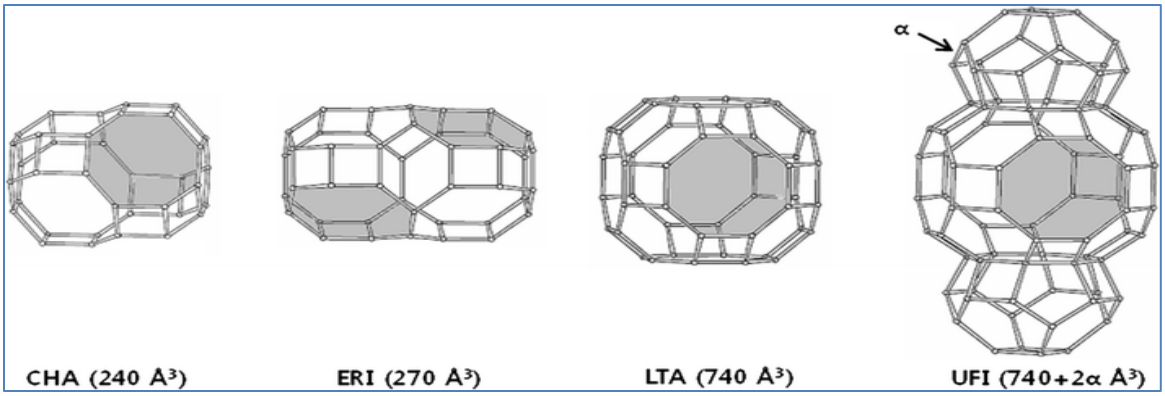

Figure 16. Shape and size of different catalyst topology used in the MTO conversion [46]

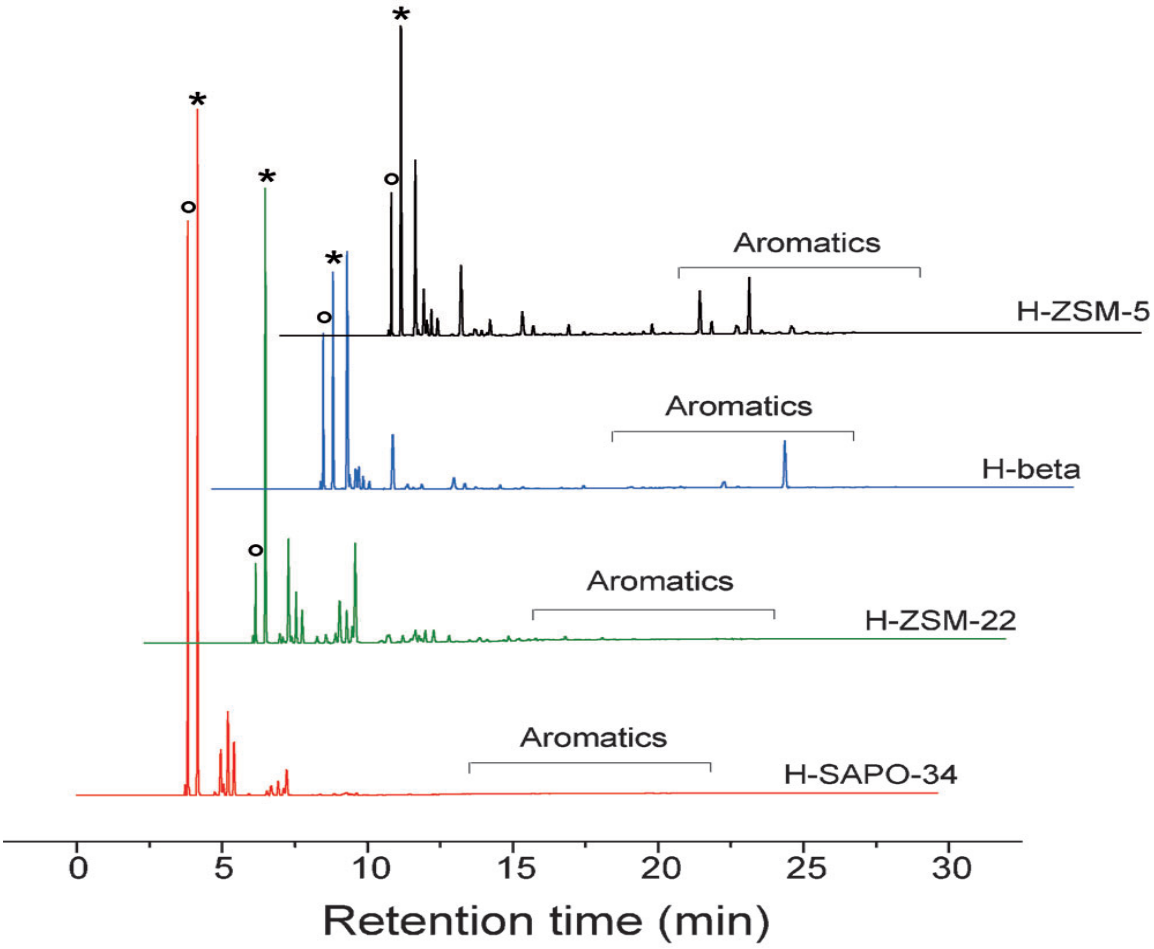

Figure 17. Chromatograms explaining the effect of different topologies on the products distribution; reaction was done under same conditions (T= 400 °C , WHSV = 2 h^{-1} [57].

2.4.3 Effect of acidity on MTO reaction

Acidity of catalysts plays a very important rule in the selectivity of products and conversion of reactants in many reactions. Zeolites which are acidic catalysts possess different densities and strength of acid sites. Some frameworks of different zeolites or even the same type of zeolite has varying amount acid sites strength and density. However, for certain reactions, acidity is needed to be reduced. This can be achieved by leaching the alumina from zeolites' framework or by the attachment of metals. Removing the alumina can be by done by steam treatment at elevated temperature (for example 500-700 °C) or by treatment the samples in acidic medium.

Attachment of metals

The selectivity towards light olefins was increased when iron and phosphorous have been impregnated over ZSM-5. The presence of phosphorous and iron on ZSM-5 decreased the acidity and thus ceased the olefins conversion to paraffin and aromatics. However, the selectivity to olefins over SAPOO-34 is relatively high due to its 8 MR pore entrance and the cage size which works to maintain active intermediates that are responsible for light olefins production. Even though, SAPO-34 showing higher selectivity to olefins, it suffers from the deactivation as a result of nonreactive intermediate formation.[40]

Acid strength:

Acid strength and density have a great effect on methanol conversion, stability of the catalyst and selectivity to light olefins. Blenken et al. [58] studied the effect of acid strength on the stability and selectivity toward olefins by using two different catalysts with the same topology; SSZ-13 and SAPO-34. The two catalysts were evaluated at different range of temperature (300 - 425°C) to investigate the influence of temperature

on the catalysts lifetime. The temperature found to have an influence on the conversion of methanol for both type of catalysts. The optimum temperature for SAPO-34 was found to be 400 °C, while H-SSZ-13 was between 300 and 350 °C. At lower temperature, SSZ-13 was more stable than SAPO-34, while at higher temperature, SAPO-34 was more stable. This could be because of the strong acidity of the H-SSZ-13 catalyst.

The selectivity of the two catalysts, SSZ-13 and SAPO-34, to propylene and ethylene is shown in **Figure 18**. The SSZ-13 catalyst with strong acidity had higher ratio of ethane to propylene ($C^{=}_2/C^{=}_3$). At a temperature of 375 and 400 °C with a 100% conversion both catalyst, had almost the same selectivity. However, when the conversion was slightly decreased, SSZ-13 showed higher selectivity to ethylene. This increase in selectivity of SSZ-13 to ethylene was explained by the diffusion limitation induced by the coke formation which was larger in the case of SSZ-13 catalyst. Ethylene molecules is smaller than propylene, thus it is easier for ethylene to diffuse than propylene when coke is formed. [58]

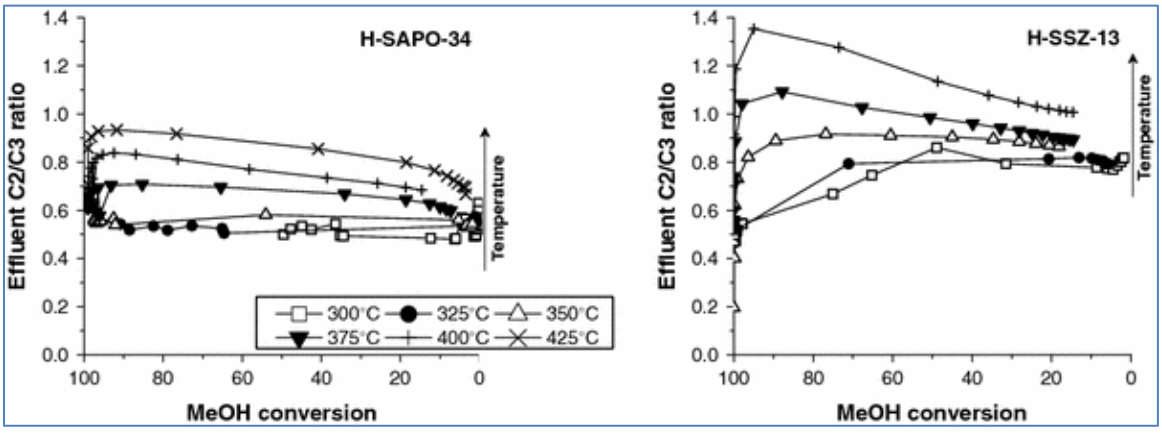

Figure 18. Effect of acid strength on selectivity of light olefins; H-SSZ-13 is more acidic than H-SAPO-34 [45]

Q. Zhu et al. [50] prepared CHA zeolite using two different methods with different strength of acidity. CHA with low acid site (Si/Al =2.4) was prepared by the conversion of FAU zeolite and CHA with stronger acid sites (Si/Al = 14, 24, 38 and 67) were prepared by using organic structure directing agent (OSDA). As it shown in **Figure 19**, strong and weak acid are related to the Al content in the zeolites framework. CHA with low Si/Al ratio (2.4) exhibited weak acidity, while CHA with higher Si/Al ratio had strong acid

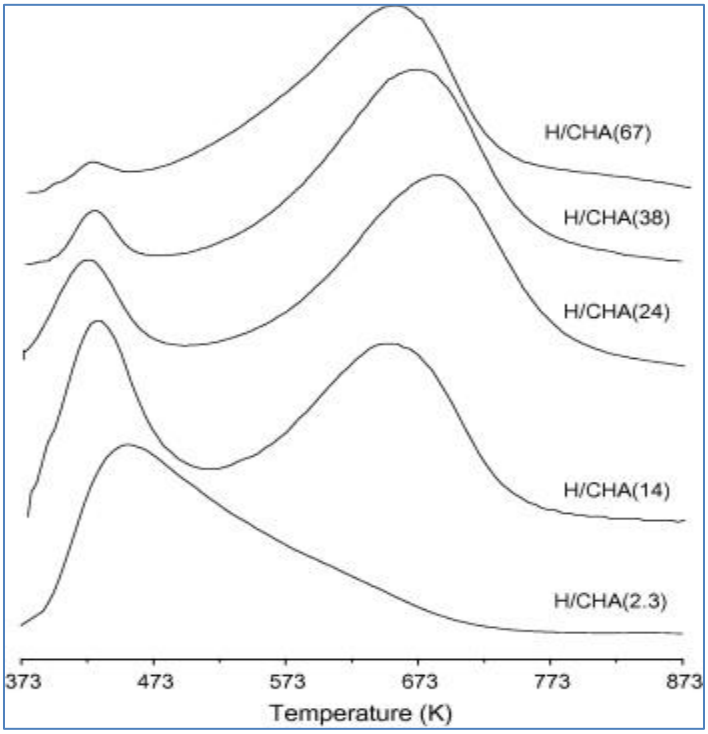

Figure 19. NH3 TPD profile of CHA zeolites synthesized by two different methods at different Si/Al ratio[41]

Table 3. Surface area, pore volume and acidity of catalysts from literature

Catalyst	Surface area (m2/g)			pore volume (cm3/g)			Acidity (m mole/g)		Si/Al	Particle size (µm)	Ref.
	$S_{micro.}$	$S_{ext.}$	S_{total}	V_{micro}	V_{meso}	V_{total}	Weak	Strong			
Sapo-34	572	18	590	0.29	0.08	0.37	0.4509	0.6420	-		[59]
FeAPSO-34	401	9	410	0.16	0.02	0.18	0.2982	0.3672	-		
CoAPSO-34	495	11	506	0.21	0.04	0.25	0.2307	0.2655	-		
NiAPSO-34	407	9	416	0.12	0.02	0.14	0.2925	0.3908	-		
LaAPSO-34	458	16	416	0.19	0.06	0.25	0.1641	0.2136	-		
CeAPSO-34	470	16	486	0.22	0.06	0.28	0.1594	0.1945	-		
CHA,K^+ form	25	20	45	0.023	0.0157	0.0387	-	-	-		[53]
CHA, Ca^+ Exchanged	513	24	537	0.2182	0.0110	0.2292	-	-			
CHA, Seeded, Ca^+ Exchanged	500	69	569	0.2972	0.1123	0.4095	-	-			
H-CHA (Conversion of FAU)			442			0.189			2.5	0.2	[50]
H-CHA (Through OSDA)			1104			0.326			14	2	
H-CHA (Through OSDA)			1086			0.311	Acidity can by read from figure 19		24	2	
H-CHA (Through OSDA)			1136			0.340			38	2	
H-CHA (Through OSDA)			908			0.332			67	1	

2.5 Reaction Mechanism of MTO process

The mechanism of the conversion of methanol to olefins is very complicated. It has been mentioned earlier that MTO was discovered by chance during the enhancement of the MTG process. Thus, to understand the reaction mechanism of olefins formation from methanol, it is preferable to study the reaction mechanism of methanol conversion to hydrocarbons (MTH) in general. After the discovery of MTH process, the formation of the first C-C bond and the reaction mechanism under which methanol is converted to hydrocarbons are the two points that are not well understood [60]. However, the general apparent reaction mechanism of the MTH process is consisting of three main steps [17, 61]:

- Dehydration of methanol to DME.
- Converting the methanol-DME- H_2O equilibrium to olefins (Formation of first C-C bond).
- Conversion of olefins to other hydrocarbons such as naphthenes, higher olefins, paraffins, and aromatics.

2.5.1 Dehydration of methanol to DME

Methanol is easily dehydrated into DME over acidic zeolites. As shown in **Figure 20**, methanol is firstly adsorbed (irreversibly) to the hydrogen on the hydroxyl bridge of a catalyst to form methoxonium ion which is a protonated form of the methanol [61]. The formation of methoxonium ion process is very fast and has no energy barrier; a proof of this has been reported somewhere else [62] using the density functional theory calculation. Then, the protonated methanol is dehydrated to form surface methoxy species ($CH3^{+}$) which reacts with methanol to form protonated DME (dimethyloxonium ion). Finally, the dimethyloxonium ion is deprotonated to form DME.

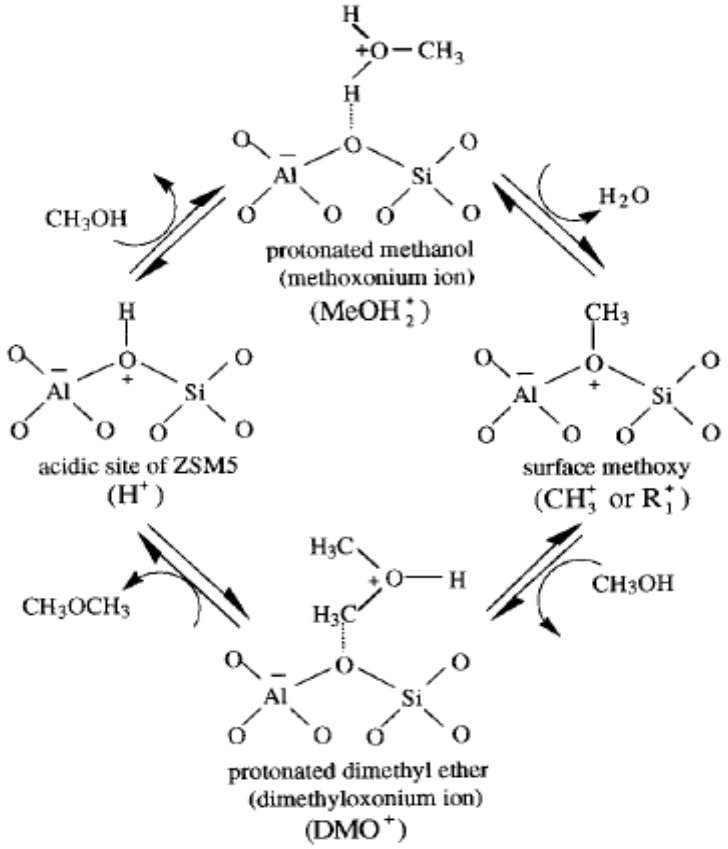

Figure 20. Reaction mechanism of the dehydration of methanol to DME over zeolite catalyst [50]

2.5.2 Formation of the first C-C bond

The formation of the first C-C bond is the limiting step in the MTO mechanism [17]. All reaction mechanisms that have been proposed for the formation of the firs C-C bond can be classified into three main methods; the direct coupling of the first carbon (methanol or DME), indirect coupling of the first carbon and the autocatalytic reaction [16]. Herein, we will discuss each method.

There are more than 20 mechanisms explaining the direct coupling of the first C-C bond [16], but carbocations, oxoniums ylides, carbenes and free radicals mechanisms are the most popular mechanisms in literature. Thus, we will briefly explore how each mechanism works.

The carbine mechanism:

The mechanism involves the formation of carbenes by the elimination of water from methanol in the presence of acidic sites as explained in Eq. 3.

$$H - CH_2 - OH \rightarrow : CH_2 + H_2O \qquad \textbf{Eq. 3}$$

Now, how can the generated carbene form the first C-C bond? At the beginning, it has been stated that after the carbene formation, carbenes undergo polymerization to form alkenes. But later on, it was figured out that the carbenes attack the C-O bond of either DME or methanol to form the first carbon-carbon bond [17].

Oxonium ylide mechanism

In this mechanism, trimethyloxonium ion is formed from the methylation of DME over Brønsted acid sites. Then the base sites deprotonate the trimethyloxonium ion to form dimethyloxonium methylide which goes through what is called Stevens rearrangement producing methylethr which can be converted to ethylene.

Free radical

The direct pairing of first carbon fails due to a number of reasons. The most important reason is that it has been found that the paring rate of the adsorbed methanol in catalyst pores was incomparable to the hydrocarbons formation [63]. Furthermore, the activation energy for the direct coupling was relatively high, around 200 Kj/mol. Moreover, Songe et al.[64] used a very pure reactants, carrier gas and catalyst from any type of C-C bond. They found that the initial methanol conversion was very small. This emphasize that the direct coupling of the first C-C bond is unlikely especially in what is called “induction period”, the induction period is the period in which conversion of methanol increases with TOS.

Ethylene is formed by through the aromatics intermediate while propylene is formed through olefins methylation and cracking reactions [65]. Thus this supports the dual cycle mechanism; the methylation responsible for propylene formation and the aromatic cycle responsible for the formation of aromatics, ethylene and catalyst deactivation. The acidity of the catalyst plays an important role in suppression of the aromatic cycle and promotion of alkene cycle [66].

The autocatalytic concept in the MTH process reaction mechanism was the stepping stone toward the indirect coupling of the first C-C bond formation. Autocatalysis means that the presence of small amount of products gives rise to rate of conversion improvement. The indirect reaction bonding mechanism was firstly proposed by Dessau and co-worker [67, 68]. In their mechanism, they proposed as there are at least some ethylene molecules or other higher olefins that are produced during the induction period, cracking and consecutive methylation take place to produce olefins [67]. Another work by Mole et. al. [69] in which they co-feeded aromatics which caused an enhancement in the methanol conversion. However, Dahl and Kolboe [70] concluded that addition of propylene and ethylene to the feed over SAPO-34 catalyst did not have strong effect on the methanol conversion, and most of the produced light olefins were from the methanol conversion rather than the feeded olefins. This poor performance of alkenes over SAPO-34 led to what is called "Hydrocarbon-pool".

Hydrocarbone pool Mechanism

The organic species (such as polymethylbenzene), which are trapped in the zeolites' framework, are known as the so called "Hydrocarbon pool". The hydrocarbon pool species work as reaction centers. These centers are repeatedly methylated by methanol followed by splitting of alkenes such as ethylene or propylene. The reaction centers differed with the type of zeolite structure, for example penta and hexamytheylbenzene are more active than lower methylbenzene in SAPO-34 and BET zeolites. In contracts to SAPO-34 and BET zeolites, lower methylbenzene found to be more active in ZSM-5 due to the narrow channels. When the aromatic base cycle and alkene base cycle work simultaneously, it called the dual cycle concept.[57]

CHAPTER 3

OSDA-free chabazite (CHA) zeolite synthesized from amorphous aluminosilicate gel in the presence of fluoride for selective methanol-to-olefins

Abstract

A series of cost-effective aluminum-rich chabazite (Al-rich CHA) zeolite with improved textural properties has been synthesized without using templates. Herein, we report a detail synthesis method for CHA zeolite without using an organic structure directing agent (OSDA-free). Pure CHA zeolites were successfully synthesized under different gel compositions. The prepared CHA samples were characterized using different characterization techniques. The crystallinity, the textural properties, the morphology and the acidity were characterized using X-ray diffraction (XRD), nitrogen physisorption, field-emission scanning electron microscopy (SEM) and ammonium temperature programing desorption (NH_3-TPD), accordingly. The BET results showed that ion-exchange enhanced the surface area from around 1 m^2/g to around 485 m^2/g. Aging time had a significant influences on the crystallization rate, particles' size and shape. The synthesized CHA zeolite was evaluated in the methanol-to-olefin (MTO) reaction at different reaction temperatures. The Conversion was maintained at 100% for 4 h at 350 °C and for 2 h at 400 and 450 °C. The selectivity to lower olefins was correlated to the reaction temperature and time on stream (TOS). The highest olefins selectivity was ca. 93.8 at 180 min TOS and reaction temperature of 350 °C.

3.1 Introduction

Zeolites are microporous crystalline solid acidic materials with channels and cavities size ranging from 0.3 to 1.5 nm [33]. Zeolites are crucial materials and due to their distinct properties have wide a range of applications in industry as adsorbents, catalysts and detergents [19, 33]. There are more than 232 zeolites frameworks recorded in the International Zeolite Association (IZA). The structure of the zeolites' framework is generally consisting of several building units. The primary building unit of zeolites is the tetrahedra of AlO_4, SiO_4 (aluminosilicate zeolites) and PO_4 in the case of silicoaluminophosphate zeolites [22]. More complex building units of zeolites are formed by the combination of the primary building units. The 4-corner sharing of the tetrahedra results in a microporous and low framework density. The framework density is defined as the number of T atoms per 1000 Å [20, 22, 23]. For understanding the structure of zeolites, it can be viewed as composite of rings which are formed by a number of tetrahedra. The name of the ring is given based on the number of tetrahedral it contains. For example, the 4-ring (4R) is consisting of 4 tetrahedra. Other tetrahedral n-rings are do exist, where n can be 4, 6, 6, 10 or 12 tetrahedra [34].

Chabazite zeolite, which exists in nature or can be synthesized in lab, owing a three dimensional network of interconnected pores with a framework density and pore dimension of 14.5 T/1000$Å^3$ and 3.8 x 3.8 Å (IZA), respectively. The CHA framework has been applied in different areas. CHA can be used in adsorption, ion-exchange application [71-73] and in catalysis in the conversion of methanol to olefins or in the NH_3 selective catalytic reduction (SCR) of NO_x [45, 55, 74, 75]. CHA zeolite can be classified based on the Si/Al ratio into CHA with high Si/Al ratio (>3, it can be as high as 7.5 [76])

and CHA with low Si/Al ratio (<3). The high Si/Al ratio is represented by SSZ-13 zeolite which has been firstly prepared by Zones in 1985 using N,N,N-trimethyl-1-adamantammonium (TMAda+) iodide as a template [52]. Other templates and a combination of templates and seed have been reported in the synthesis of SSZ-13 for the purpose of cost reduction [45-47, 51, 54]. Although, the CHA in which its synthesis method involves the use of templates shows excellent activity in the MTO reaction, the unusual price of templates hindered the use of CHA as a catalyst in the industry. Thus, a less expensive method for CHA synthesis is highly required.

Researchers paid a lot of efforts to make the synthesis method of CHA zeolite cheaper and thus appealing to the industry. These have been achieved by: (i) combining less expensive templates with the TMAda iodide [51], (ii) using less expensive template and seed [54], (iii) conversion of FAU zeolite with the presence of templates [49], (iv) template free conversion of FAU zeolites [41-43, 48], (v) OSDA free using seed [44] and (vi) OSDA free using fluoride route [53]. Fabricating CHA zeolite without using OSDA resulted in low Si/Al ration. The low silica zeolite decreases the activity of the CHA zeolites. However, the low silica CHA can be post-treated to reduce the alumina content. Ji et al prepared CHA zeolite by hydrothermal conversion of Y-zeolite and then post-treated using steam and acid to remove the alumina from the CHA framework [41]. In their work, they steamed the as-synthesized CHA (Si/Al =2.4) at different temperatures to get CHA with different Si/Al ration. The dealuminated CHA showed better activity in the MTO reaction than the parent CHA.

In this work, we reported detail synthesis of cost-effective pure CHA zeolites without using any type of templates. After that, we characterized the prepared and modified

zeolites using different characterization techniques, and finally we tested the synthesized zeolite in MTO reaction.

3.2 Experimental

3.2.1 Materials and Chemicals

Colloidal silica TM-40colloidal silica, 40wt.%, suspended in water (Aldrich), De-ionized water (produced in our labs labs.), ammonium fluoride, aluminum hydroxide PRS (Panreac), ammonium nitrate >= 98% (Sigma-Aldrich), potassium hydroxide 85% pellets (Panreac) and sodium hydroxide 85% pellets (Panreac).

3.2.2 Synthesis of CHA zeolites

Pure chabazite (CHA) zeolite has been prepared hydrothermally without using any organic structure directing agent (OSDA). Our preparation method was adapted from a procedure reported elsewhere [53], but with a modified gel and wide investigations of different synthesis parameters. Aluminum hydroxide was added to an aqueous solution of potassium hydroxide under heating. Subsequently, after cooling to room temperature, ammonium fluoride and colloidal silica were added and stirred for different aging times. The final gel was hydrothermally treated in a PTFE-lined stainless steel autoclave. Thereafter, the product was separated, washed with deionized water, dried and ion-exchanged.

For preparing 40 g of the final gel, 4.21 g of potassium hydroxide was added to 17.23 g of deionized water and placed in an oil-bath at 80 °C. To the aqueous solution of potassium hydroxide, a 3 g of aluminum hydroxide was added and stirred for 30 min under heating. After cooling to room temperature, 1.07 and 14.44 g of ammonium

fluoride and colloidal silica were added, respectively. The final gel (also named as *gel# 1*) with a molar composition of 1 SiO_2: 0.2 Al_2O_3: 0.39 K_2O: 0.3 NH_4F: 15 H_2O was aged for x hours at room temperature, x= 6, 12, 24 and 48. Following this, the final gel was crystallized in a convection oven at 160 °C for y hours, y= 48, 72, 96 and 120. Finally the product was separated and washed with deionized water until a neural pH around 7 was obtained. The same procedure was followed, when we prepared CHA using gel # 2, 3, 4 and 5, see **Table 4** for gels composition. For the incorporation of metals (Ni, Fe, Zn, Mg and Fe), the same procedure was followed using gel # 1 at different aging and crystallization times. The required amount (**Table 5**) of the corresponding metal was added at a stage prior to the addition of ammonium fluoride.

The as synthesized samples, which were in potassium form (K-CHA), were ion-exchanged using ammonium nitrate (NH_4NO_3) as a source of proton. For each gram of the sample, we used 50 mL of 2 M of NH_4NO_3 and treated under reflux (80 °C) for *3 h.* The ion-exchanged was repeated one more time with fresh solution of ammonium nitrate.

3.2.3 Methanol-to-olefins

The synthesized and modified catalysts with different metals were evaluated for MTO reaction using a fixed bed reactor. The reaction was conducted at 350, 400 and 450 °C using 50 mg of the prepared catalyst with a Weight Hourly Space Velocity (WHSV) of 0.95 h^{-1}. Prior to the reaction analysis, the catalysts were calcined at 500 °C for 1 h under the flow of He. The reaction products were analyzed using an on-line Shimadzu GC-2014 chromatograph equipped with a flame ionization detector and a capillary column HP-PLOT (30 m × 0.53 mm, 6 μm film thickness).

3.2.4 Characterization techniques

The catalyst structure was investigated using ^{27}Al, and ^{29}Si Nuclear Magnetic Resonance (NMR) spectroscopy and X-ray diffraction (XRD). The XRD patterns were recorded using Rigaku Miniflex diffractometer equipped with Cu Kα radiation (λ = 0.15406 nm) at 2θ angle ranging from 5 to 50° with a scan speed of 3° per minute and a step size of 0.02.

Ammonia temperature programmed desorption (NH_3–TPD) was conducted to investigate the acidity of the zeolites. The NH_3–TPD analysis was performed on a Chemisorb 2750 Micrometrics chemisorption analyzer over 100 mg of the prepared zeolites. The sample was preheated at 600°C (heating rate 30 °Cmin^{-1}) under the flow of He (25 ml. min^{-1}) for 30 min After allowing the sample to cool to 100 °C, NH_3 was allowed to flow over the ample with a flow rate of 25 mL. min^{-1} for 30 min. Subsequently, He flow was reconnected for 1 h to remove the weakly adsorb NH_3. Finally, the temperature was ramped to 800 ^oC at a ramping rate of 10 °C min^{-1} and the amount desorbed of ammonia was recorded using the TCD detector on a 0.5 s basis.

The elemental compositions of the samples were measured using X-ray fluorescence (XRF), while the morphology of the samples were investigated using field-emission scanning electron microscope (FE-SEM) and energy dispersive X-ray (EDX).

The surface area, pore volume and pore size distribution were measured using the physisorption of Nitrogen in ASAP 2020 (Micromeritics). Prior to analysis, the samples were heated up to 350 °C and dwelled for 6 hours. The sample temperature during the analysis was maintained at -196 °C. The t-plot was used to measure the volume of

micropores, surface area, and the external surface area, while the pore size distribution was estimated using Horvath–Kawazoe model method.

Table 4. Different molar compositions used in the synthesis of CHA zeolite.

Gel #	Molar composition
1	$1SiO_2 : 0.2Al_2O_3 : 0.39K_2O : 0.3NH_4F : xH_2O$
2	$1SiO_2 : 0.2Al_2O_3 : 0.39K_2O : yNH_4F : 15H_2O$
3	$1SiO_2 : zAl_2O_3 : 0.39K_2O : 0.3NH_4F : 15H_2O$
4	$1SiO_2 : 0.2Al_2O_3 : w\ K_2O : 0.3NH_4F : 15H_2O$
5	$1SiO_2 : 0.2Al_2O_3 : wK_2O : 0.04Na_2O : 0.3NH_4F : 15H_2O$

Table 5. Experimental conditions for MeCHA zeolites

Run#	Me/SiO2 (mole ratio)	Me	Aging Time (h)	Crystallization time (d)	Phase	Relative crystallinity*
MeCHA1	0.05	B	24	3	CHA(Am.)	37 (49)
MeCHA 2	0.05	B	24	4	CHA	67 (89)
MeCHA 3	0.05	B	48	3	CHA	100 (132)
MeCHA 4	0.1	B	24	4	Am.(CHA)	22 (29)
MeCHA 5	0.1	B	24	6	CHA	42 (55)
MeCHA 6	0.1	B	48	5	CHA	71 (94)
MeCHA 8	0.02	Ni	24	2	CHA(Am.)	57 (63)
MeCHA 9	0.02	Ni	24	3	CHA	98 (107)
MeCHA 10	0.02	Ni	48	3	CHA	100 (109)
MeCHA 11	0.02	Mg	24	3	CHA(Am.)	65 (49
MeCHA 12	0.02	Mg	48	3	CHA	56 (42)
MeCHA 13	0.02	Mg	24	4	CHA*	100 (75)
MeCHA 14	0.02	Zn	24	3	Am.	-
MeCHA 15	0.02	Zn	48	3	Am.	-
MeCHA 16	0.02	Zn	24	6	CHA	34
MeCHA 17	0.02	Fe	24	4	CHA(Am.)	57 (55)
MeCHA 18	0.02	Fe	24	5	CHA	70 (68)
MeCHA 19	0.02	Fe	48	3	CHA	100 (96)

*: the crystallinity outside the bracket is with relative to highest crystalline MeCHA, while the one inside the bracket is relative to CHA free of metals.

3.3 Results and discussion

3.3.1 Effect of H_2O/SiO_2 ratio on CHA formation

Table 4 shows different formula of the silicoaluminate gel used in this study. The first batch prepared was Run# 1, which had the same gel composition as reported in the literature [53]. However, the published procedure was not reproducible and we were unable to synthesize pure CHA from this batch even at long crystallization times, (up to 5 days). Nevertheless, by altering the water content of the first batch and fixing the crystallization time to 5 days as shown in **Table 6** (Run# 5) pure CHA zeolite was successfully formed with H_2O/SiO_2 molar ratio of 15. **Figure 21** shows the XRD patterns of the CHA zeolite prepared at x= 15 and the reference CHA. It is obvious that the XRD patterns of the prepared CHA at x = 15 are in well agreement with the reference one; all characteristic peaks and even small peaks are matching with the reference. A further decrease in H_2O/SiO_2 ratio to 10 resulted in CHA phase but with Merlinoite (MER) phase as an impurity. The XRD patterns of the CHA zeolite synthesized at different water contents are shown in **Figure 22**. From the XRD patterns, the increase in H_2O/SiO_2 ratio from 15 up to 35, did not favor the formation of CHA zeolite and amorphous phases were dominating.

Table 6. Water content and crystallization time under which CHA zeolite was formed.

#	Gel #	x	T (°C)	Si/Al[a]	Aging time (h)	Crystallization time(h)	Phase
1	1	35	160	2.5	6	120	Am.
2	1	28.5	160	2.5	6	120	Am.
3	1	25	160	2.5	6	120	Am.
4	1	20	160	2.5	6	120	Am. (Oth.)
5	1	15	160	2.5	6	120	CHA
6	1	10	160	2.5	6	120	CHA*
7	1	15	160	2.5	6	108	CHA
8	1	15	160	2.5	6	96	CHA (am.)
9	1	15	160	2.5	6	72	Am. (CHA)
10	1	15	160	2.5	6	48	Am.

a: gel Si/Al ratio

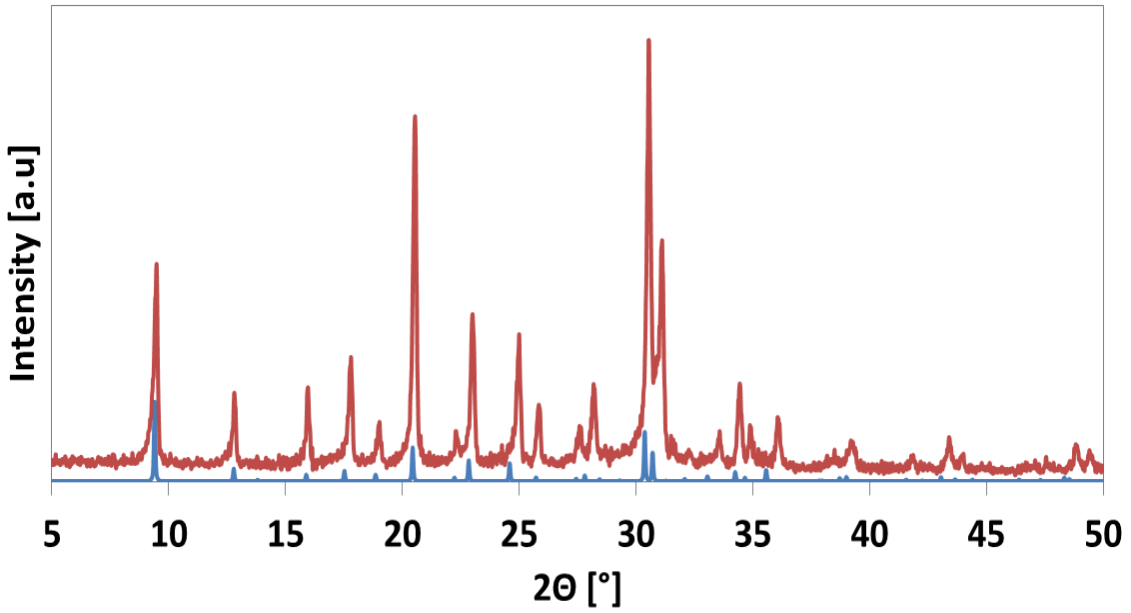

Figure 21. XRD patterns of the as-synthesized CHA (Run# 5) compared to the reference CHA zeolite

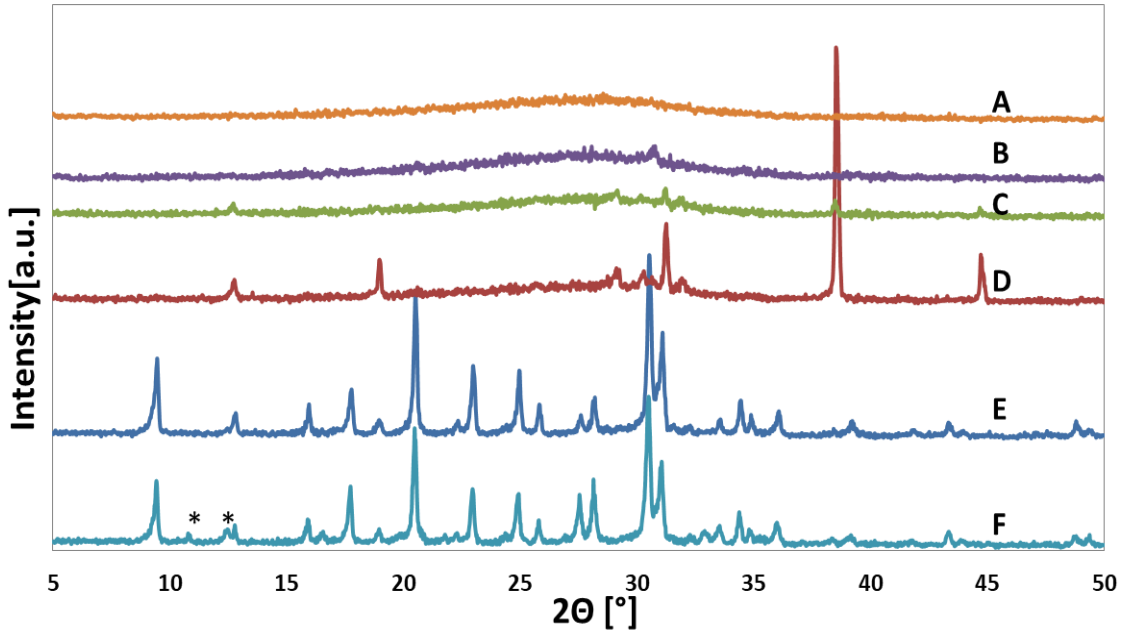

Figure 22. . XRD patterns of samples prepared from Gel # 1 at different H_2O/SiO_2 ratios; (A) $H2O/SiO_2$ = 35, (B) H_2O/SiO_2 = 28, (C) H_2O/SiO_2 = 25, (D) H_2O/SiO_2 = 20, (E) H_2O/SiO_2 = 15, (F) H_2O/SiO_2 = 10.

Peaks with * symbol represents the MER phase.

Figure 23 shows the solid-state ^{27}Al magic-angle spinning (MAS) NMR spectra of the ion-exchanged samples. The typical spectrum reveals a main peak around 58 ppm attributed to tetrahedral coordination of Al species. A small peak corresponding to the octahedral coordination of Al was observed at around 0 ppm. The presence of additional structure of Al species (the octahedral) might be because of the ion-exchange [44] or by the calcination as dealumination takes place [29].

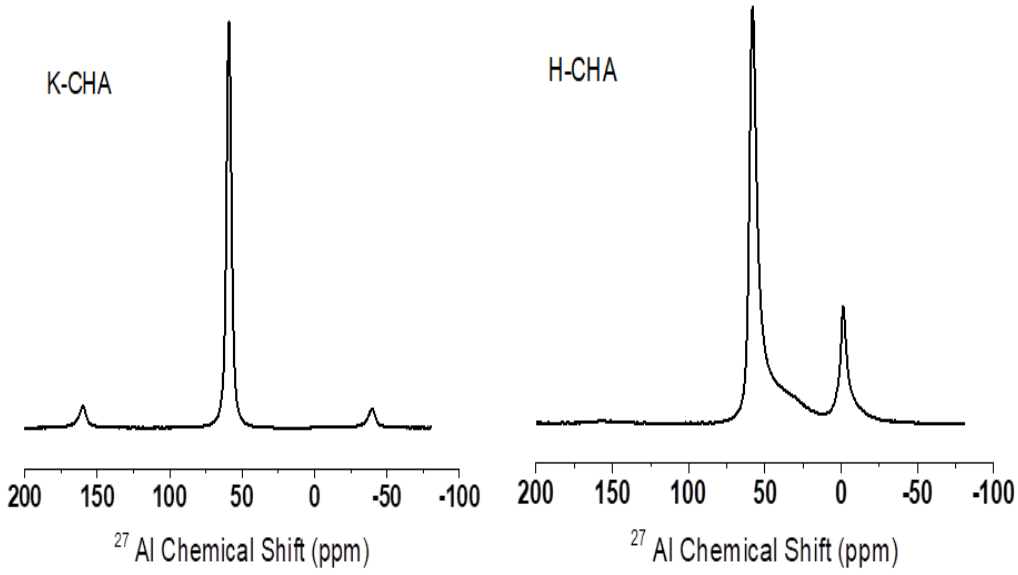

Figure 23. ^{27}Al MAS NMR spectra of the synthesized CHA before and after ion-exchange and calcination.

Table 7. Effect of aging time on the crystallization of CHA zeolite.

#	Gel #	x	T (°C)	Si/Al[a]	Aging time (h)	Crystallization time(h)	Phase
11	1	15	160	2.5	12	72	CHA(Am.)
12	1	15	160	2.5	12	96	CHA
13	1	15	160	2.5	12	120	CHA
14	1	15	160	2.5	24	60	CHA(Am.)
15	1	15	160	2.5	24	72	CHA
16	1	15	160	2.5	24	96	CHA
17	1	15	160	2.5	24	120	CHA
18	1	15	160	2.5	48	60	CHA
19	1	15	160	2.5	48	72	CHA
20	1	15	160	2.5	48	96	CHA

a: gel Si/Al ratio

3.3.2 Effect of aging time on crystallization

The effect of aging time has been investigated using Gel# 1 with x= 15. We studied the effect of aging time at 4 different periods as presented in **Table 7**. The aging time had a significant influence on the crystallization time. Samples aged for longer time, required less crystallization time. For example, the minimum crystallization time for the samples aged for 6 h was between 96 and 108 h, while for those aged for 48 h require only 60 h to get pure and highly crystalline CHA zeolite. The XRD patterns of samples aged for 6 h at different crystallized times are shown in **Figure 24**, whereas the XRD patterns of samples aged for 12, 24 and 48 h with different crystallization times are shown in **Figure A1**, **A2**, and **A3** (see the appendix). An obvious picture for understanding the formation of CHA zeolites under different aging and crystallization time is depicted in **Figure 25**. The higher the aging time was, the lower the crystallization time required. All points on the line and above it represent conditions where a pure CHA zeolite can be formed, while points below the line are a combination of CHA and amorphous phase. The effect of aging time on the crystallization rate of different type of OSDA-free zeolite has been observed elsewhere [77-80]. M. Ahmed et al. varied the aging time from 3 to 24 h at room temperature over EU-1 zeolite. They found that the crystallinity was increased with the increase of aging time from 3 to 12 h. A further increase in aging (up to 24 h) negatively affected the crystallinity and purity of EU-1 zeolite. In contrast, we found a continuous increase in the crystallization rate with the increase of aging time. This could be because of the type of silica source (colloidal silica Ludox TM 40%) used in the synthesis of CHA zeolite. The rule of various silica sources in studying the effect of aging time on the crystallization rate has been studied by Qinghua and his coworkers on

TPA-silicalite-1 [81]. They found that the colloidal silica Ludox TM required a longer aging time to have similar effect as other sources of silica.

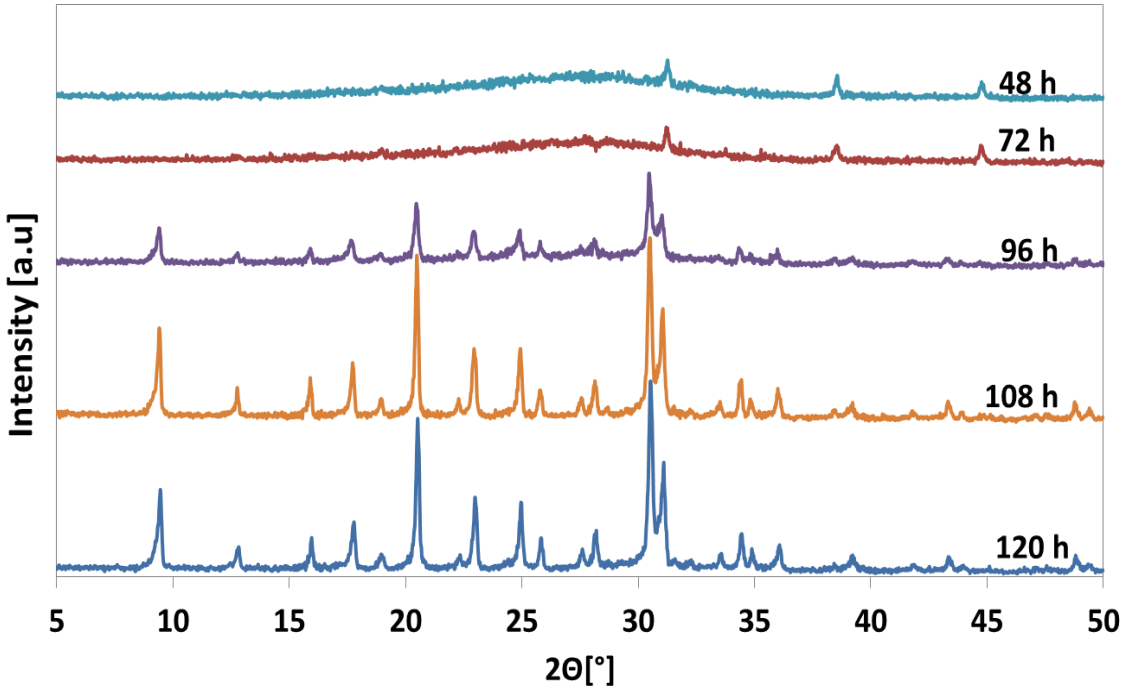

Figure 24. XRD patterns of samples prepared from Gel # 1 with x (H2O/SiO2) = 15 at 6 h of aging and different crystallization times.

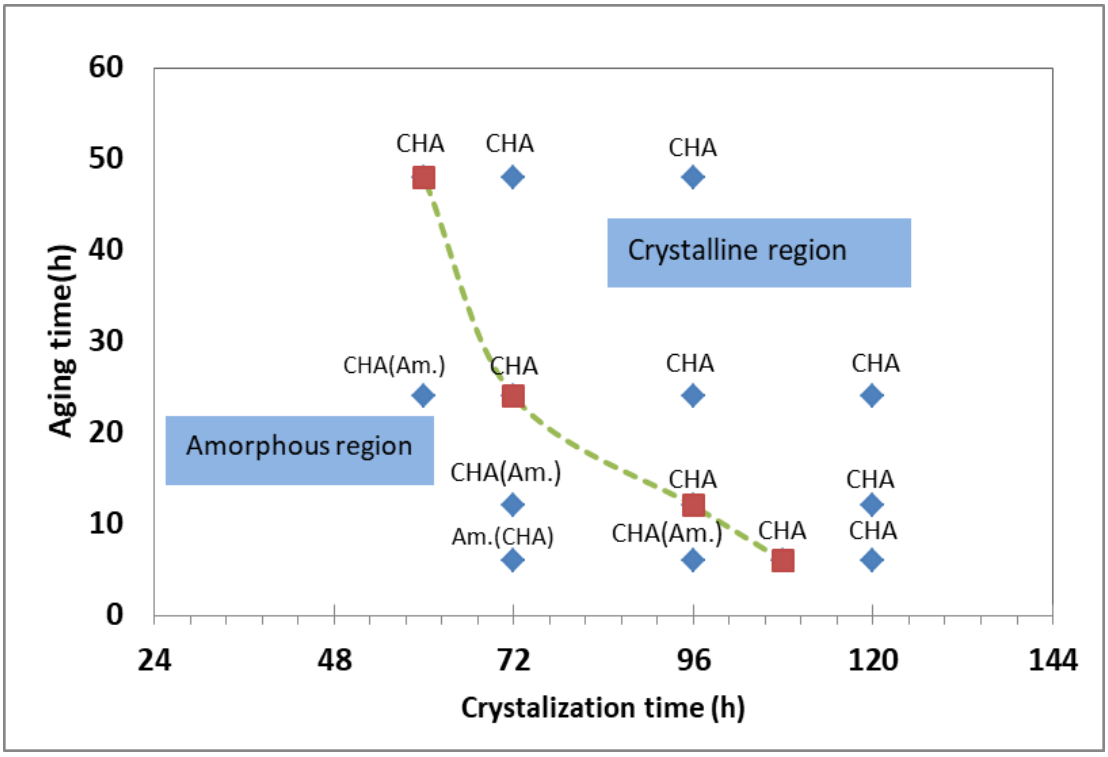

Figure 25. Formation of CHA zeolite at different aging and crystallization times.

3.3.3 Effect of aging time on morphology

Aging time did not only lower the crystallization time but it also influenced the morphology (particles' shape and size) of the prepared CHA zeolites. Samples prepared at lower aging time had different particle shape and size than samples prepared at higher aging time. Generally, the particles are small cuboids, which are agglomerated to form large particles that are similar to a swollen-disk like shape. **Figure 26** shows FE-SEM images of CHA zeolite which was aged for 6, 24 and 48 h with a corresponding minimum crystallization time. For the aging time of 6 h and crystallization time of 108 h, the swollen disk-like particles' shape seems to be interconnected to form a flower-like shape. The size of these interconnected particles ranged between 15 to 20 µm, while the small cuboids which are the components of the larger particles had a size of 1.2-2 µm. The increase in aging time affected both the swollen disk-like shape and the small

cuboids. The flower-like shape was not anymore interconnected and appeared to be more dispersed with a size ranging between 10 and 18 μm when the aging time was 24 h. Moreover, the size of the small cuboids was as small as 0.8 μm, even at 24 h aging time. A more increase in aging time up to 48 h caused a desertion to the swollen disk-like shape as they become more spread and irregular in shape. Additionally, the small cuboids size decreased to 400 nm. Alfaro et al [77] found that the particle size was decreasing with the increase of aging time of LTA zeolite. Other studies [79, 80]in the literature are in-agreement with our finding.

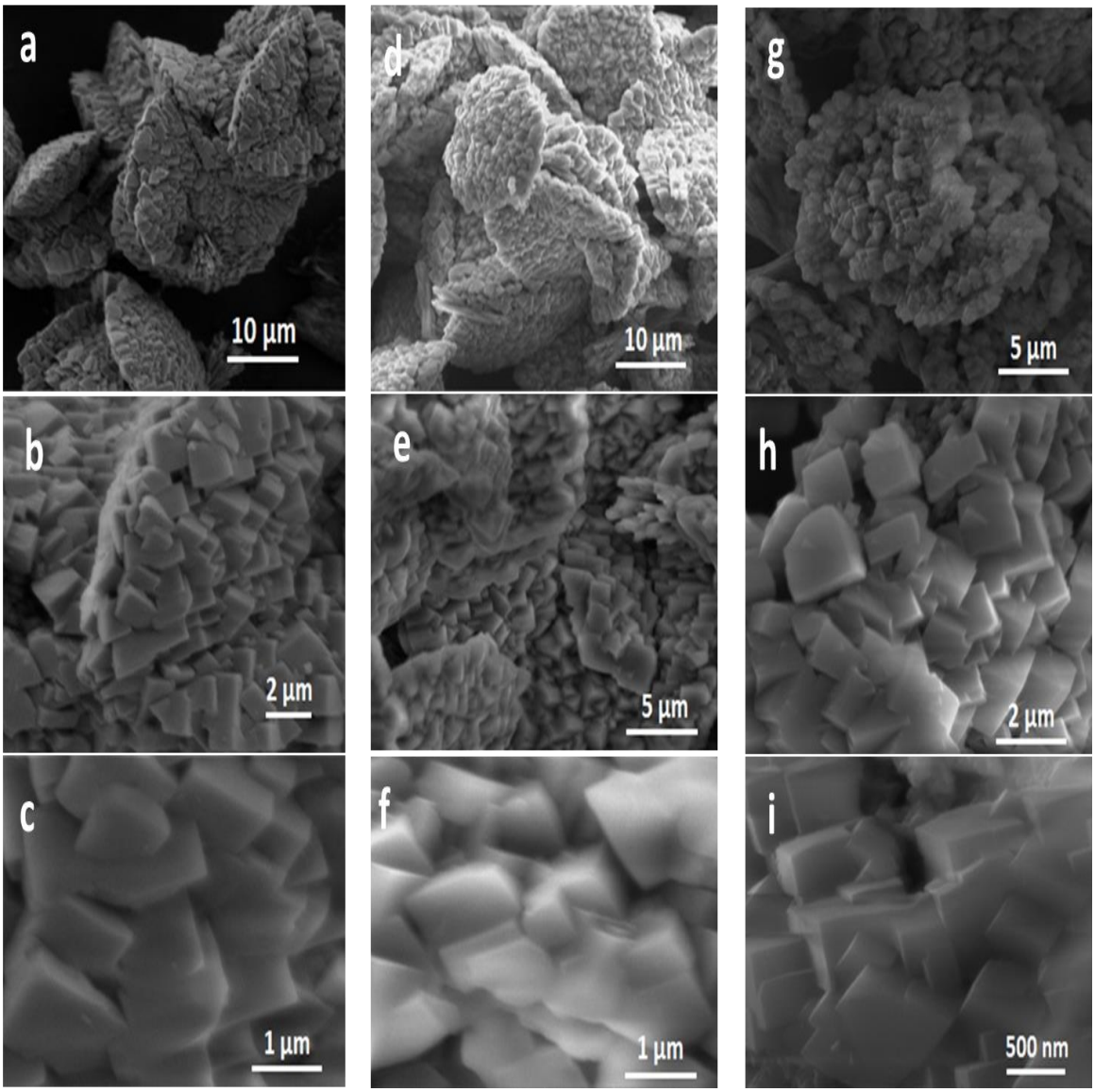

Figure 26. FE-SEM images at different magnifications of CHA zeolites prepared at aging time of 6 h (a, b and c), 24 h (d, e and f) and 48 h (g, h and i) at a minimum time of crystallization.

3.3.4 Effect of varying Al_2O- NH_4F-K_2O / SiO_2 ratios

Table 8 shows different gel compositions (Gel# 2, 3 & 4) of the precursor solution. The Si/Al ratio has been varied in the gel composition in order to have CHA zeolites with different Si/Al ratio. However, an increase in the Si/Al ratio either by decreasing the source of aluminum or by increasing the source of silica resulted in MER as a competitive phase or an amorphous phase as shown in **Figure 27**. Similarly, altering the concentration of K_2O and NH_4 did not favor the formation of CHA zeolite. The introduction of small concentration of Na_2O beside K_2O (Gel# 5, Run# 25 & 26, **Table 8**) for the purpose of varying alkaline metals suppressed the formation of CHA zeolite and favor the growth of MER phase.

Table 8. Effect of altering fluoride and aluminum content on the formation of CHA zeolite

#	Gel #	y	z	w	Si/Al[a]	T (°C)	Aging time (h)	Crystallization time(h)	Phase
21	3	-	0.1	-	5	160	6	96	Am.
22	3	-	0.15	-	3.33	160	24	72	MER
23	2	0.4	-	-	2.5	160	24	72	Am
24	2	0.25	-	-	2.5	160	24	72	CHA(Oth.)
25	4	-	-	0.3	2.5	160	24	72	Am.(CHA)
26	5	-	-	0.35	2.5	160	24	72	MER(CHA)

a: gel Si/Al ratio

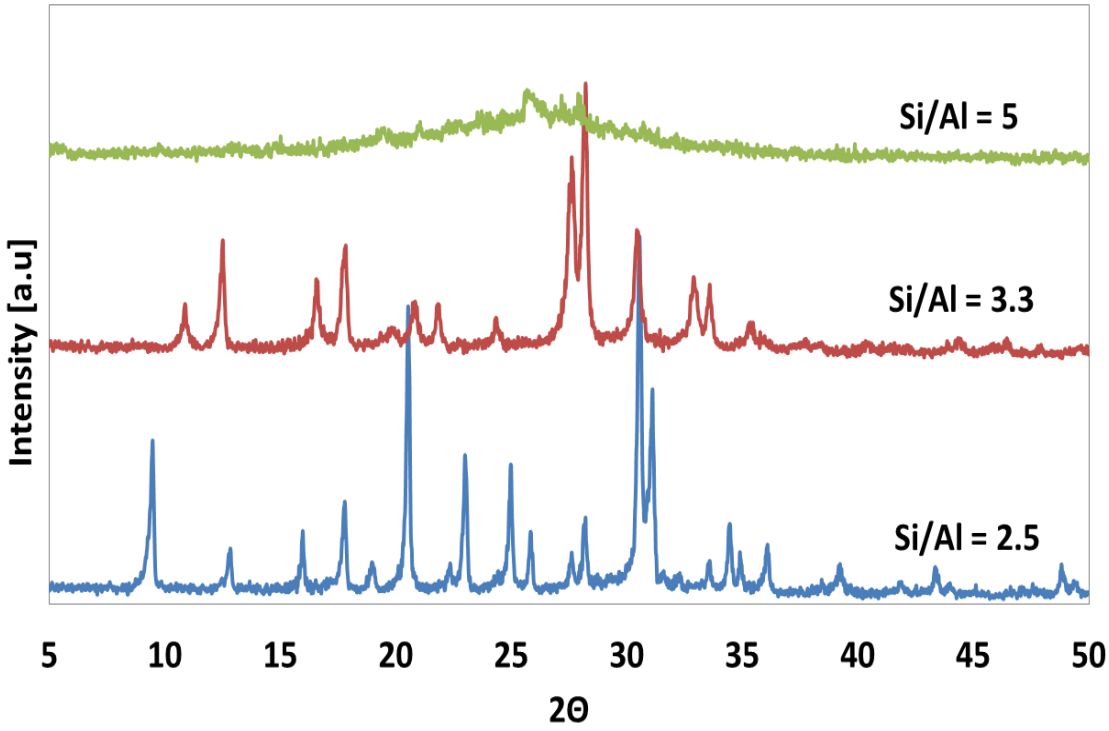

Figure 27. XRD patterns of samples prepared at different bulk Si/Al ratios.

3.3.5 Surface area and pore volume distribution

Ion-exchange of the as-synthesized zeolite was carried out using 2 M of ammonium nitrate at 75 °C for 3 h. **Table 9** shows the physical properties of the prepared CHA samples before and after ion-exchange. The as-synthesized material in potassium form (K-CHA) had a small surface area, while the ion-exchanged sample in H-form (H-CHA) showed an excellent enhancement in the surface area and pore volume. The parent sample (K-CHA), initially, had a BET surface area of 0.962 m^2/g and total pore volume of 0.0032 cm^3/g. After ion-exchange, the BET surface area and pore volume increased to 485 m^2/g and 0.217 cm^3/g, respectively. The poor adsorption of the parent sample is due

to the large size of the potassium cation (K^+) which might block the pore of the CHA framework [82]. A poor adsorption of CHA in K-form and an enhancement in adsorption when the CHA zeolite was ion-exchanged with Ca^+ and Na^+ has been observed elsewhere [43, 82, 83] and summarized in **Table 9**. Nedyalcova and his coworkers [43]found that CHA in potassium form had a surface area of ca. 7.9 m^2/g and then enhanced to ca. 396 m^2/g after ion exchange. Similarly, Shang et. al [83] reported a micropore volume of 0.0008 cm^3/g when the CHA was in potassium form.

Figure 28 presenting the N_2 adsorption/desorption isotherm of K-CHA and H-CHA zeolites. The isotherm belongings to type I and IV isotherm, which is the common isotherm type of CHA zeolite [84, 85]. The pore width of H-CHA zeolite was calculated using the Horvath–Kawazoe model with a main peak at ca. 5.1 Å, as shown in **Figure 29**.

Table 9. Surface area, pore volume and Si/Al ratio of the CHA samples.

Sample	Surface Area (m^2/g)				Pore volume (cm^3/g)			Si/Al[a]	Ref.
	S_{ext}	S_{micR}	$S_{BET.}$	S_L	V_{micro}	V_{meso}	V_{tot}		
K-CHA	0.09	0.87	0.96	1.371	0.0005	0.0027	0.0032	-	Current work
H-CHA	25	461	485	584	0.1952	0.0219	0.2172	2.5	Current work
K-CHA	-	-	17.82	-	0.002	0.05	0.052	2.2	[82]
Na-CHA	-	-	257.3	-	0.1	0.053	0.153	-	[82]
K-CHA	18	2	-	20	0.0008	-	-	2.2	[83]
K-CHA	-	-	7.84	--	-	-	-	2.3	[43]
H-CHA	-	-	396.2	--	-	-	-	2.3	[43]

[a] products Si/Al ratio by XRF; S_L: Langmuir surface area.

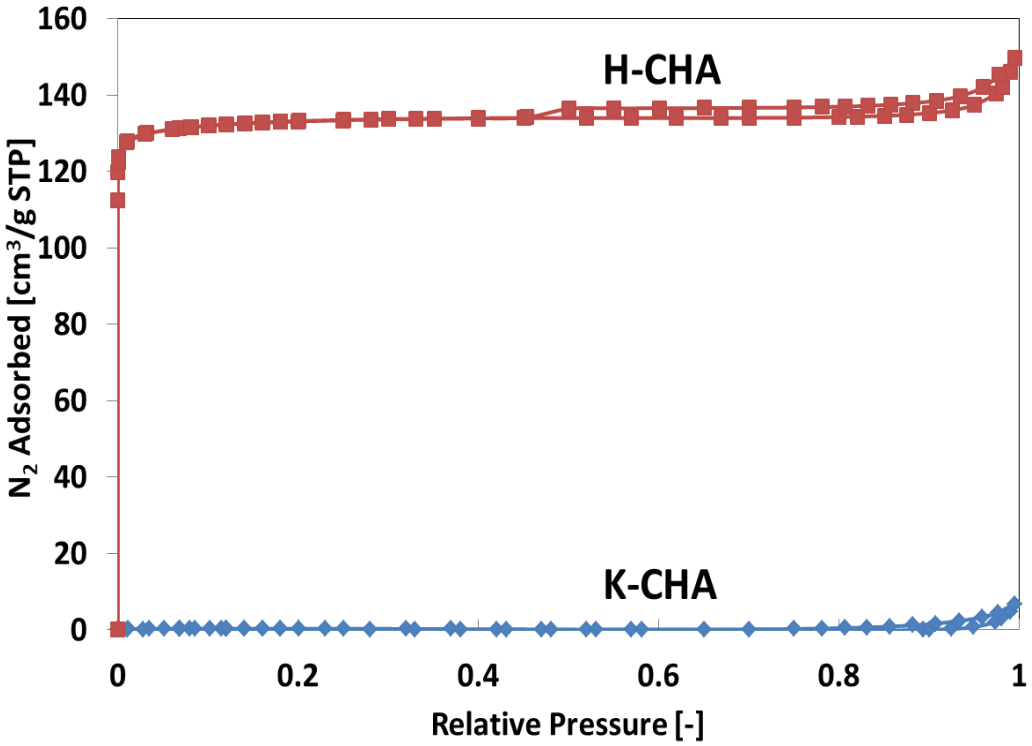

Figure 28. N2 adsorption/desorption isotherms of the as-synthesized CHA (K-CHA), and after ion-exchanged with ammonium nitrate (H-CHA).

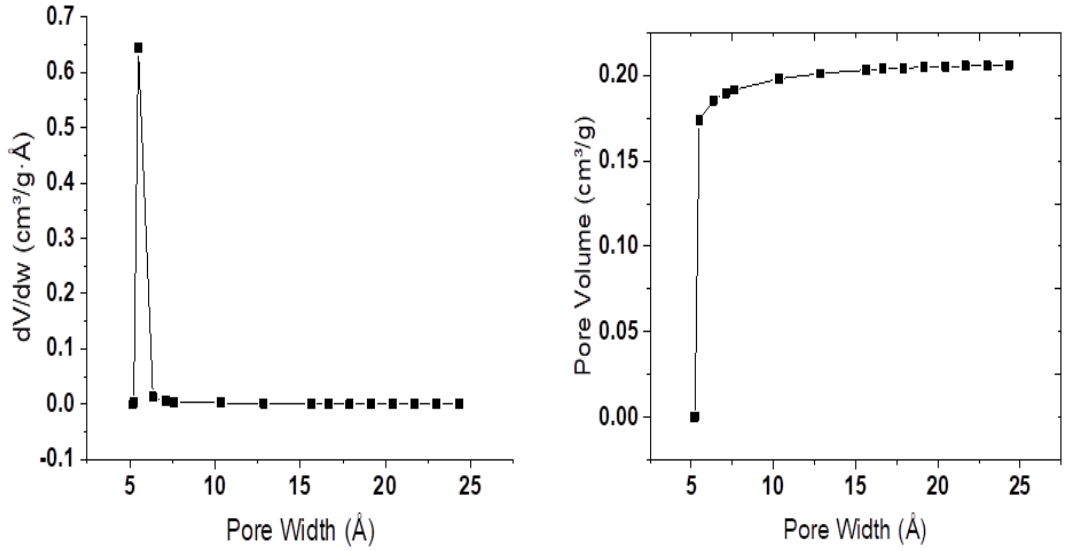

Figure 29. Micropores of synthesized and modified CHA zeolite samples using Horvath–Kawazoe model

The NH_3-TPD profile of the as synthesized CHA zeolite before and after ion-exchange is depicted in **Figure 30**. The sample in K-form had only a single small peak at T~175 °C attributed to weak acid sites. However, after ion-exchange (H-CHA), the TPD profile of ammonia showed two peaks at T = 195 °C and 475 °C corresponding to weak and strong acid sites, respectively.

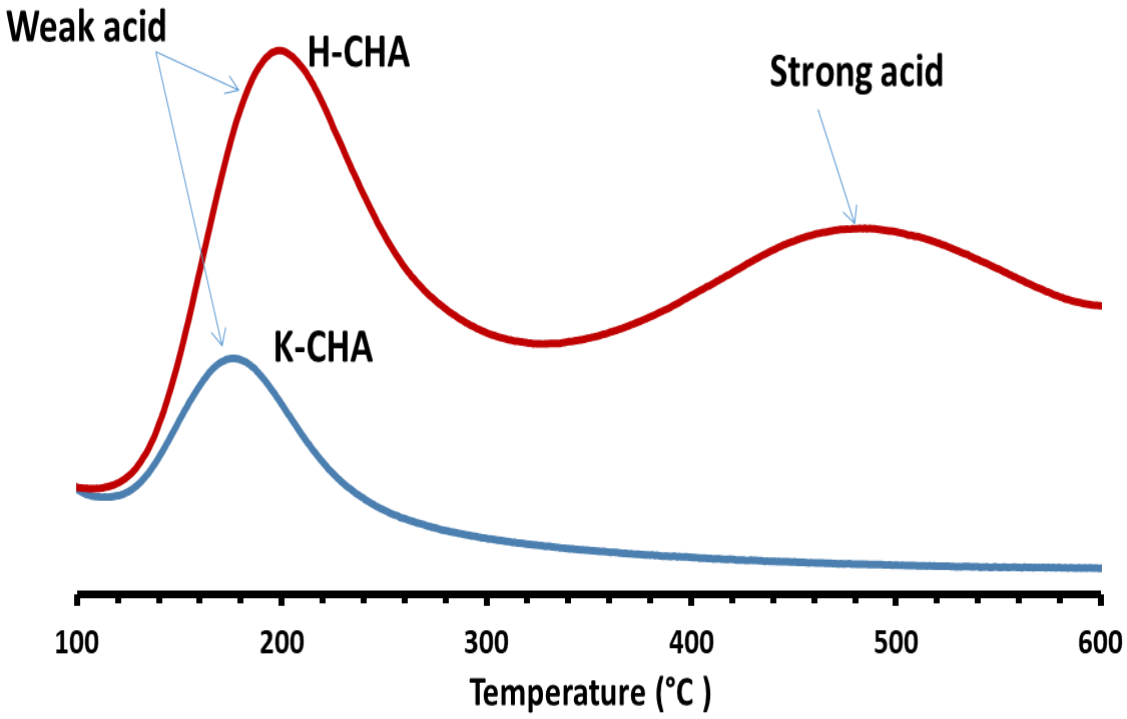

Figure 30. NH3-TPD profiles of the as-prepared CHA zeolite in K-Form (K-CHA) and after ion-exchanged with 2 M of ammonium nitrate (H-CHA).

3.3.6 CHA activity in MTO reaction

The activity of the synthesized CHA zeolites was evaluated in the MTO reaction at three temperatures (350, 400 and 450°C) with a WHSV of 0.95 h^{-1} in a fixed bed reactor. The selectivity and conversion of the CHA zeolites at the three temperatures are shown in **Figure 31** and **32**, respectively. From **Figure 31**, it is obvious that Al-rich CHA at lower reaction temperature (350°C) was more stable than at 400 and 450 °C. At 350°C, the conversion was maintained ca. 100% for more than 180 min, while at 400 and 450 °C the conversion decreased below 100% at TOS ca. 60 min. The increase in deactivation rate of CHA, which contains a high percent of alumina as a function of temperature was reported also by Bleken, et. al [58]. Bleken and his coworkers studied the effect of temperatures on SAPO-34 and SSZ-13. SSZ-13 is more acidic and is similar in acidity to our Al-rich CHA zeolite. Thus our results are in agreement with the behavior of SSZ-13 as shown in **Figure 33**.

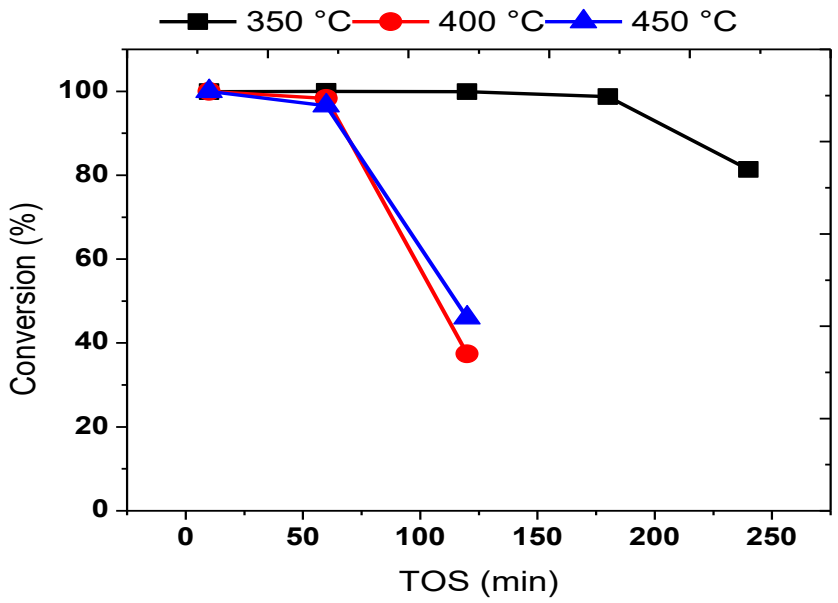

Figure 31. . Conversion of methanol over Al-rich CHA as a function of temperatures.

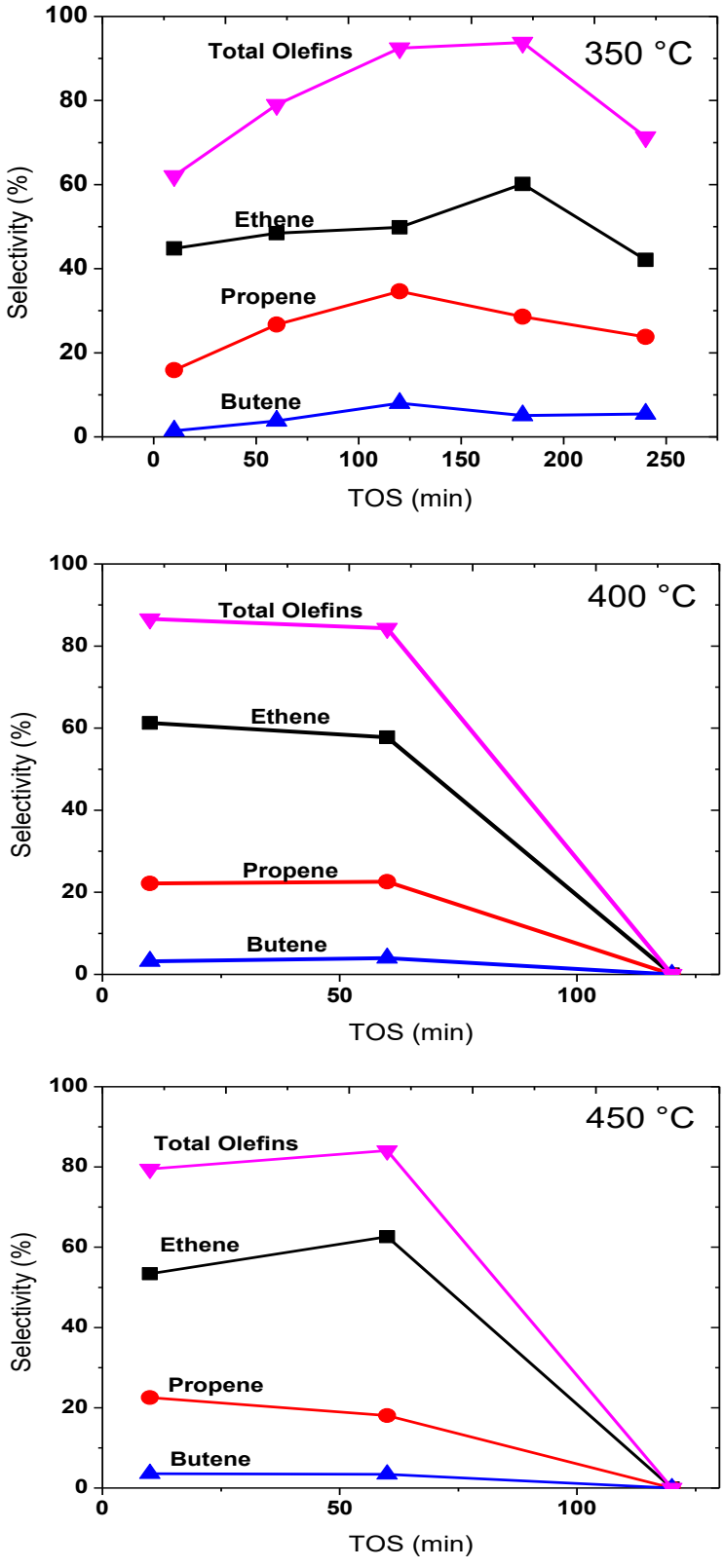

Figure 32. Selectivity to olefins as a function of temperatures.

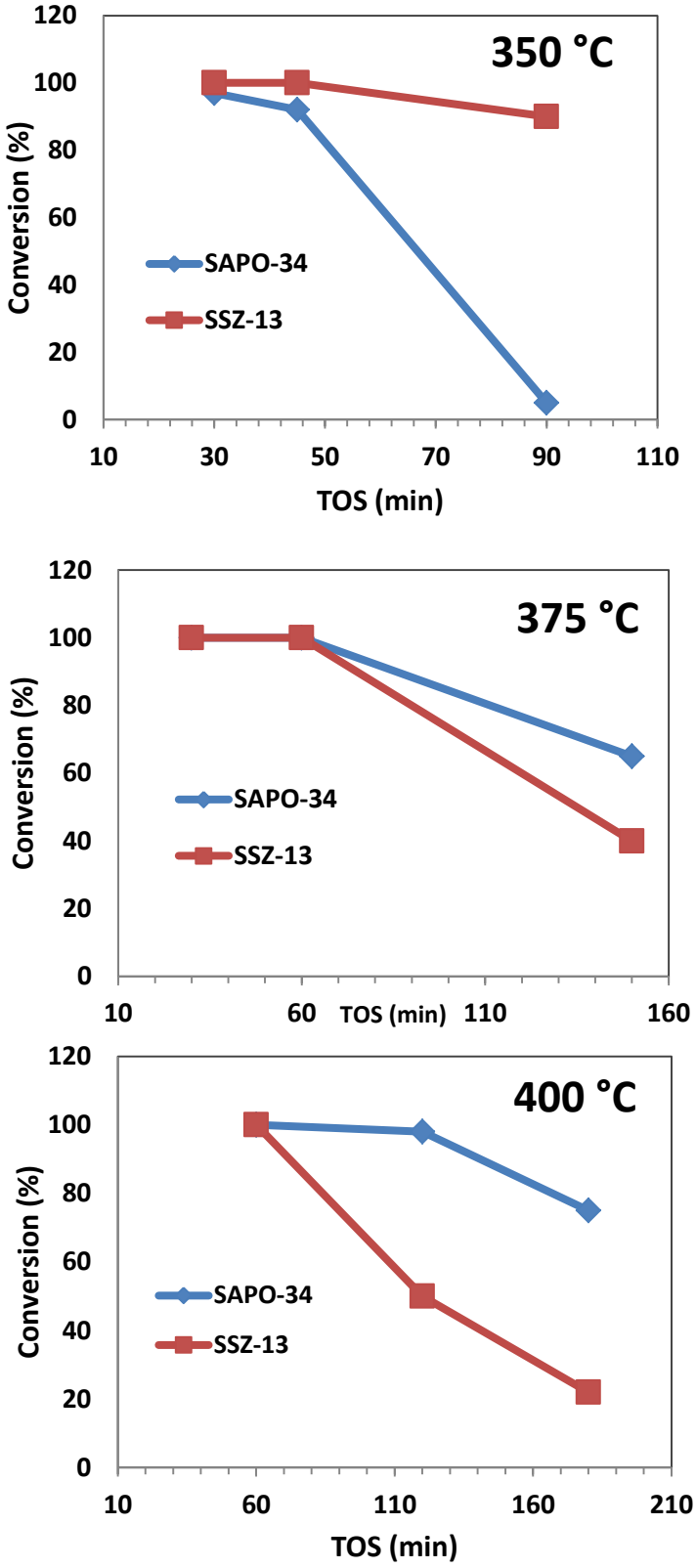

Figure 33. Effect of temperature on catalyst stability [58].

The selectivity to olefins as a function of temperatures is shown in **Figure 32**. At 350°C, the selectivity to light olefins was increased with TOS before the catalyst deactivated. At the beginning of the reaction, total olefins selectivity was ca. 62% and increased up to 93.8% at TOS of 180 min. In contrast, at higher temperatures (400 and 450°C), the selectivity to light olefins was higher at the initial of the reaction as presented in **Table 10**. The increase in selectivity to olefins with the increase of TOS and temperature was reported in the literature [86, 87]. The low selectivity to olefins at the initial of the reaction might be because part of olefins is consumed to form different hydrocarbon species. Additionally, propylene is more reactive at lower temperatures and has a tendency to form oligomers. The tendency of oligomers formation decreases with the increase of temperature as they crack to form more ethylene [86].

Table 10. Products distribution as a function of temperatures over Al-rich CHA.

	350℃				**400℃**			**450℃**		
TOS	**10**	**60**	**120**	**180**	**10**	**60**	**120**	**10**	**60**	**120**
Conv. (%)	99.9	100.0	99.9	98.7	100.0	98.3	37.4	100.0	96.6	46.0
Propene (%)	15.87	29.3	34.7	28.6	22.2	22.6	0.0	22.53	18.1	0.0
Ethene (%)	44.8	53.1	50.0	60.1	61.2	57.8	0.0	53.4	62.6	0.0
Butenes (%)	1.4	4.2	8.1	5.1	3.2	4	0.0	3.6	3.4	0.0
Total Olefins (%)	62.1	86.6	92.8	93.8	86.6	84.3	0.0	79.5	84.1	0.0
DME (%)	0.00	0.0	0.1	2.7	0.00	1.9	97.3	0.00	2.6	99.0
Paraffins (%)	36.9	12.2	4.3	2.5	12.1	13.2	0.4	19.3	10.0	0.8
C4s (%)	1.42	4.17	8.05	5.2	3.2	4.0	0.00	3.6	3.7	0.00
over C5s (%)	1.01	1.25	2.837	1.1	1.35	0.52	2.291	1.15	3.37	0.257

The selectivity comparison of Al-rich CHA to the commercial ZSM-5 and SSZ-13 at the same reaction conditions is depicted in **Figure 33**. At TOS 60 min, SSZ-13 showed the highest selectivity, however at higher TOS (120 and 180 min) our Al-rich CHA was the most selective catalyst. In agreement with literature, selectivity to olefins, particularly ethylene, was decreased with the increase of TOS [58, 86]. This decrease in the selectivity was explained by the pore blockage caused by carbon deposition which hinders the diffusion of propylene [58]. The pore blockage is more obvious when the reaction temperature was 450 °C as a result of coke formation.

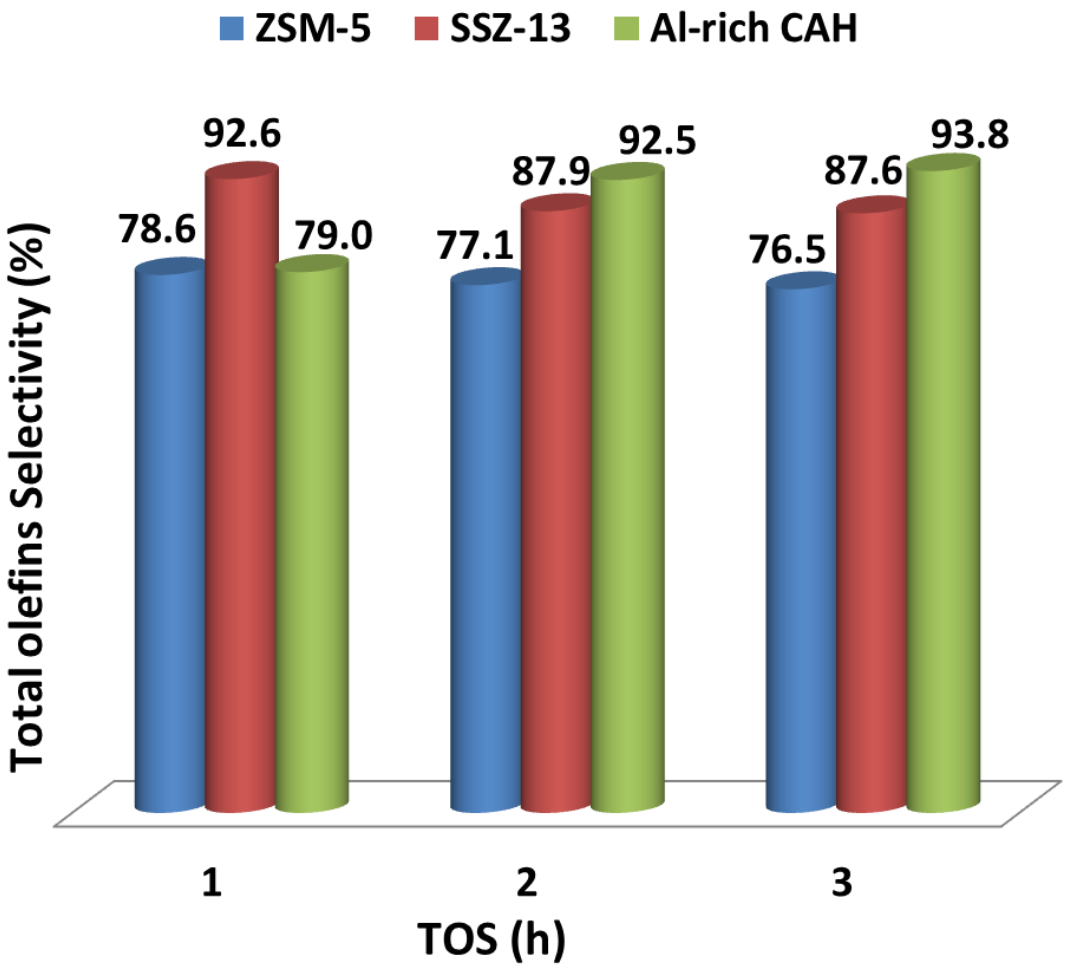

Figure 34. Comparison of olefins selectivity of Al-rich CHA commercial ZSM-5 and SSZ-13

3.3.7 Incorporation of metals

Different metals have been incorporated to the framework of CHA zeolites as indicated in **Table 5**. Only selected samples have been evaluated in the MTO reaction. Figure 35 shows the conversion of methanol of MeCHA zeolites. All MeCHA catalysts showed a 100% conversion of methanol. However, only BCHA and NiCHA maintained 100% conversion of methanol after 1 h of TOS, while the other MeCHA zeolites deactivated after 10 min TOS.

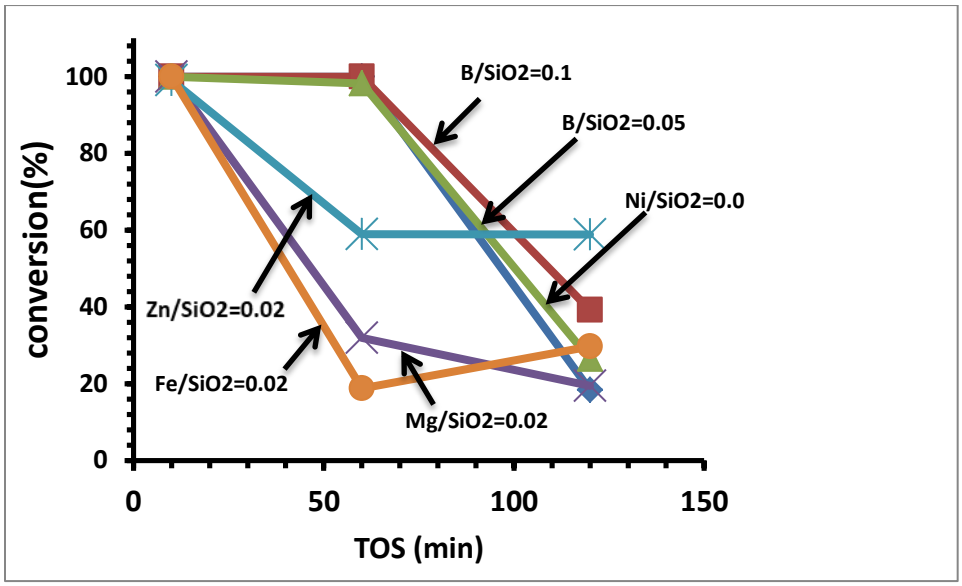

Figure 35 . Conversion of methanol over MeCHA zeolites; reaction temperature 350 °C, WHSV =0.95 h^{-1}

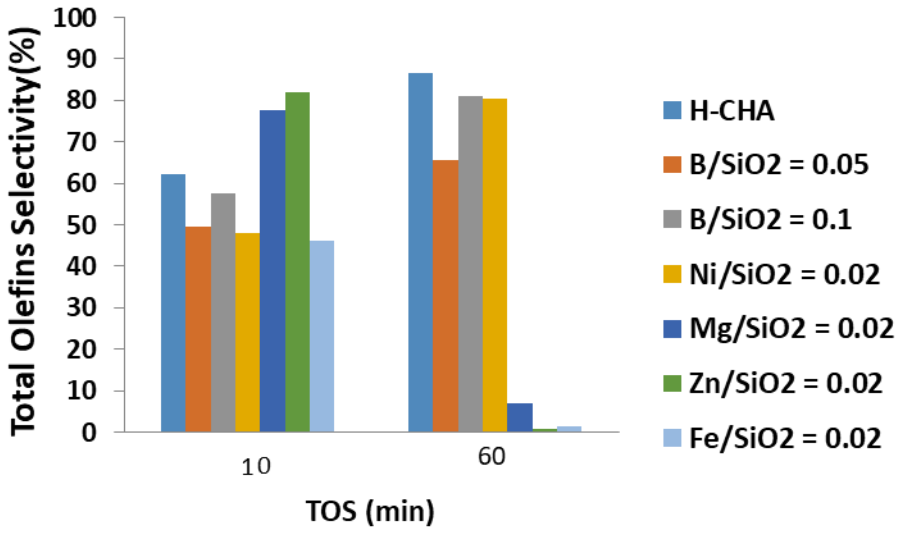

Figure 36. Total olefins selectivity of MeCHA zeolites compared to the parent CHA zeolite.

Figure 36 shows the total olefins selectivity of MeCHA zeolites after 10 and 60 min of the beginning of the reaction. After 10 min TOS, the CHA zeolites incorporated with magnesium (Mg/SiO_2 = 0.02) and zinc (Zn/SiO_2 = 0.02) were the most selective catalysts. The total olefins selectivity for ZnCHA was ca 82%, while for MgCHA it was ca. 78%. The enhancement in the total olefins selectivity for ZnCHA and MgCHA compared to parent CHA (H-CHA) was ca. 20 and 16 %, respectively. However, these two catalysts deactivated rapidly and showed no activity when TOS was 60 min. The CHA incorporated with nickel (Ni/SiO_2 = 0.02) and boron at different concentrations B/SiO_2 = 0.05 and B/SiO_2 = 0.1) showed comparable selectivity to olefins after 60 min of the reaction. Both NiCHA and BCHA (B/SiO_2 =0.1) maintained a total selectivity ca. 80% which is lowere than the parent CHA by ca. 6%. Thus, the metal incorporation to the framework of CHA zeolite by in-situ method enhanced the enhanced the activity of the catalyst at the beginning of reaction. After 60 min TOS, all MeCHA zeolites were deactivated and showed no activity in the MTO reaction.

3.3.8 Conclusions

Cost-effective Al-rich CHA zeolite was successfully synthesized without using templates. The CHA zeolite was synthesized under different experimental conditions than what was reported in the literature. The Si/Al ratios of the gel had a crucial role in the formation of pure CHA zeolite. A slight increase in Si/Al ratio (Si/Al=3.3) caused formation of impurities of other phase (MER). Higher H_2O/SiO_2 ratio affected the crystallinity of CHA zeolite, in which lower H_2O/SiO_2 ratio favored the formation of MER phase. The aging time influenced both the particles' shape and size, and the rate of crystallization. At longer aging time, smaller CHA particles were synthesized with shorter crystallization times. The synthesized CHA zeolite in H-form (H-CHA) showed a higher surface area and pore volume than the K-form (K-CHA). The reaction evaluation of H-CHA showed that the Al-rich CHA zeolite was very selective to olefins. The deactivation rate and initial selectivity to olefins were linked to the reaction temperature. The selectivity of the Al-rich CHA zeolite in the MTO reaction was comparable to the commercial ZSM-5 and SSZ-13 catalysts. Ni, Mg, Fe, B and Zn were successfully incorporated to the CHA framework by in-situ method. The incorporation of metals affected negatively the stability of the catalyst. However, the metal incorporation had a significant enhancement to the total olefins selectivity at the beginning of the reaction. Thus MeCHA zeolites are promising MTO catalysts to be used in a fluidized bed reactor.

3.3.9 Acknowledgements

The authors would like to acknowledge the funding provided by SABIC for Center of Research Excellence in Nanotechnology at King Fahd University of Petroleum & Minerals (KFUPM).

CHAPTER 4

Microwave-Assisted Hydrothermal Synthesis of Al-rich CHA Zeolite from Amorphous Aluminosilicate Gel in the Presence of a Seed

Abstract

Cost-effective aluminum (Al) rich CHA zeolite was synthesized by seed-assisted hydrothermal synthesis under microwave irradiation to shorten the crystallization time. Al-rich CHA zeolite was successfully synthesized within 6 h. The Al CHA was synthesized under different stirring rates and evaluated for the methanol-to-olefins reaction at three different temperatures in a fixed bed reactor. After the successful synthesis of the SDA-Free CHA zeolite, boron was incorporated by in-situ synthesis. The XRD pattern revealed that the synthesized CHA was crystalline. The performance evaluation revealed that reaction temperature and TOS affected both the catalyst's stability and selectivity to light olefins. At lower temperature (350 °C), the Al-rich CHA was more stable and less selective to light olefins at the beginning of the reaction. The selectivity was increased from 41.8% at TOS of 10 min up to 85.0% at TOS of 120 min. In contrast, the selectivity of olefins at TOS of 10 min was 55.0 and ca. 79.6% when the reaction temperatures were 400 °C and 450 °C, respectively. Incorporation of boron only enhanced the olefins selectivity at the initial stages of the reaction. At 350 °C, the total olefins selectivity was increased from 41.8% for parent CHA to 71.5% for CHA with Si/B=13.

4.1 Introduction

Zeolites are crystalline porous materials with tunable and distinct properties. They are mainly composed of aluminum, silicon, oxygen and phosphorous in some frameworks. There are more than 220 zeolites frameworks recorded in the international zeolite association (IZA). Each framework has its own property such as pore diameter, crystal habit, pore dimension, framework density and compositions, to mention but a few. Due to these exceptional properties, they have been applied in wide range of applications. For example, zeolites are be used in separation, adsorption, ion-exchange and purifications [88-90]. Zeolites properties such as high surface area, well defined channels and cavities, controlled adsorption capacity, availability of active sites, shape selective and hydrothermal stability open plethora applications in hydrocarbon catalysis [32, 89, 90]. One of the most challenging reactions is the conversion of methanol-to- olefins (MTO), which is the focus of this study. Many factors are still explored to optimize MTO process, including development of better effective catalyst.

There are different types of zeolites frameworks used in the MTO reaction [7, 91-95]; however, zeolites with MFI and CHA topology have been proved to have superior activities. These two frameworks exhibited different selectivities to light olefins and slower deactivation rate. The selectivity is governed by the pore and cage size, while the deactivation rate is affected by the catalyst's acidity [6, 40, 94]. Thus, ZSM-5, which has a medium pore opening and can be synthesized with varying amount of acid sites, is an outstanding catalyst in the MTO reaction in term of stability, but it produces a wide range of products. In contrast, SAPO-34 with small pore opening and contains on large amount

of acid sites is the most selective catalysts to light olefins, but it suffers from severe deactivation.

The synthesis method of CHA zeolites involves the use of the expensive template N,N,N-trimethyl-1-adamantammonium iodide as structure directing agent (SDA) [52]. Other strategies for CHA synthesis in which a combination of the expensive template with cheaper SDAs have been reported in the literature [54]. Bull and his coworkers were patented for the conversion of a pre-synthesized zeolite (FAU) to CHA without using templates [96]. However, the synthesis of CHA zeolite from the conversion of FAU zeolites produces CHA with low silica content (Si/Al = 2-2.5) that has a negative effect in the MTO process. Imai et al [44] reported a direct SDA-Free synthesis of CHA zeolite from amorphous silicoaluminate gel in the presence of seed. In this study, we focused on the production of cost-effective CHA zeolite utilizing the microwave-assisted hydrothermal synthesis (MAHyS) from the amorphous of silicoaluminate gel.

In this study, we focused on the production of a cost-effective Al-rich CHA zeolite utilizing the microwave-assisted hydrothermal synthesis (MAHyS). Microwave is a powerful platform with a wide range of applications. Regardless of its massive use in food coking, the first use of microwave in laboratory was in drying and moisture analysis [97]. Then, the microwave technology has been utilized in the field of material synthesis of inorganic chemistry in the late 1970s and in organic synthesis in the 1980s [98]. The first report for chemical synthesis (organic synthesis) has been published in 1986 by Gedye et al. [99]. After 1990, the number of publications using microwave technology have been noticeably increased because the commercialization of the technology. Regarding the synthesis of zeolite using microwave, Mobile Oil Corporation in 1988

patented on the zeolite synthesis using microwave [100], while the first article concerning the synthesis of NaA and ZSM-5 zeolites was published by Arafat et al in 1993 [101]. Since that time, the number of articles reported on the synthesis of zeolites using microwave heat was continuously increased [102-108]. The main benefits of the microwave synthesis are shorter synthesis time, reduced particle size and uniform particle shapes. Rapid synthesis (MAHyS) of Al-rich CHA has been established within this study, eventhough the Al content supposed to slower the crystallization growth [109].

4.2 Experimental

4.2.1 Synthesis of Al-rich CHA

Pure chabazite (CHA) zeolite was successfully synthesized under microwave radiations. The synthesized CHA was prepared in the presence of a CHA Seed from amorphous silicoaluminate gel without any addition of templates. The compositions of the amorphous gel was adopted from the literature [44]. Our synthesis procedure includes the addition of aluminium iso-propoxide to an alkaline solution of sodium and potassium hydroxide. Then, fumed silica and a required amount of seeds were added. After that, the final gel was crystallized in a microwave lab station (400 W, MicroSYNTH, Milestone, Italy) at 170 °C for certain hours. In a typical preparation, 0.5 g and 0.23 g of sodium and potassium hydroxide, respectively, were dissolved in 37.6 g of deionized water. To this alkaline solution, 0.43 g of aluminum iso-propoxide was added and stirred at 450 rpm for about 1 h. Prior to the addition of 0.25 g of seeds, 1.25 g of fumed silica was added and stirred for 30 min. The final gel was crystallized at 170 °C for *x* hours, (*x*= 5, 6, 6.5, 7 and 8 hours) at a stirring rate of 50 rpm. After optimizing the crystallization time at 50 rpm, we synthesized CHA zeolite at higher stirring rate (400 rpm). Then, we incorporated

boron at 400 rpm for different crystallization times as shown in **Table 14**. The required amount of boron was introduced after the addition of aluminum and then the experimental procedure was the same as if the sample was free of boron. Thereafter, the product was separated by centrifugation, washed with deionized water, dried and ion-exchanged.

The ion-exchanged was performed using ammonium nitrate (NH_4NO_3) as a source of proton. For each gram of the sample, we used 50 mL of 2 M of NH_4NO_3 and then the solution was heated using microwave at 85 °C for 25 min, at a heating rate 17 °C per minute. The ion-exchanged was repeated one more time with a fresh solution of ammonium nitrate. Finally, the samples were calcined to obtain H-CHA at 500 °C for 4 h, at heating rate of 5 °C/ min.

4.2.2 Characterization techniques

Structure and morphology analysis

The crystallinity of the synthesized samples was explored using X-ray diffraction (XRD) machine, Rigaku Miniflex diffractometer equipped with Cu Kα radiation (λ = 0.15406 nm). The XRD patterns were recorded in 2θ angle ranging from 5 to 50° with a scan speed of 3° per minute and step size of 0.02. The crystallinity (**Table 14**) was calculated by the relative intensities of mean peaks at 2θ ~ 9.5, 20.5, 30.7 and 31.2° as follow:

$Crystallinity = \frac{\sum(mean\ peaks\ of\ x\ sample)}{\sum(mean\ peaks\ of\ pure\ CAH\ sample)}$, where the pure was Run# 7.

The ^{27}Al, and ^{29}Si solid state Nuclear Magnetic Resonance (NMR) was used to study the coordination of the aluminum and silicon in the CHA framework. The elemental compositions of the samples were measured using X-ray fluorescence (XRF) and energy

dispersive X-ray (EDX), while the morphology of the samples was investigated using the field-emission scanning electron microscope (FE-SEM).

Acidity analysis

We conducted the ammonia temperature programmed desorption (NH_3-TPD) to investigate the acidity of the zeolites. Typically, a 100 mg of H-CHA zeolite was used for the acidity measurement in a Chemisorb 2750 Micrometrics Chemisorption analyzer. Firstly, we preheated the sample at 600 °C (heating rate 30 °C.min^{-1}) for 30 min under the flow of helium (25 mL. min^{-1}). Then, the samples were cooled to 100 °C and allow ammonia to flow over the samples for 30 min at rate of 25 mL. min^{-1}. To remove the weakly adsorbed ammonia, the samples were flushed with helium at the same previous conditions for 60 min. Finally, we heated the sample up to 650 °C at heating rate of 10 °C. min^{-1} and the amount desorbed of ammonia was collected using a TCD detector.

Surface area and pore volume distribution

The N_2 adsorption /desorption isotherm was conducted to study the textural properties of the synthesized catalysts. The samples firstly were degassed at 300°C for 12 h and then the analysis was performed in a liquid nitrogen bath at −195.86°C. The surface and pores volume were calculated using the BET method, while the micropores distribution and micropore area were calculated using the Horváth–Kawazoe and the t-plot methods, respectively.

4.2.3 Catalytic Evaluation

The activities of the synthesized and modified catalysts with different concentrations of boron were evaluated in a fixed bed reactor with a WHSV of 0.94 h^{-1} over 50 mg of the catalyst. Prior to the analysis, the samples firstly were calcined for 1 h and then evaluated at three different temperatures; 350, 400 and 450 °C. An on-line Shimadzu GC-2014 chromatograph equipped with a flame ionization detector and a capillary column HP-PLOT (30 m × 0.53 mm, 6 μm film thickness) was used to quantify the products distribution.

4.3 Results and Discussion

Table 11. Experimental conditions for microwave-assisted hydrothermal synthesis (MAHyS) of CHA zeolite.

Run#	Crystallization Time (h)	T (^oC)	Seed	Stirring (rpm)	Phase	Si/Al[a]	Si/B[a]	Relative Crystallinity
1	5	170	-	50	MER	10	-	-
2	6	170	-	50	MER	10	-	-
3	8	170	-	50	MER	10	-	-
4	5	170	CHA	50	CHA (Am.)	10	-	-
5	6	170	CHA	50	CHA (Am.)	10	-	-
6	7	170	CHA	50	CHA*	10	-	
7	6.5	170	CHA	50	CHA	10	-	100
8	6.5	170	CHA	400	CHA*	10	-	
9	6	170	CHA	400	CHA	10	-	90
10	6	170	CHA	400	CHA (Am.)	10	50	
11	6.5	170	CHA	400	CHA (Am.)	10	50	
12	7	170	CHA	400	CAH*	10	50	
13	7	170	CHA	400	CHA*	10	20	94
14	7	170	CHA	400	CHA (Am.)	10	13	41

[a]: ratios of the amorphous silicoaluminate gel.
*: the CHA phase is containing on a tiny impurities, very small peak appeared at $2\Theta = 12.4^o$

4.3.1 Seed-Free Crystallization

To synthesize pure Al-rich CHA from amorphous aluminosilicate gel, firstly, we investigated the synthesis without using a CHA seed for three different crystallization periods; 5, 6 and 8 h. As shown in **Figure 37**, CHA zeolite was not obtained in the absence of a CHA seed. The seed-free synthesis only favors the formation of another phase of zeolite, namely MER. This finding is in well agreement with previously reported crystallization work using conventional heating [44].

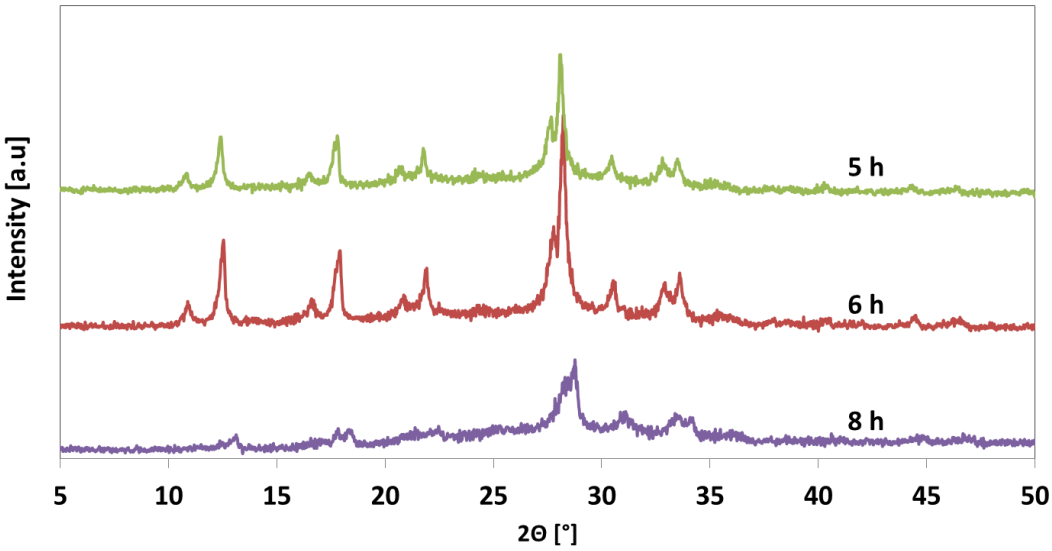

Figure 37. XRD patterns of CHA samples crystallized by MAHyS without using seed at different crystallization times.

4.3.2 Seed-assisted Crystallization

Once the CHA seed has been added to the gel, 20 wt.% of silica, CHA zeolites was formed at different crystallization times. **Figure 38** shows the XRD patterns of the as-synthesized CHA zeolites using microwave heating. It is obvious from the XRD patterns that crystallization time has a great influence on the formation of CHA zeolite. Higher

crystallinity and pure CHA zeolite was achieved at a crystallization time of 6.5 h and a string rate of 50 rpm. All peaks of the pure CHA zeolite were in well agreement with the CHA reference. Shorter crystallization times, 5 and 6 h, resulted in a combination of CHA and amorphous phase. When the crystallization time was increased to 7 h, crystallinity was maintained but a minor peak of an impurity (MER) phase appeared at 2Θ= 12.4°. In line with our previously reports for different zeolite frameworks, we successfully synthesized CHA with significantly shorter time (6 h) than MOR [110] and MTT [105] zeolite under microwave radiation. However, the increase in crystallization time stimulated the appearance of impurity phase.

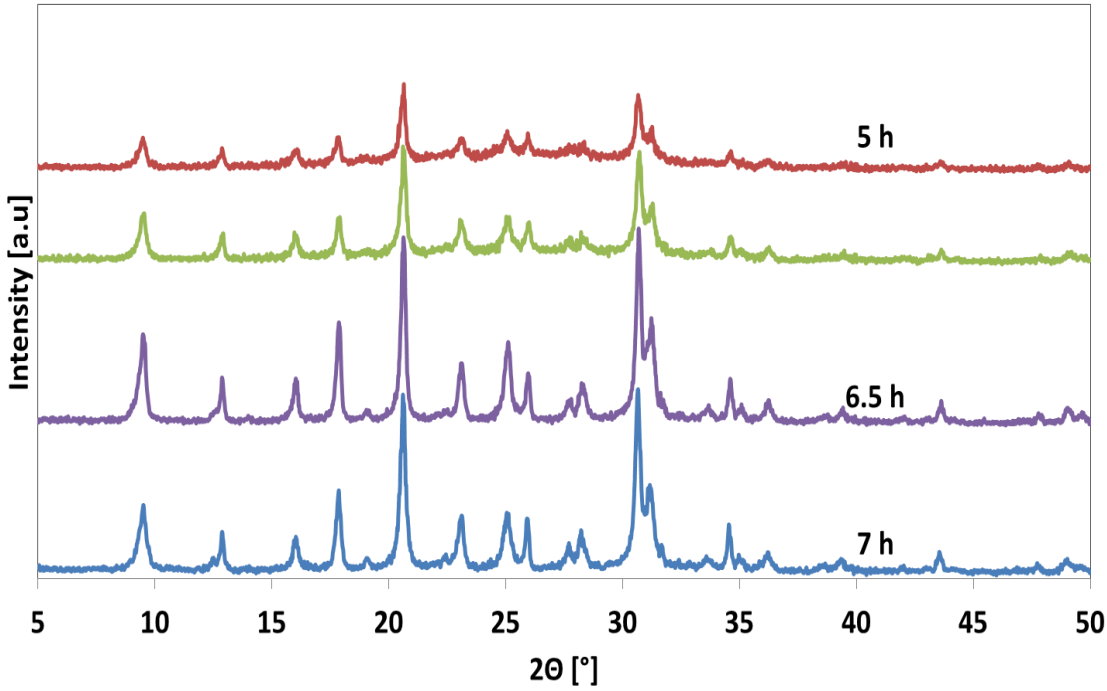

Figure 38. Synthesis of CHA zeolite by MAHyS in the presence of seed (20 wt. % of silica) at different crystallization times with stirring rate of 50 rpm.

4.3.3 Effect of Stirring

The preparation of Al-CHA zeolite using conventional heating, was carried out at slow steering rate, 20 rpm, using a tumbling oven. Therefore, in our study, we initiated the synthesis at very slow stirring rate and then we increased the speed of the stirring rate to investigate its effect on crystal growth, morphology and catalyst activity. The initial stirring rate was 50 rpm. At this stirring rate, pure CHA zeolite was formed at crystallization time of 6.5 h and 170 °C (Run# 7). At the same conditions, but with higher stirring rate (400 rpm), CHA zeolite was formed but with an additional small peak of MER phase at 2Θ= 12.4° as shown in **Figure 39**. The additional peak is attributed to a MER framework. However, when crystallization time was decreased to 6 h, still with 400 rpm stirring rate, we were able to get pure CHA zeolite. This implies that stirring rate influences the rate of crystallization. The higher stirring rate was the lower the required crystallization time. The effect of stirring rate on crystallization has been noticed elsewhere [105, 111, 112]. It has been reasoned that higher stirring rate would prevent the mass-transfer limitations. Thus, the lower mass-transfer limitation would give rise to higher nucleation and crystallization rate[30].

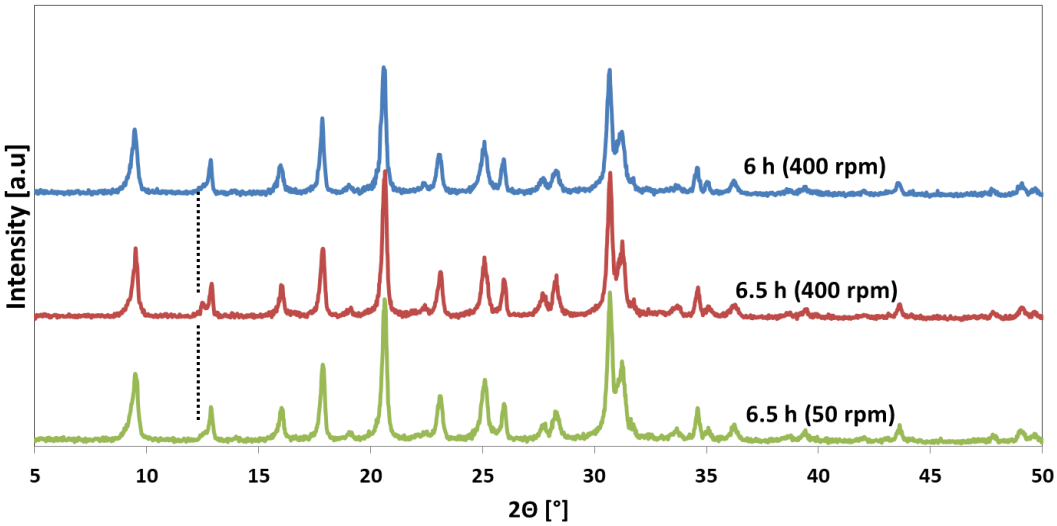

Figure 39. XRD patterns of the synthesized CHA by MAHyS at different crystallization times and different stirring speeds.

Figure 40 shows the ^{27}Al, and ^{29}Si solid state NMR spectra for the samples synthesized at different stirring rates. The ^{27}Al NMR spectra show a sharp peak at around 58 ppm corresponding to tetrahedral coordination, and a tiny resonance at around 0 ppm attributed to the octahedral environment. The ^{29}Si resonance spectra (for both samples synthesized at 50 and 400 rpm) show two large peaks located at ca. -109 ppm and -105 ppm, corresponding to Si(0Al) and Si(1Al) coordination, respectively. Another two minor ^{29}Si resonance spectra centered at ca. -99 ppm and -93 ppm were attributed to Si(2Al) and Si(3Al) coordination, respectively.

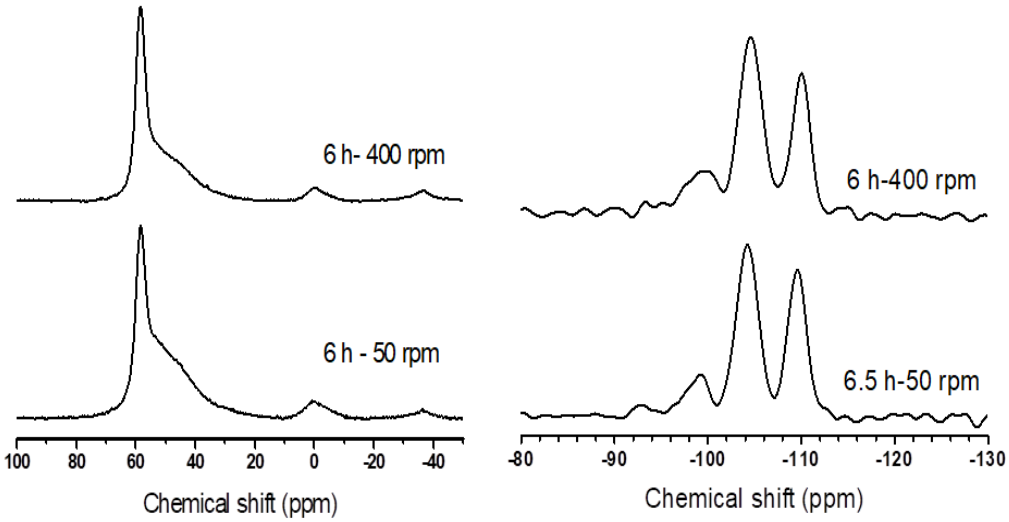

Figure 40. The 27Al and 29Si MAS NMR spectra of the CHA zeolites by MAHyS synthesized at different stirring rates

4.3.4 Effect of boron incorporation on crystallization

We studied in-situ incorporation of boron at different concentrations. Firstly, we attempted to incorporate boron with a Si/B molar ratio of 50 over Run# 9, crystallization time 6 h and at a stirring rate of 400 rpm. However, the addition of boron decreased the rate of crystallization, and we obtained a combination of amorphous and CHA phases after the addition of boron, as shown in **Figure 41**. The crystallinity was 90% for CHA free of boron and then decreased to 40% after the boron incorporation at the same experimental conditions. Thus, to obtain a well crystalline and pure CHA phase, we had to optimize both the crystallization time and stirring rate. Therefore, crystallization time was increased up to 7 h, while the stirring rate was maintained at 400 rpm, but this resulted in the appearance of a small peak at 2Θ= 12.4° (Run# 12). With the same stirring

speed, we have increased the boron concentration so that the Si/B ratios were 20 and 13. The increase in Si/B ratio from 20 to 13 suppressed the peak appeared at 2Θ = 12.4° as shown in **Figure 41**. **Table 12** presents the elemental compositions (in wt. %) of the samples synthesized before and after boron incorporation. The boron addition influenced the Si/Al ratio; the highest Si/Al ratio was 4.54 corresponding to the highest amount of boron.

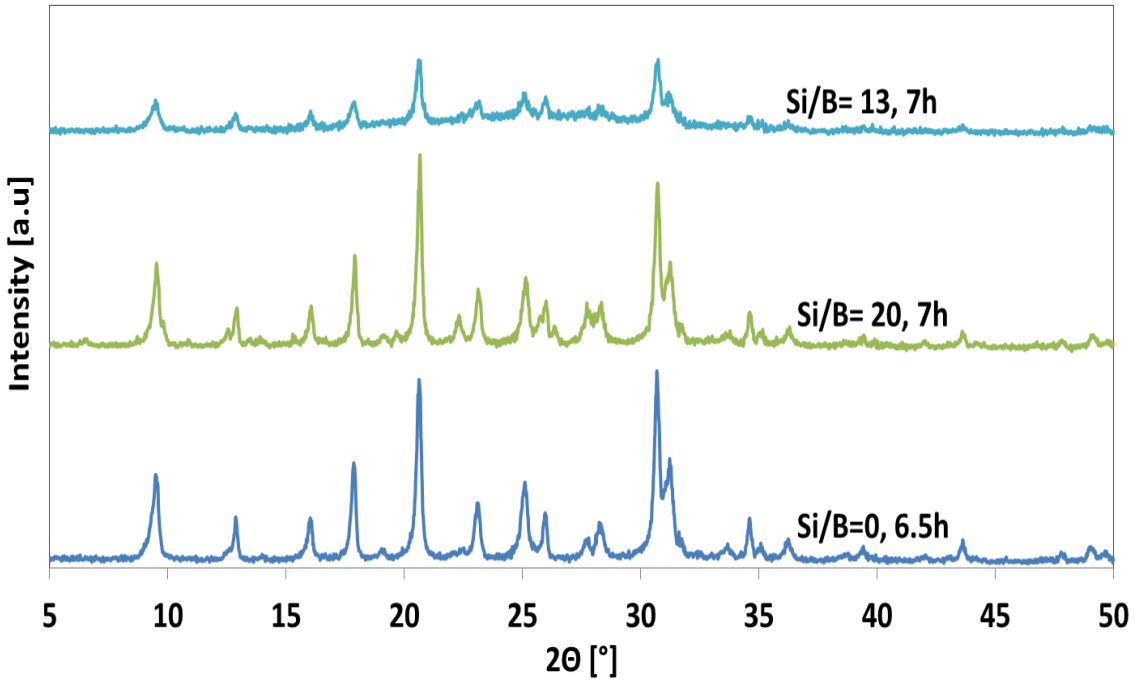

Figure 41. XRD patterns of the synthesized CHA zeolite by MAHyS at different concentrations of boron

Table 12. Elemental compositions of as-synthesized CHA zeolites prepared using microwave (MAHyS) heating.

Sample	Al	Si	B	Si/Al	Si/B	Si/B[a]
Run#7	7.90	29.59	-	3.75	-	-
Run#13	7.77	30.51	8.4	3.93	3.85	1.08
Run#14	6.05	27.48	12.98	4.54	2.13	2.14

4.3.5 Physical properties and morphology of Al-rich CHA zeolite

The amount and strength of acidic sites of the synthesized samples were evaluated using NH_3-TPD. The TPD analysis has been conducted for selected samples as presented in **Table 13** and shown in **Figure 42**. All the analyzed samples had two peaks that usually appeared in the NH_3-TPD profile, the l-peak and h-peak [113], which were observed at a temperature of 120-400 and 400-650 °C, respectively. The peaks appeared in the NH_3-TPD profile expressed different amounts of acid type. Samples synthesized without the incorporation of boron or with lower Si/B ratio had similar amount of acid; the samples synthesized from Run # 7, 9 and 13 had similar densities of acid sites as shown in **Table 13**. **Figure 43** shows the typical N_2 adsorption-desorption of Al-rich CHA with minor presence of mesopores (Type IV). **Table 13** presents the comparison of the physical properties of CHA zeolites synthesized using conventional and microwave heating. The presented BET results reveal that the microporous CHA zeolite synthesized using

microwave heating possess high surface area (up to 578 m^2/g) and the presence of mesopores (ca. 25%). CHA synthesized using microwave heating had relatively fewer amounts of acid sites, which was reflected later on the catalyst stability in the MTO reaction as explained in Section 4.3.6. The Al-rich CHA zeolite synthesized at 50 and 400 rpm exhibited almost similar pore volume and sizes, which were calculated using Horváth–Kawazoe method as depicted in **Figure 44**. This shows that mesoporisoty is not highly affected by the stirring speed.

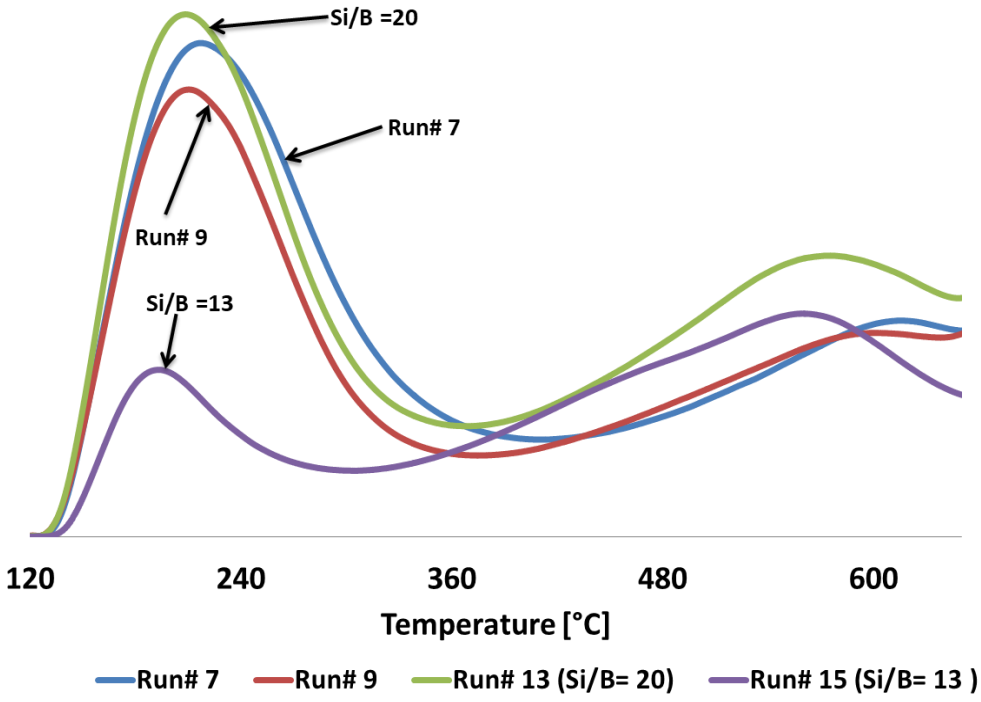

Figure 42. NH_3-TPD of the CHA samples synthesized under microwave irradiation with different stirring rates and different concentrations of boron.

Table 13. Physical properties of the CHA zeolites prepared microwave (MAHyS) and conventional heating.

Sample	Surface Area [m^2/g]				Pore Volume [cm^3/g]			Acid amount [mmol g^{-1}]		
	S_{BET}			S_L	V_{micro}	V_{meso}	V_{tot}	weak	strong	Total
	S_{ext}	S_{micro}	S_{tot}							
T-CHA	66.8	512	578	704	0.217	0.077	0.294	-	-	0.90
Run# 7	42.5	535	577	698	0.227	0.070	0.297	0.55	0.30	0.85
Run# 9	41.1	505	546	660	0.214	0.057	0.271	0.46	0.30	0.76
Run# 13	-	-	-	-	-	-	-	0.55	0.43	0.98
Run# 14	-	-	-	-	-	-	-	0.19	0.35	0.54

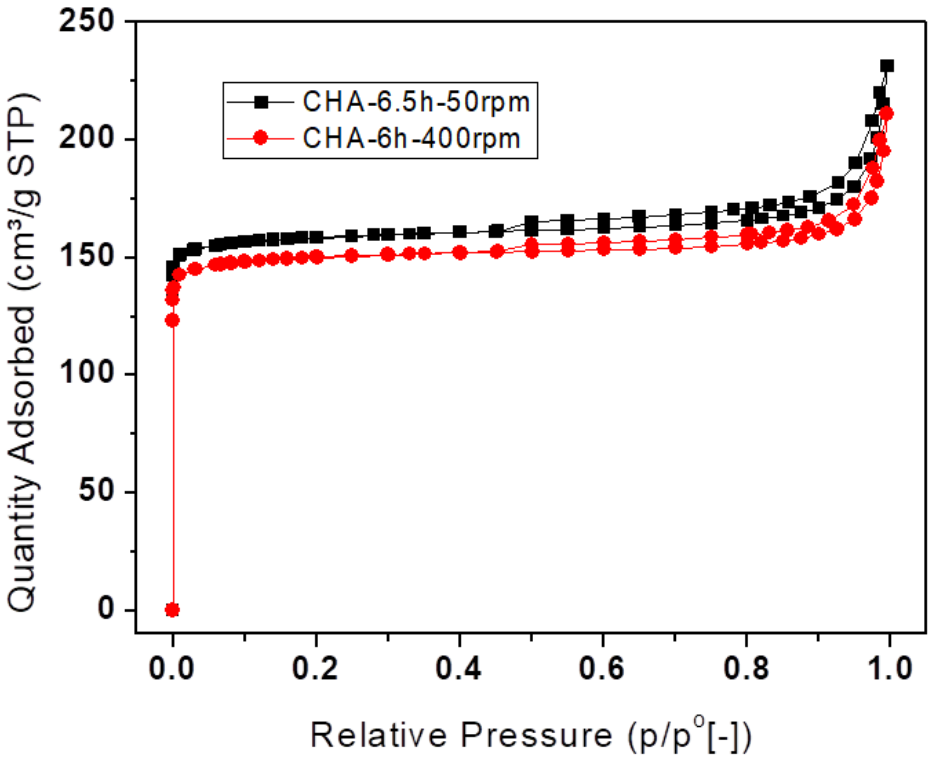

Figure 43. N2 adsorption/desorption isotherm of samples from Run# 7 (CHA-6.5h-50rpm) and Run# 9 (CHA-6h-400rpm).

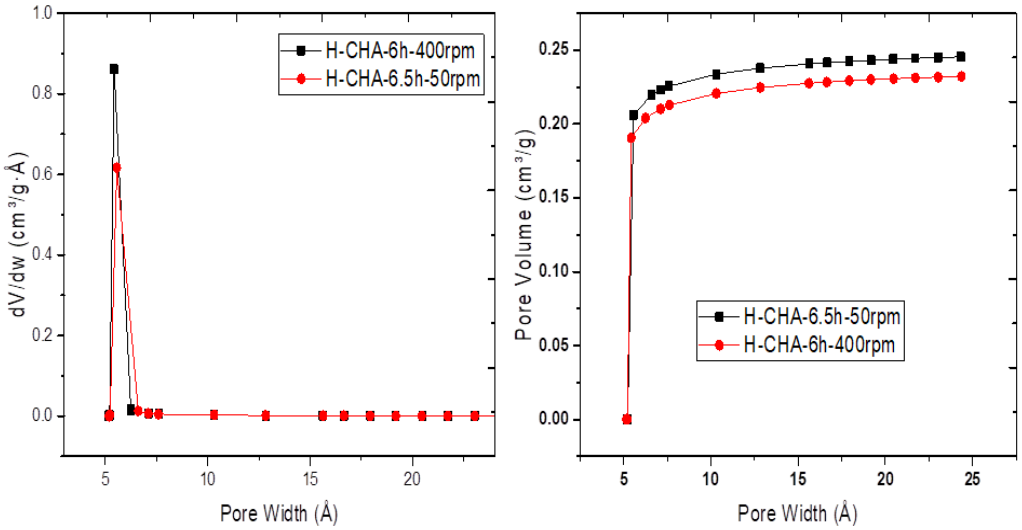

Figure 44. Cumulative pore volume distribution using Horvath-Kawazoe plot.

The SEM images of the samples shown in **Figure 45** revealed that the obtained CHA particles are in a nano size range of around 150 nm. These small particles are agglomerated in a very ordered way to form a sheet, which is similar in shape to corn flakes sheets. These corn flakes like shapes have a thickness ranging between ~ 130 and 160 nm.

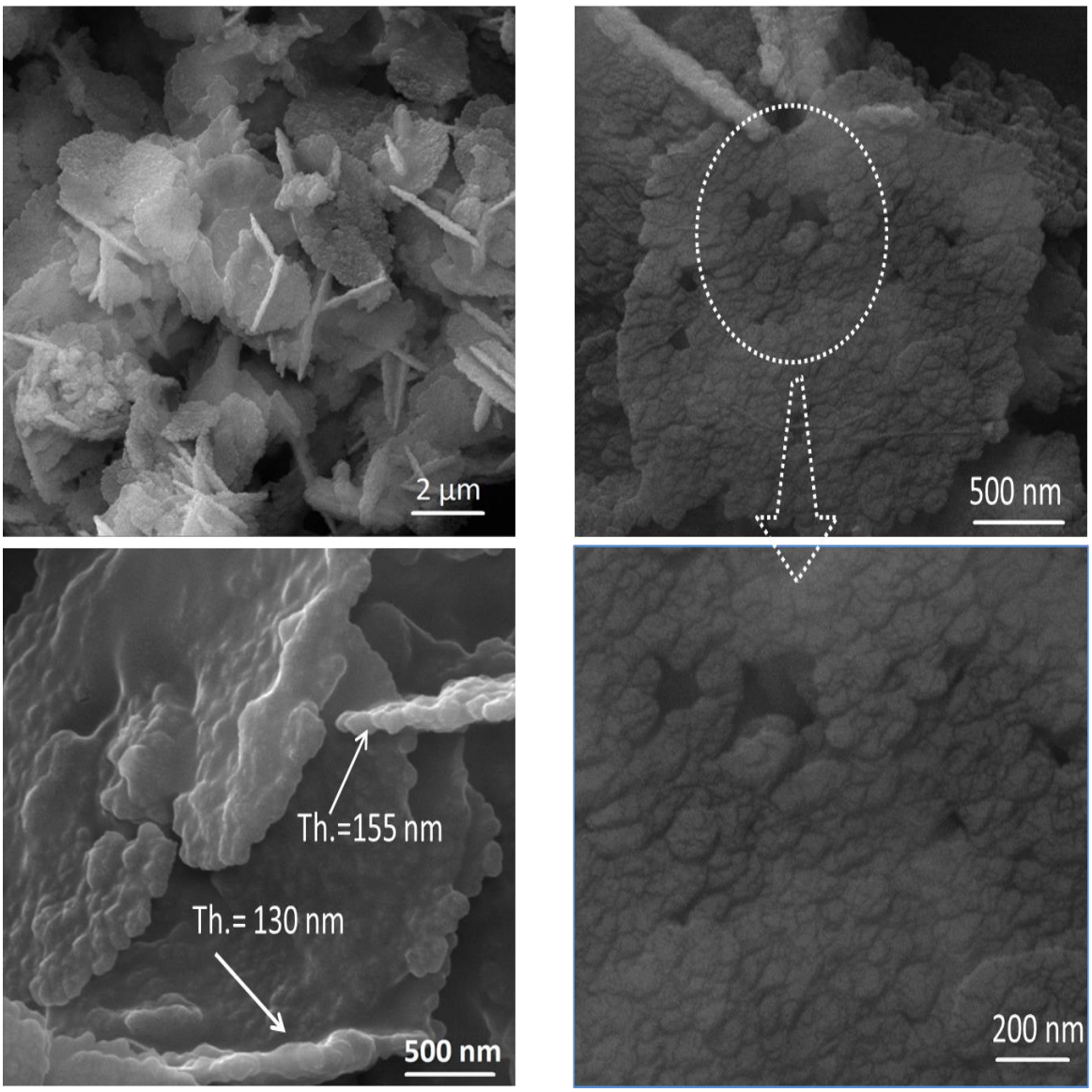

Figure 45. FE-SEM images of the CHA zeolites synthesized by MAHyS in the presence of seed at different crystallization times and stirring rates; Run# 7 (left side) and Run# 9 (right side).

4.3.6 Catalyst Evaluation

The catalytic performance of the synthesized samples has been evaluated in methanol-to-olefins reaction using a fixed bed reactor. Firstly, we studied the effect of reaction temperature on catalysts activity over Run# 7 of Chapter 4. **Figure 46** shows the conversion and selectivities to light olefins at three different temperatures; 350, 400 and 450 °C. At all reaction temperatures, the conversion maintained 100% for the first 60 min with different selectivities to light olefins. At 120 min time on stream (TOS), the sample which was tested at 400 °C started to deactivate with a conversion decreased to around 80%, while for the samples tested at 350 and 450 °C the conversion was maintained above 92%. After 150 min, all catalysts suffered from severe deactivation. In term of stability, CHA sample tested at 350 °C is the most stable than at 400 and 450 °C. This finding is in agreement with our previous finding in chapter 3 and also with literature [58], in which zeolites with high amount of acid sites deactivate faster at higher temperatures.

Table 14 shows the products distribution of the MTO reaction over CHA zeolite catalyst evaluated at the three different temperatures. Obviously, both the reaction temperature and TOS had an influence on the selectivity toward light olefins. At the initial stage of the reaction (TOS = 10 min), the selectivity was maximum ca.80% when the reaction temperature was 450 °C, and minimum (ca. 42%) at 350 °C. Then, with the increase of TOS, the selectivity of olefins (especially ethylene) was increased at all reaction temperatures. In contrast to ethylene, the propylene selectivity was increased slightly at temperatures of 350 and 400 °C. However, when the temperature was 450 °C, the selectivity to propylene decreased with the increase of TOS. The increase in ethylene

selectivity at higher temperature was due to coke formation, which blocked the pore and disturbed the diffusion of propylene [58]. Another reason is the reactivity of propylene, which undergoes oligomerization reaction to form large oligomers, which cannot diffuse out through the CHA pore [86]. These large oligomers later crack to form ethylene [86].

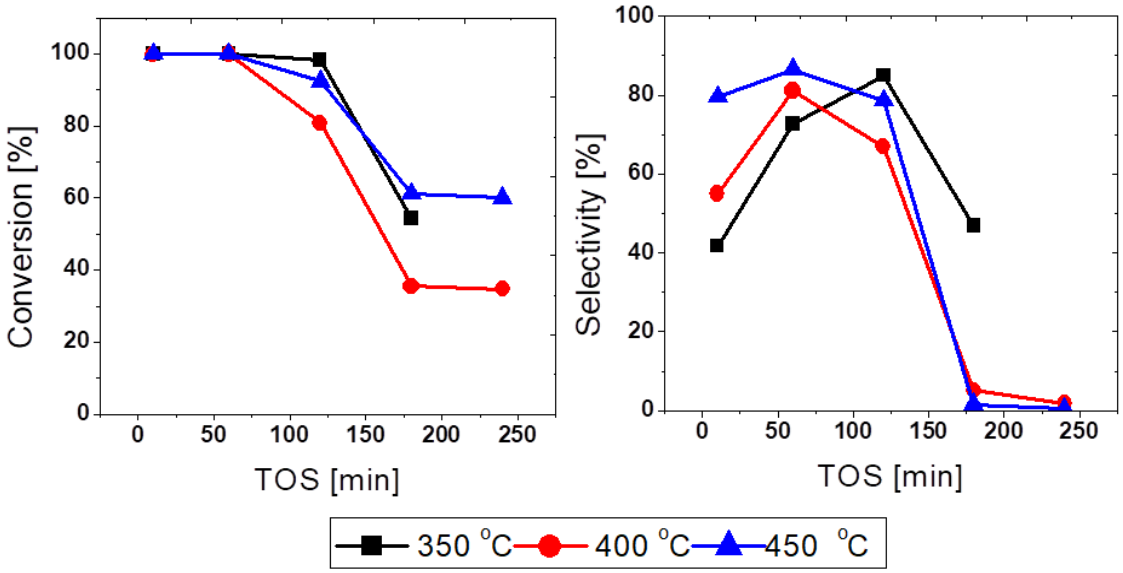

Figure 46 . Conversion of methanol and selectivity to total light olefins over CHA zeolite evaluated at different temperatures.

Table 14. Product distribution of CHA zeolite (Run# 7) at different temperatures.

Temperature (°C)	**350**			**400**			**450**		
TOS (min)	**10**	**60**	**120**	**10**	**60**	**120**	**10**	**60**	**120**
Conv. (%)	**100**	**100**	**98.2**	**99.9**	**100**	**80.8**	**100**	**100**	**92.5**
Propene (%)	14.53	32.93	30.34	20.05	30.15	17.4	23.13	21.99	15.01
Ethene (%)	18.6	30.8	48.6	30.6	45	46.7	53.2	61.5	60.5
Total Olefins (%)	41.76	72.68	84.96	54.98	81.11	66.82	79.6	86.54	78.7
DME (%)	0	0	9.66	0	0	28.93	0	0	10.68
Paraffins (%)	56.39	24.86	4.38	45.02	17.37	4.02	19.87	12.63	10.12
C4s (%)	8.6	8.9	6	5.8	6	2.7	3.3	3.1	3.2
Over C5s (%)	1.85	2.46	1.01	0	1.52	0.24	0.53	0.83	0.5

MTO reaction was also performed over the CHA zeolite synthesized at 400 rpm to investigate the effect of stirring on the catalyst activity. The performance of the catalyst at higher stirring rate was slightly better in term of selectivity to light olefins than the one at lower stirring rate, as shown in **Figure 47**. For example, the maximum total olefins selectivity was 92.26 over the 400 rpm catalyst, while over the 50 rpm catalyst, the selectivity was 84.96, as shown in **Table 15**. This relative enhancement in the catalyst activity is due to the slightly lower acidity of the sample prepared at 400 rpm, as presented in **Table 13** and **Figure 42**.

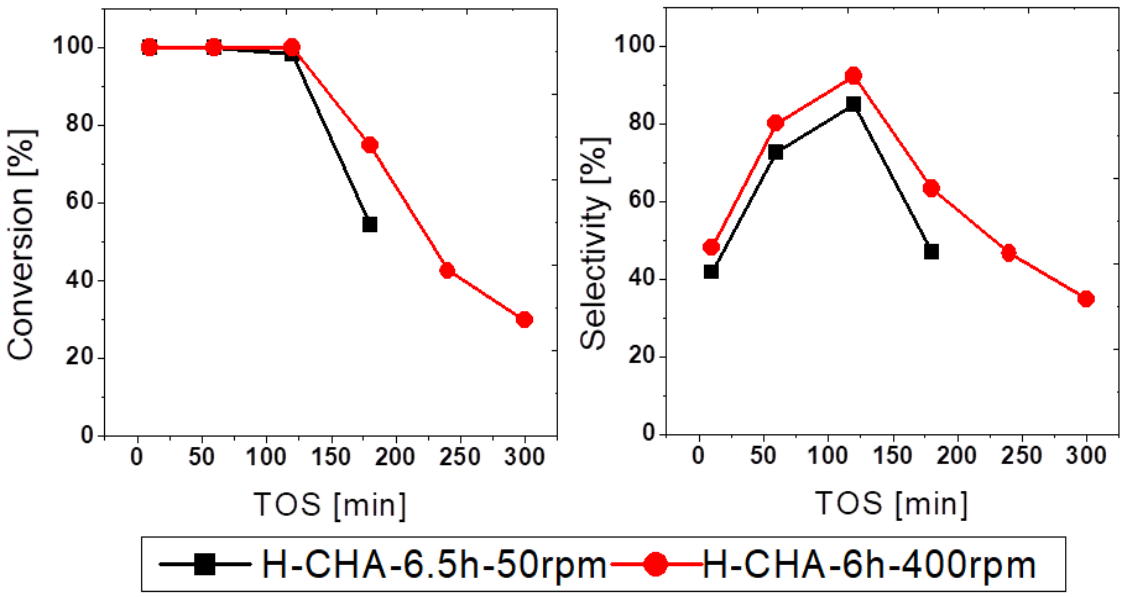

Figure 47. Methanol conversion and selectivity to total light olefins synthesized at different stirring rates; H-CHA-6.5h-50rpm (Run# 7) and H-CHA-6h-400rpm (Run# 9)

Table 15. Product distribution of CHA samples incorporated with boron at reaction temperature of 350 °C.

Sample	CHA-6h-400rpm (Run# 9)			Si/B =20 (Run# 13)			Si/B =13 (Run# 14)		
TOS (min)	**10**	**120**	**180**	**10**	**60**	**120**	**10**	**60**	**120**
Conv. (%)	**100**	**100**	**74.8**	**100**	**100**	**96.1**	**100**	**72.9**	**43.6**
Propene (%)	16.7	39.13	22.85	14.5	34.2	26.43	27.41	16.79	0
Ethene (%)	22.4	45.4	33.41	18	33	48	34.2	23.7	3.8
Total olefins (%)	48.09	92.26	63.34	40.93	75.7	80.93	71.49	44.94	4.48
DME (%)	0	0.783	32.5	0	0	13.83	0	50.68	92
Paraffins (%)	50.39	5.8	3.5	57.27	22.22	4.04	25.08	3.77	3.52
C4s (%)	9	7.7	4.12	8.5	9	6.5	9.9	4.5	0.7
Over C5s (%)	1.52	1.16	0.66	1.79	2.08	1.2	3.43	0.62	0

Table 16 shows a comparison of products distribution between the CHA synthesized under microwave radiation and the CHA synthesized using conventional heating [44] at the same reaction conditions and gel composition. Obviously, our Al-rich CHA zeolite showed a higher stability and, relatively, higher selectivity to light olefins. The higher stability of our catalyst might be because of the slightly lower amount of acid sites as presented in **Table 13**. The boron incorporation had a negligible effect on the selectivity and catalyst stability. At lower boron incorporation (Si/B =20), as shown in **Table 15** and **Figure 48**, methanol conversion and total olefins selectivity were decreased from 100 to 96% and from 92.3 to 80.9%, respectively as compared to the parent CHA zeolite (Run# 9). Although a higher content of boron incorporation decreased the stability of the catalyst, the sample showed higher selectivity to olefins at the initial of the reaction (TOS= 10 min) as compared to the parent CHA catalyst. Qingium Zhu et. al[114] synthesized a borosilicate CHA zeolite which was evaluated in the MTO reaction. In agreement with our finding, the incorporation of boron of the borosilicate CHA reduced the catalyst stability and activity toward light olefins as shown in **Figure 49**.

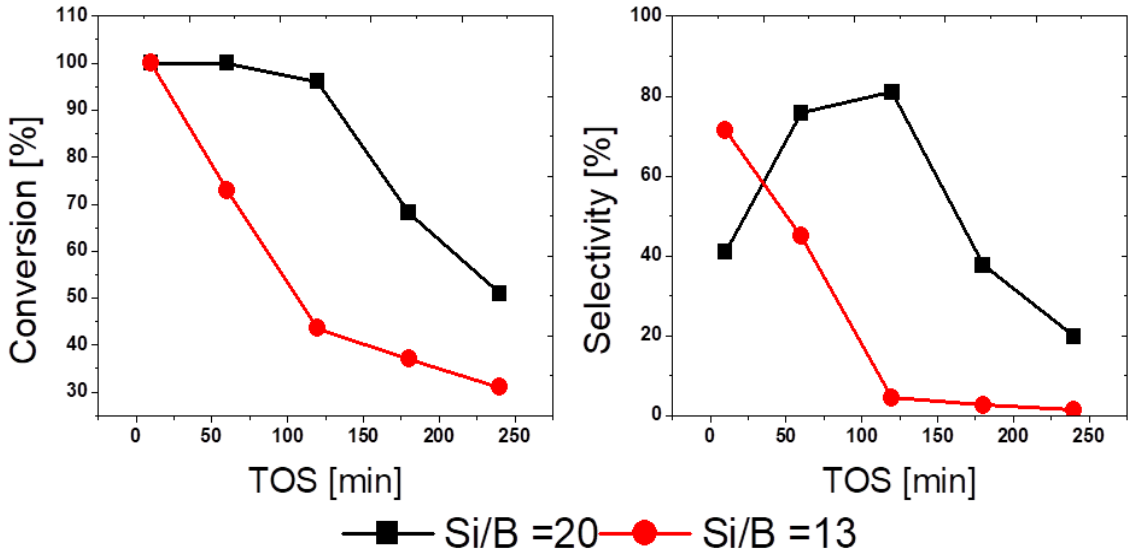

Figure 48. Methanol conversion and selectivity to total light olefins over samples synthesized at different concentrations of boron; Si/B =20 (Run# 13) and Si/B =13 (Run#14).

Table 16. Physical properties and product distribution of the MTO reaction of CHA zeolites synthesized using conventional and microwave (MAHyS) heating.

Sample	Conversion	Acid amount [mmol g^{-1}]	Selectivity		Ref.
			$C2^{=}$	$C3^{=}$	
T-CHA	100	0.90	31.9	36.8	[44]
Run# 6	100	0.85	30.8	32.9	Current work
Run# 9*	100	0.76	45.4	39.1	Current work

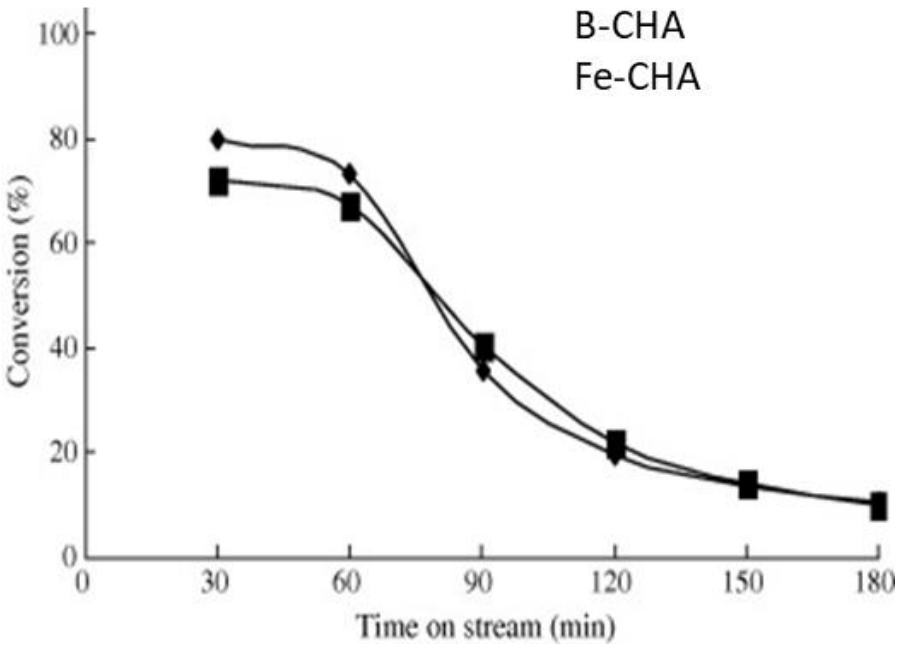

Figure 49. Conversion of methanol over borosilicate and ferrous-silicate CHA zeolites

4.3.7 Conclusions

Up to our knowledge, for the first time, microwave irradiation has been utilized to synthesize an OSDA-Free Al rich CHA zeolite. Microwave heating decreased the crystallization time from 24 to 6 h. The synthesized CHA zeolites samples showed excellent activity in the MTO reaction. The selectivity to lower olefins was linked to the higher reaction temperatures and TOS. At higher temperature, 450 °C, the synthesized CHA zeolite was more selective to light olefins especially at the beginning of the reaction. Similarly, as TOS increased, the selectivity to light olefins was increased as well. This increase in selectivity with TOS was not significant at a reaction temperature of 450 °C. The highest boron incorporated CHA catalyst increased only the amount of

olefins produced at the beginning of the reaction, while the low content boron incorporation did not contribute significantly to the activity of CHA catalyst.

4.3.8 Acknowledgements

The authors would like to acknowledge the funding provided by KACST through NSTIP project # 13-NAN1702-04.

CHAPTER 5

Conclusions and Recommendations

This chapter will restate the conclusions of the two approach used in this study, and will give recommendations.

For the first approach, Cost-effective Al-rich CHA zeolite was successfully synthesized without using templates. The CHA zeolite was formed under different experimental conditions than what was reported in the literature. The Si/Al ratios of the gel had a crucial role in the formation of pure CHA, with a slight increase in Si/Al ratio (Si/Al=3.3), impurities of other phase (MER) were formed. Higher H_2O/SiO_2 ratio affected the crystallinity of CHA zeolite, while lower H_2O/SiO_2 ratio favored the formation of the MER phase. The aging time influenced both the particles' shape and size, and the rate of crystallization. At longer aging time, smaller CHA particles were synthesized with shorter crystallization time. The synthesized CHA zeolite in H-form (H-CHA) showed a high surface area and pore volume than the K-form (K-CHA). The reaction evaluation mesurements of H-CHA showed that the Al-rich CHA zeolite was very selective to olefins. The deactivation rate and initial selectivity to olefins were linked to the reaction temperature. The selectivity of the Al-rich CHA zeolite in the MTO reaction was comparable to the commercial ZSM-5 and SSZ-13catalysts. Ni, Mg, Fe, B and Zn were successfully incorporated to the CHA framework by an in-situ method. The incorporation of metals affected negatively the stability of the catalyst. However, the

metal incorporation had a significant enhancement to the total olefins selectivity at the beginning of the reaction.

For the second approach, up to our knowledge, for the first time, microwave irradiation has been utilized to synthesize an OSDA-Free Al rich CHA zeolite. Microwave heating decreased the crystallization time from 24 to 6 h. The synthesized CHA zeolites samples showed excellent activity in the MTO reaction. The selectivity to lower olefins was linked to the higher reaction temperatures and TOS. At higher temperature, 450 °C, the synthesized CHA zeolite was more selective to light olefins especially at the beginning of the reaction. Similarly, as TOS increased, the selectivity to light olefins was increased as well. This increase in selectivity with TOS was not significant at a reaction temperature of 450 °C. The highest boron incorporated CHA catalyst increased only the amount of olefins produced at the beginning of the reaction, while the low content boron incorporation did not contribute significantly to the activity of CHA catalyst.

5.1 Recommendations

MOT reaction is one the most important reactions that significantly depends on the catalyst's acidity, morphology and topology. CHA zeolite is the most suitable topology for the MTO reaction, in which the small pore opening of the CHA cage strictly hinders the formation of aromatics. Regarding the acidity and morphology, the catalysts that we developed suffered from the fast deactivation due to the high alumina content which gives rise to higher acidity. Thus, to have a more efficient CHA catalyst, further modifications are highly recommended. We recommend post-modifications to the CHA catalyst to reduce the alumina content. The partial removal of aluminum can be achieved by applying acid and steam treatments. Moreover, impregnation of alkaline metals is

highly recommended for acidity reduction. Finally, we recommend fabricating CHA catalysts with small particles size by applying ball milling technique.

Appendix

Symbol	Detail preparation method	Reference
A	The prepared aluminosilicate gel with the molar composition of 3.1-3.8Na2O:1.0Al2O3:10–35SiO2:200H2O:2.0–3.0Cu-TEPA was prepared by mixing 0.514g of sodium aluminate and 0.380 g of sodium hydroxide in required amount of demineralized water. Then, 1.149 g of copper sulfate pentahydrate (CuSO4.H2O) was added to the previous solution. Next, 1.07g of TEPA was added and stirred for 1 hr. Following this, 3.6 ml of a 31.6wt.% silica solution was added dropwise under vigorous stirring for 2 or 3 hours. Finally, the final gel was transferred to a Teflon and heated for 3 up to 6 days at 140 °C.	[45, 46]
B		
C	The CHA zeolite was prepared by the conversion of FAU zeolite with the presence of benzyl trimethyl ammonium hydroxide as SDA. The FAU zeolite was firstly prepared from NH4-Zeolite with Si/Al =2.8 and the then prepared FAU was dealuminated using steam and H2SO4. Seeds with Si/Al =16 have been used to assist the synthesis. In detail, educate amount of dealuminated FAU zeolite was added to a solution containing of the BTMAOH and sodium hydroxide or sodium chloride, optional. Finally, the final mixture was transferred to Teflon and hydrothermally treated at 125 ℃ for 7-21 days.	[48]
D	CHA zeolite was prepared from amorphous aluminosilicate gel using SSZ-13 seeds. The amorphous gel having a molar composition of 1 SiO2: 0.05 Al2O3: 0.40 Na2O: 0.09 K2O: 100 H2O prepared, firstly, by adding the aluminum isopropoxide to aqueous solution of sodium hydroxide and potassium hydroxide. After string for 1 h, fumed silica was added and stirred for have and hour. Following this, SSZ-13 seeds 20wt.% of the silica were added to the final solution and stirred for 10 minutes. Finally the gel was transferred to Teflon-lined stailess steel autoclave and hydrothermally heated with tumbling rate of 20 rpm for one day.	[44]
E	High silica CHA was synthesized using TEA as OSDA and FAU zeolite (CBV-720) as source of alumina and silica. The CHA formed at temperatures of 160 and 140 at various gel compositions. The effect of TEAOH, H2O and NaOH was studied. TEAOH/Si =0.4 and NaOH/Si =0.2 and at different water content (H2O/Si = 5,15 and 25) CHA was obtained. The PH of the synthesis gel was 12.7.	[49]

F	CHA zeolite was prepared by the conversion of FAU zeolite, HY zeolite (Si/Al = 2.8, TOSOH). The synthesis of CHA zeolite was achieved by mixing the HY-zeolite to an aqueous solution of potassium hydroxide with a final gel molar composition of 5.5 SiO2–1.0 Al2O3–4.0 KOH–224 H2O. The final mixture was stirred for 2 hours and then transferred to a polypropylene bottle, and heated at 100 °C for 5 days.	[50]
G	Chabazite SSZ-13 with a gel composition of 10 TMAdOH: 10 Na2O:3 Al2O3: 100 SiO2: 4400 H2O was synthesized by first mixing 2 g of 1M of sodium hydroxide, 2g of deionized water and 4g of 0.5M of TMAdOH. Then, 0.05g of aluminum hydroxide was added to the later solution and stirred vigorously for 30 minutes. After that, a 0.6g of fumed silica was added and the solution stirred at room temperature till it homogenized. Finally, the final gel was transferred to Teflon-lined stainless autoclave and heated at 160 °C for 4 days.	[51]
H	SSZ-13 was prepared by first mixing a solution composing of 0.45 g Na_2 O, 1.46 g SiO_2, 3.10 g H_2 O with 6 ml of water and 1.56 g of the TMADAI ion. Then, another solution composing of 6 ml H2O 0.24 g of $Al_2(SO_4)_3.16H_2O$ and 0.67 g NaOH added to the first solution and stirred till homogeneous gel was obtained. After that, the final gel was transferred to a stainless steel pressure reactor and crystallized for 6 days at 140 °C.	[52]
I	Materials:Ammonium fluoride, sodium fluoride and potassium fluoride (sigma Aldrich) Molar composition: 1SiO2:xAl2O3: 0.39K2O:yNH4F:35H2O,x=0.05-0.33, y=0.1-0.5. Typical synthesis: an amount of aluminum hydroxide was added to an alkaline solution containing (7.0 g potassium hydroxide +67.6g of demineralized water) under heating at 80 °C. Then cold to room temperature. After that, an amount of ammonium fluoride and Ludox TM-40 colloidal silica (Sigma–Aldrich, 40 wt.% SiO2 water suspension) were added in the clear alkaline aluminate solution. This mixture stirred at room temperature for 6h and then transferred to Teflon and hydrothermally treated at 160 °C for several time.	[44]
J	20g of Hi-Sil 233 (source of silicon oxide) placed in a vessel. Reheis F-2000 alumina (1.7 grams) was dissolved in 5 grams of a 50% aqueous NaOH solution and then added to the Hi-Sil 233 in the vessel. The resulting mixture is mixed thoroughly. To the resulting mixture was added 1 gram of SSZ-13 seed crystals, and the mixture thoroughly mixed again for 5 minutes. 23.3 Grams of a 2.36 mmole/gram solution of benzyl trimethylammonium hydroxide was added slowly to the mixture while mixing. 8 Grams of D.I. water was added slowly and the resulting mixture mixed thoroughly for 1 hour. The resulting mixture was in the form of slightly wet granules with a volatiles content of 59.6%.	

ABW	ACO	AEI	AEL	AEN	AET	AFG	AFI	AFN	AFO	AFR	AFS	AFT	AFV	AFX
AFY	AHT	ANA	APC	APD	AST	ASV	ATN	ATO	ATS	ATT	ATV	AVL	AWO	AWW
BCT	BEC	BIK	BOF	BOG	BOZ	BPH	BRE	BSV	CAN	CAS	CDO	CFI	CGF	CGS
CHA	-CHI	-CLO	CON	CSV	CZP	DAC	DDR	DFO	DFT	DOH	DON	EAB	EDI	EEI
EMT	EON	EPI	ERI	ESV	ETL	ETR	EUO	EZT	FAR	FAU	FER	FRA	GIS	GIU
GME	GON	GOO	HEU	IFO	IFR	-IFU	IFW	IFY	IHW	IMF	IRN	IRR	-IRY	ISV
ITE	ITG	ITH	ITR	ITT	-ITV	ITW	IWR	IWS	IWV	IWW	JBW	JNT	JOZ	JRY
JSN	JSR	JST	JSW	KFI	LAU	LEV	LIO	-LIT	LOS	LOV	LTA	LTF	LTJ	LTL
LTN	MAR	MAZ	MEI	MEL	MEP	MER	MFI	MFS	MON	MOR	MOZ	MSE	MSO	MTF
MTN	MTT	MTW	MVY	MWF	MWW	NAB	NAT	NES	NON	NPO	NPT	NSI	OBW	OFF
OKO	OSI	OSO	OWE	-PAR	PAU	PCR	PHI	PON	POS	PSI	PUN	RHO	-RON	RRO
RSN	RTE	RTH	RUT	RWR	RWY	SAF	SAO	SAS	SAT	SAV	SBE	SBN	SBS	SBT
SEW	SFE	SFF	SFG	SFH	SFN	SFO	SFS	SFW	SGT	SIV	SOD	SOF	SOS	SSF
SSY	STF	STI	STT	STW	-SVR	SVV	SZR	TER	THO	TOL	TON	TSC	TUN	UEI
UFI	UOS	UOV	UOZ	USI	UTL	UWY	VET	VFI	VNI	VSV	WEI	-WEN	YUG	ZON

Figure A1. Different frameworks of zeolites recorded in the international zeolites association

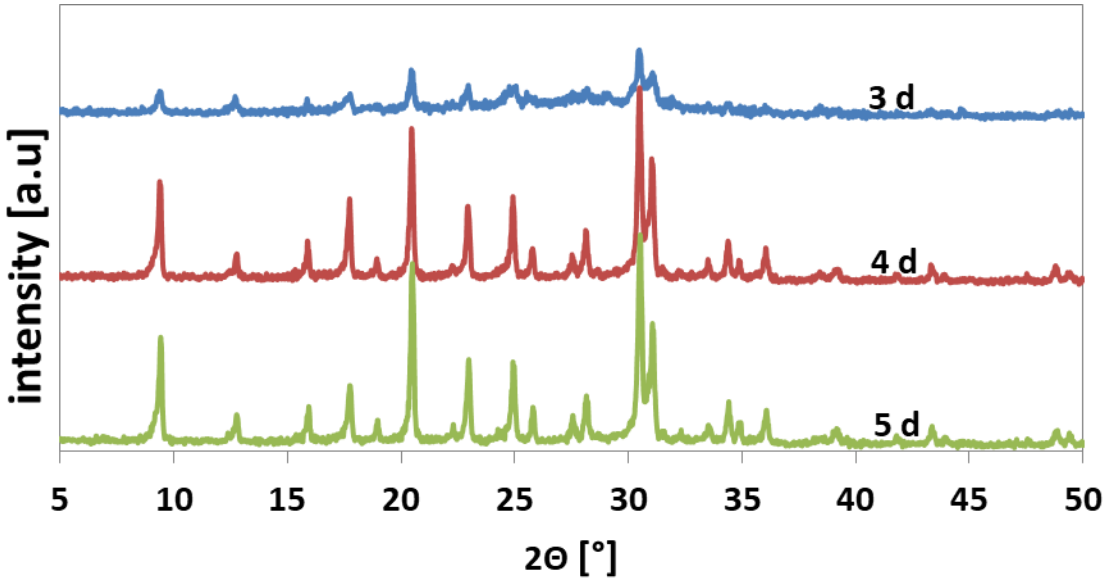

Figure A2. XRD patterns of samples prepared at aging time of 12 h for different crystallization times with H2O/SiO2 of 15.

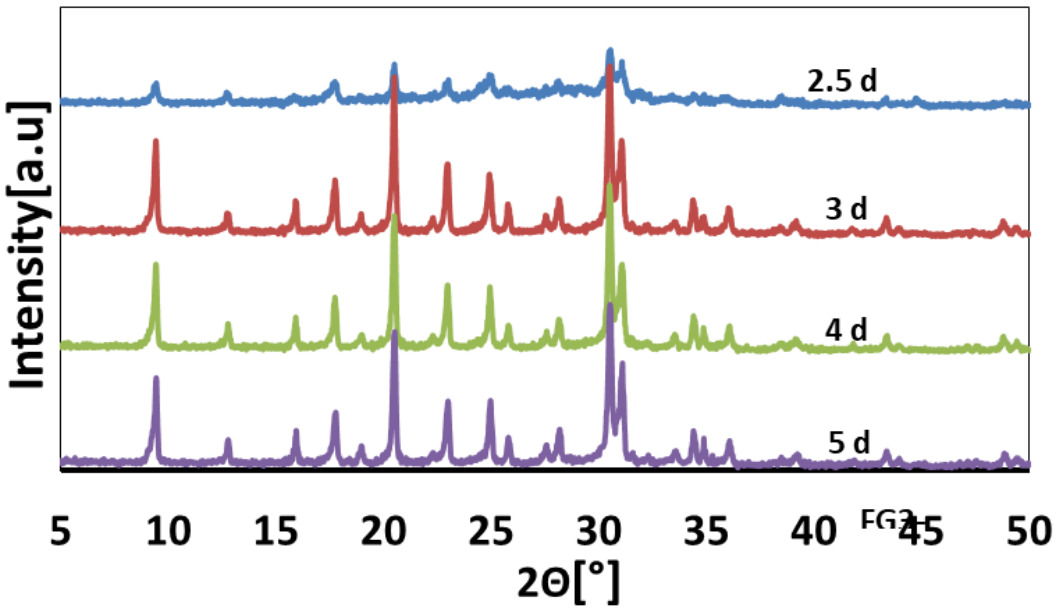

Figure A3.XRD patterns of samples prepared at aging time of 24 h for different crystallization times, H2O/SiO2 =15

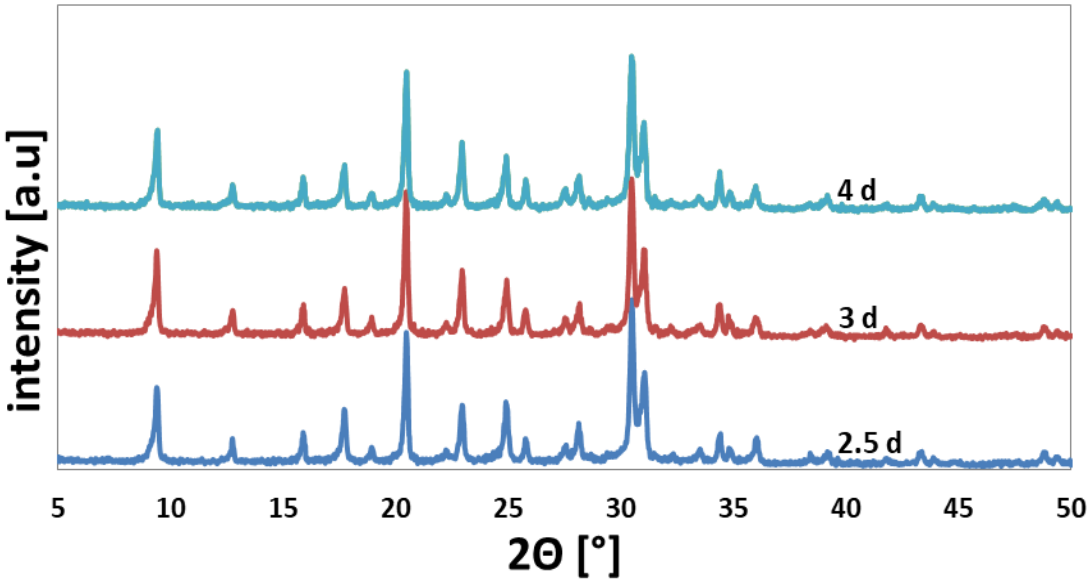

Figure A4. XRD patterns of samples prepared at aging time of 48h at different crystallization times, H2O/SiO2 =15

References

[1] J. Lefevere, S. Mullens, V. Meynen, and J. Van Noyen, "Structured catalysts for methanol-to-olefins conversion: a review," *Chemical Papers,* vol. 68, pp. 1143-1153, 2014.

[2] T. Ren, M. Patel, and K. Blok, "Olefins from conventional and heavy feedstocks: Energy use in steam cracking and alternative processes," *Energy,* vol. 31, pp. 425-451, 3// 2006.

[3] Y. Xiang, J. Zhou, B. Lin, X. Xue, X. Tian, and Z. Luo, "Exergetic evaluation of renewable light olefins production from biomass via synthetic methanol," *Applied Energy,* vol. 157, pp. 499-507, 11/1/ 2015.

[4] I. Amghizar, L. A. Vandewalle, K. M. Van Geem, and G. B. Marin, "New Trends in Olefin Production," *Engineering,* vol. 3, pp. 171-178, 4// 2017.

[5] OPEC, Nexant-EU-OPEC Energy Dialogue, vienna, Presentation2014.

[6] W. Dai, X. Wang, G. Wu, N. Guan, M. Hunger, and L. Li, "Methanol-to-Olefin Conversion on Silicoaluminophosphate Catalysts: Effect of Brønsted Acid Sites and Framework Structures," *ACS Catalysis,* vol. 1, pp. 292-299, 2011/04/01 2011.

[7] I. Yarulina, J. Goetze, C. Gucuyener, L. van Thiel, A. Dikhtiarenko, J. Ruiz-Martinez, *et al.*, "Methanol-to-olefins process over zeolite catalysts with DDR topology: effect of composition and structural defects on catalytic performance," *Catalysis Science & Technology,* vol. 6, pp. 2663-2678, 2016.

[8] F. J. Keil, "Methanol-to-hydrocarbons: process technology," *Microporous and Mesoporous Materials,* vol. 29, pp. 49-66, 6// 1999.

[9] P. Tian, Y. Wei, M. Ye, and Z. Liu, "Methanol to Olefins (MTO): From Fundamentals to Commercialization," *ACS Catalysis,* vol. 5, pp. 1922-1938, 2015/03/06 2015.

[10] C. D. Chang and A. J. Silvestri, "The conversion of methanol and other O-compounds to hydrocarbons over zeolite catalysts," *Journal of Catalysis,* vol. 47, pp. 249-259, 1977/05/01 1977.

[11] C. D. Chang, "Hydrocarbons from Methanol," *Catalysis Reviews,* vol. 25, pp. 1-118, 1983/01/01 1983.

[12] M. Stöcker, "Methanol-to-hydrocarbons: catalytic materials and their behavior1," *Microporous and Mesoporous Materials,* vol. 29, pp. 3-48, 6// 1999.

[13] J. Q. Chen, A. Bozzano, B. Glover, T. Fuglerud, and S. Kvisle, "Recent advancements in ethylene and propylene production using the UOP/Hydro MTO process," *Catalysis Today,* vol. 106, pp. 103-107, 10/15/ 2005.

[14] J. F. Haw, W. Song, D. M. Marcus, and J. B. Nicholas, "The Mechanism of Methanol to Hydrocarbon Catalysis," *Accounts of Chemical Research,* vol. 36, pp. 317-326, 2003/05/01 2003.

[15] W. Song, Y. Wei, and Z. Liu, "Chemistry of the Methanol to Olefin Conversion," in *Zeolites in Sustainable Chemistry: Synthesis, Characterization and Catalytic Applications*, F.-S. Xiao and X. Meng, Eds., ed Berlin, Heidelberg: Springer Berlin Heidelberg, 2016, pp. 299-346.

[16] U. Olsbye, S. Svelle, M. Bjørgen, P. Beato, T. V. W. Janssens, F. Joensen, *et al.*, "Conversion of Methanol to Hydrocarbons: How Zeolite Cavity and Pore Size Controls Product Selectivity," *Angewandte Chemie International Edition,* vol. 51, pp. 5810-5831, 2012.
[17] N. Nesterenko, J. Aguilhon, P. Bodart, D. Minoux, and J. P. Dath, "Chapter 5 - Methanol to Olefins: An Insight Into Reaction Pathways and Products Formation A2 - Sels, Bert F," in *Zeolites and Zeolite-Like Materials*, L. M. Kustov, Ed., ed Amsterdam: Elsevier, 2016, pp. 189-263.
[18] M. Ye, H. Li, Y. Zhao, T. Zhang, and Z. Liu, "Chapter Five - MTO Processes Development: The Key of Mesoscale Studies," in *Advances in Chemical Engineering*. vol. 47, G. B. Marin and J. Li, Eds., ed: Academic Press, 2015, pp. 279-335.
[19] G. Busca, "Chapter 7 - Zeolites and Other Structurally Microporous Solids as Acid–Base Materials," in *Heterogeneous Catalytic Materials*, ed Amsterdam: Elsevier, 2014, pp. 197-249.
[20] R. Martinez-Franco, M. Moliner, J. R. Thogersen, and A. Corma, *ChemCatChem*, vol. 5, p. 3316, 2013.
[21] R. Xu, W. Pang, J. Yu, Q. Huo, and J. Chen, "Introduction," in *Chemistry of Zeolites and Related Porous Materials*, ed: John Wiley & Sons, Ltd, 2010, pp. 1-18.
[22] R. Xu, W. Pang, J. Yu, Q. Huo, and J. Chen, "Structural Chemistry of Microporous Materials," in *Chemistry of Zeolites and Related Porous Materials*, ed: John Wiley & Sons, Ltd, 2010, pp. 19-116.
[23] C. Baerlocher, L. B. McCusker, and D. H. Olson, "Introduction and explanatory notes," in *Atlas of Zeolite Framework Types (Sixth Edition)*, ed Amsterdam: Elsevier Science B.V., 2007, pp. 3-11.
[24] J. Klinowski, "Solid-state NMR studies of molecular sieve catalysts," *Chemical Reviews*, vol. 91, pp. 1459-1479, 1991/11/01 1991.
[25] M. Boronat and A. Corma, "Factors Controlling the Acidity of Zeolites," *Catalysis Letters*, vol. 145, pp. 162-172, January 01 2015.
[26] K. J. Farnworth and P. J. O'Malley, "Brønsted acid site models for zeolites: a comparative density functional, Hartree-Fock and semi-empirical molecular orbital study," *Electronic Journal of Theoretical Chemistry*, vol. 1, pp. 172-182, 1996.
[27] D. Coster, A. L. Blumenfeld, and J. J. Fripiat, "Lewis Acid Sites and Surface Aluminum in Aluminas and Zeolites: A High-Resolution NMR Study," *The Journal of Physical Chemistry*, vol. 98, pp. 6201-6211, 1994/06/01 1994.
[28] J. Huang, Y. Jiang, V. R. R. Marthala, B. Thomas, E. Romanova, and M. Hunger, "Characterization and Acidic Properties of Aluminum-Exchanged Zeolites X and Y," *The Journal of Physical Chemistry C*, vol. 112, pp. 3811-3818, 2008/03/01 2008.
[29] B. A. Aufdembrink, D. P. Dee, P. L. McDaniel, T. Mebrahtu, and T. L. Slager, "Spectroscopic Characterization of Acidity in Chabazite," *The Journal of Physical Chemistry B*, vol. 107, pp. 10025-10031, 2003/09/01 2003.
[30] G. Nasser, T. Kurniawan, K. Miyake, A. Galadima, Y. Hirota, N. Nishiyama, *et al.*, "Dimethyl ether to olefins over dealuminated mordenite (MOR) zeolites

derived from natural minerals," *Journal of Natural Gas Science and Engineering*, vol. 28, pp. 566-571, 2016/01/01/ 2016.
[31] G. A. Nasser, T. Kurniawan, T. Tago, I. A. Bakare, T. Taniguchi, Y. Nakasaka, *et al.*, "Cracking of n-hexane over hierarchical MOR zeolites derived from natural minerals," *Journal of the Taiwan Institute of Chemical Engineers*, vol. 61, pp. 20-25, 2016/04/01/ 2016.
[32] T. Kurniawan, O. Muraza, A. S. Hakeem, and A. M. Al-Amer, "Mechanochemical Route and Recrystallization Strategy To Fabricate Mordenite Nanoparticles from Natural Zeolites," *Crystal Growth & Design*, vol. 17, pp. 3313-3320, 2017/06/07 2017.
[33] C. Martínez and A. Corma, "5.05 - Zeolites A2 - Reedijk, Jan," in *Comprehensive Inorganic Chemistry II (Second Edition)*, K. Poeppelmeier, Ed., ed Amsterdam: Elsevier, 2013, pp. 103-131.
[34] F. L. Raúl, "Introduction to the Structural Chemistry of Zeolites," in *Handbook of Zeolite Science and Technology*, ed: CRC Press, 2003.
[35] J. Weitkamp and M. Hunger, "Preparation of zeolites via the dry-gel synthesis method," in *Studies in Surface Science and Catalysis*. vol. 155, A. Gamba, C. Colella, and S. Coluccia, Eds., ed: Elsevier, 2005, pp. 1-12.
[36] C. A. Fyfe, J. M. Thomas, J. Klinowski, and G. C. Gobbi, "Magic-Angle-Spinning NMR (MAS-NMR) Spectroscopy and the Structure of Zeolites," *Angewandte Chemie International Edition in English*, vol. 22, pp. 259-275, 1983.
[37] C. Suryanarayana and M. G. Norton, "X-Rays and Diffraction," in *X-Ray Diffraction: A Practical Approach*, ed Boston, MA: Springer US, 1998, pp. 3-19.
[38] *Microscopes techniques*. Available: http://nptel.ac.in/courses/102103015/module3/lec2/2.html
[39] Y. Kumita, J. Gascon, E. Stavitski, J. A. Moulijn, and F. Kapteijn, "Shape selective methanol to olefins over highly thermostable DDR catalysts," *Applied Catalysis A: General*, vol. 391, pp. 234-243, 1/4/ 2011.
[40] J. W. Park, J. Y. Lee, K. S. Kim, S. B. Hong, and G. Seo, "Effects of cage shape and size of 8-membered ring molecular sieves on their deactivation in methanol-to-olefin (MTO) reactions," *Applied Catalysis A: General*, vol. 339, pp. 36-44, 4/15/ 2008.
[41] Y. Ji, M. A. Deimund, Y. Bhawe, and M. E. Davis, "Organic-Free Synthesis of CHA-Type Zeolite Catalysts for the Methanol-to-Olefins Reaction," *ACS Catalysis*, vol. 5, pp. 4456-4465, 2015/07/02 2015.
[42] N. Yamanaka, M. Itakura, Y. Kiyozumi, Y. Ide, M. Sadakane, and T. Sano, "Acid stability evaluation of CHA-type zeolites synthesized by interzeolite conversion of FAU-type zeolite and their membrane application for dehydration of acetic acid aqueous solution," *Microporous and Mesoporous Materials*, vol. 158, pp. 141-147, 8/1/ 2012.
[43] R. Nedyalkova, C. Montreuil, C. Lambert, and L. Olsson, "Interzeolite Conversion of FAU Type Zeolite into CHA and its Application in NH3-SCR," *Topics in Catalysis*, vol. 56, pp. 550-557, 2013.
[44] H. Imai, N. Hayashida, T. Yokoi, and T. Tatsumi, "Direct crystallization of CHA-type zeolite from amorphous aluminosilicate gel by seed-assisted method in the

absence of organic-structure-directing agents," *Microporous and Mesoporous Materials,* vol. 196, pp. 341-348, 9/15/ 2014.
[45] L. Ren, Y. Zhang, S. Zeng, L. Zhu, Q. Sun, H. Zhang, *et al.*, "Design and Synthesis of a Catalytically Active Cu-SSZ-13 Zeolite from a Copper-Amine Complex Template," *Chinese Journal of Catalysis,* vol. 33, pp. 92-105, 1// 2012.
[46] L. Ren, L. Zhu, C. Yang, Y. Chen, Q. Sun, H. Zhang, *et al.*, "Designed copper-amine complex as an efficient template for one-pot synthesis of Cu-SSZ-13 zeolite with excellent activity for selective catalytic reduction of NOx by NH3," *Chemical Communications,* vol. 47, pp. 9789-9791, 2011.
[47] R. Xu, R. Zhang, N. Liu, B. Chen, and S. Zhang Qiao, "Template Design and Economical Strategy for the Synthesis of SSZ-13 (CHA-Type) Zeolite as an Excellent Catalyst for the Selective Catalytic Reduction of NOx by Ammonia," *ChemCatChem,* vol. 7, pp. 3792-3792, 2015.
[48] M. Itakura, I. Goto, A. Takahashi, T. Fujitani, Y. Ide, M. Sadakane, *et al.*, "Synthesis of high-silica CHA type zeolite by interzeolite conversion of FAU type zeolite in the presence of seed crystals," *Microporous and Mesoporous Materials,* vol. 144, pp. 91-96, 10// 2011.
[49] N. Martin, M. Moliner, and A. Corma, "High yield synthesis of high-silica chabazite by combining the role of zeolite precursors and tetraethylammonium: SCR of NOx," *Chemical Communications,* vol. 51, pp. 9965-9968, 2015.
[50] Q. Zhu, J. N. Kondo, R. Ohnuma, Y. Kubota, M. Yamaguchi, and T. Tatsumi, "The study of methanol-to-olefin over proton type aluminosilicate CHA zeolites," *Microporous and Mesoporous Materials,* vol. 112, pp. 153-161, 7/1/ 2008.
[51] L. Wu, V. Degirmenci, P. C. M. M. Magusin, N. J. H. G. M. Lousberg, and E. J. M. Hensen, "Mesoporous SSZ-13 zeolite prepared by a dual-template method with improved performance in the methanol-to-olefins reaction," *Journal of Catalysis,* vol. 298, pp. 27-40, 2// 2013.
[52] S. I. Zones, "Zeolite SSZ-13 and its method of preparation," ed: Google Patents, 1985.
[53] B. Liu, Y. Zheng, N. Hu, T. Gui, Y. Li, F. Zhang, *et al.*, "Synthesis of low-silica CHA zeolite chabazite in fluoride media without organic structural directing agents and zeolites," *Microporous and Mesoporous Materials,* vol. 196, pp. 270-276, 9/15/ 2014.
[54] S. J. Miller and L. T. Yuen, "Preparation of molecular sieve ssz-13," ed: Google Patents, 2008.
[55] L. Xie, F. Liu, L. Ren, X. Shi, F.-S. Xiao, and H. He, "Excellent Performance of One-Pot Synthesized Cu-SSZ-13 Catalyst for the Selective Catalytic Reduction of NOx with NH3," *Environmental Science & Technology,* vol. 48, pp. 566-572, 2014/01/07 2014.
[56] G. Seo, J.-H. Kim, and H.-G. Jang, "Methanol-to-Olefin Conversion over Zeolite Catalysts: Active Intermediates and Deactivation," *Catalysis Surveys from Asia,* vol. 17, pp. 103-118, 2013.
[57] S. Teketel, U. Olsbye, K.-P. Lillerud, P. Beato, and S. Svelle, "Selectivity control through fundamental mechanistic insight in the conversion of methanol to hydrocarbons over zeolites," *Microporous and Mesoporous Materials,* vol. 136, pp. 33-41, 2010/12/01/ 2010.

[58] F. Bleken, M. Bjørgen, L. Palumbo, S. Bordiga, S. Svelle, K.-P. Lillerud, *et al.*, "The Effect of Acid Strength on the Conversion of Methanol to Olefins Over Acidic Microporous Catalysts with the CHA Topology," *Topics in Catalysis,* vol. 52, pp. 218-228, 2009.
[59] M. Sedighi, M. Ghasemi, M. Sadeqzadeh, and M. Hadi, "Thorough study of the effect of metal-incorporated SAPO-34 molecular sieves on catalytic performances in MTO process," *Powder Technology,* vol. 291, pp. 131-139, 4// 2016.
[60] S. Ilias and A. Bhan, "Mechanism of the Catalytic Conversion of Methanol to Hydrocarbons," *ACS Catalysis,* vol. 3, pp. 18-31, 2013/01/04 2013.
[61] T.-Y. Park and G. F. Froment, "Kinetic Modeling of the Methanol to Olefins Process. 1. Model Formulation," *Industrial & Engineering Chemistry Research,* vol. 40, pp. 4172-4186, 2001/10/01 2001.
[62] S. R. Blaszkowski and R. A. van Santen, "Theoretical Study of the Mechanism of Surface Methoxy and Dimethyl Ether Formation from Methanol Catalyzed by Zeolitic Protons," *The Journal of Physical Chemistry B,* vol. 101, pp. 2292-2305, 1997/03/01 1997.
[63] D. Lesthaeghe, V. Van Speybroeck, G. B. Marin, and M. Waroquier, "Understanding the Failure of Direct C□C Coupling in the Zeolite-Catalyzed Methanol-to-Olefin Process," *Angewandte Chemie International Edition,* vol. 45, pp. 1714-1719, 2006.
[64] W. Song, D. M. Marcus, H. Fu, J. O. Ehresmann, and J. F. Haw, "An Oft-Studied Reaction That May Never Have Been: Direct Catalytic Conversion of Methanol or Dimethyl Ether to Hydrocarbons on the Solid Acids HZSM-5 or HSAPO-34," *Journal of the American Chemical Society,* vol. 124, pp. 3844-3845, 2002/04/01 2002.
[65] I. Yarulina, S. Bailleul, A. Pustovarenko, J. R. Martinez, K. D. Wispelaere, J. Hajek, *et al.*, "Suppression of the Aromatic Cycle in Methanol-to-Olefins Reaction over ZSM-5 by Post-Synthetic Modification Using Calcium," *ChemCatChem,* vol. 8, pp. 3057-3063, 2016.
[66] M. Westgård Erichsen, K. De Wispelaere, K. Hemelsoet, S. L. C. Moors, T. Deconinck, M. Waroquier, *et al.*, "How zeolitic acid strength and composition alter the reactivity of alkenes and aromatics towards methanol," *Journal of Catalysis,* vol. 328, pp. 186-196, 8// 2015.
[67] R. M. Dessau, "On the H-ZSM-5 catalyzed formation of ethylene from methanol or higher olefins," *Journal of Catalysis,* vol. 99, pp. 111-116, 1986/05/01/ 1986.
[68] R. M. Dessau and R. B. LaPierre, "On the mechanism of methanol conversion to hydrocarbons over HZSM-5," *Journal of Catalysis,* vol. 78, pp. 136-141, 1982/11/01/ 1982.
[69] T. Mole, J. A. Whiteside, and D. Seddon, "Aromatic co-catalysis of methanol conversion over zeolite catalysts," *Journal of Catalysis,* vol. 82, pp. 261-266, 1983/08/01/ 1983.
[70] I. M. Dahl and S. Kolboe, "On the reaction mechanism for propene formation in the MTO reaction over SAPO-34," *Catalysis Letters,* vol. 20, pp. 329-336, September 01 1993.
[71] L. J. Smith, H. Eckert, and A. K. Cheetham, "Site Preferences in the Mixed Cation Zeolite, Li,Na-Chabazite: A Combined Solid-State NMR and Neutron

Diffraction Study," *Journal of the American Chemical Society,* vol. 122, pp. 1700-1708, 2000/03/01 2000.
[72] I. Daems, R. Singh, G. Baron, and J. Denayer, "Length exclusion in the adsorption of chain molecules on chabazite type zeolites," *Chemical Communications,* pp. 1316-1318, 2007.
[73] A. Zecchina, S. Bordiga, J. G. Vitillo, G. Ricchiardi, C. Lamberti, G. Spoto, *et al.*, "Liquid Hydrogen in Protonic Chabazite," *Journal of the American Chemical Society,* vol. 127, pp. 6361-6366, 2005/05/01 2005.
[74] F. Gao, E. D. Walter, M. Kollar, Y. Wang, J. Szanyi, and C. H. F. Peden, "Understanding ammonia selective catalytic reduction kinetics over Cu/SSZ-13 from motion of the Cu ions," *Journal of Catalysis,* vol. 319, pp. 1-14, 11// 2014.
[75] L. Ren, L. Zhu, C. Yang, Y. Chen, Q. Sun, H. Zhang, *et al.*, "Designed copper-amine complex as an efficient template for one-pot synthesis of Cu-SSZ-13 zeolite with excellent activity for selective catalytic reduction of NOx by NH3," *Chemical Communications,* vol. 47, pp. 9789-9791, 2011.
[76] D. E. Akporiaye, I. M. Dahl, H. B. Mostad, and R. Wendelbo, "Aluminum Distribution in Chabazite: An Experimental and Computational Study," *The Journal of Physical Chemistry,* vol. 100, pp. 4148-4153, 1996/01/01 1996.
[77] S. Alfaro, C. Rodríguez, M. A. Valenzuela, and P. Bosch, "Aging time effect on the synthesis of small crystal LTA zeolites in the absence of organic template," *Materials Letters,* vol. 61, pp. 4655-4658, 9// 2007.
[78] M. Borel, M. Dodin, T. J. Daou, N. Bats, B. Harbuzaru, and J. Patarin, "SDA-Free Hydrothermal Synthesis of High-Silica Ultra-nanosized Zeolite Y," *Crystal Growth & Design,* vol. 17, pp. 1173-1179, 2017/03/01 2017.
[79] M. H. M. Ahmed, O. Muraza, and A. M. Al Amer, "Effect of synthesis parameters and ion exchange on crystallinity and morphology of EU-1 zeolite," *Journal of Alloys and Compounds,* vol. 617, pp. 408-412, 2014/12/25/ 2014.
[80] X. Yin, Z. Li, S. Wang, N. Chu, J. Yang, and J. Wang, "Hydrothermal synthesis of hierarchical zeolite T aggregates using tetramethylammonium hydroxide as single template," *Microporous and Mesoporous Materials,* vol. 201, pp. 247-257, 2015/01/01/ 2015.
[81] Q. Li, B. Mihailova, D. Creaser, and J. Sterte, "Aging effects on the nucleation and crystallization kinetics of colloidal TPA-silicalite-1," *Microporous and Mesoporous Materials,* vol. 43, pp. 51-59, 2001/03/01/ 2001.
[82] F. N. Ridha, Y. Yang, and P. A. Webley, "Adsorption characteristics of a fully exchanged potassium chabazite zeolite prepared from decomposition of zeolite Y," *Microporous and Mesoporous Materials,* vol. 117, pp. 497-507, 1/1/ 2009.
[83] J. Shang, G. Li, R. Singh, P. Xiao, J. Z. Liu, and P. A. Webley, "Potassium Chabazite: A Potential Nanocontainer for Gas Encapsulation," *The Journal of Physical Chemistry C,* vol. 114, pp. 22025-22031, 2010/12/23 2010.
[84] L. Sommer, D. Mores, S. Svelle, M. Stöcker, B. M. Weckhuysen, and U. Olsbye, "Mesopore formation in zeolite H-SSZ-13 by desilication with NaOH," *Microporous and Mesoporous Materials,* vol. 132, pp. 384-394, 8// 2010.
[85] J. Liang, J. Su, Y. Wang, Z. Lin, W. Mu, H. Zheng, *et al.*, "CHA-type zeolites with high boron content: Synthesis, structure and selective adsorption properties," *Microporous and Mesoporous Materials,* vol. 194, pp. 97-105, 8// 2014.

[86] X. Wu, M. G. Abraha, and R. G. Anthony, "Methanol conversion on SAPO-34: reaction condition for fixed-bed reactor," *Applied Catalysis A: General,* vol. 260, pp. 63-69, 2004/03/25/ 2004.
[87] E. Borodina, F. Meirer, I. Lezcano-González, M. Mokhtar, A. M. Asiri, S. A. Al-Thabaiti, *et al.*, "Influence of the Reaction Temperature on the Nature of the Active and Deactivating Species during Methanol to Olefins Conversion over H-SSZ-13," *ACS Catalysis,* vol. 5, pp. 992-1003, 2015/02/06 2015.
[88] M. A. Snyder and M. Tsapatsis, "Hierarchical Nanomanufacturing: From Shaped Zeolite Nanoparticles to High-Performance Separation Membranes," *Angewandte Chemie International Edition,* vol. 46, pp. 7560-7573, 2007.
[89] A. Corma, "From Microporous to Mesoporous Molecular Sieve Materials and Their Use in Catalysis," *Chemical Reviews,* vol. 97, pp. 2373-2420, 1997/10/01 1997.
[90] Y. Tao, H. Kanoh, L. Abrams, and K. Kaneko, "Mesopore-Modified Zeolites: Preparation, Characterization, and Applications," *Chemical Reviews,* vol. 106, pp. 896-910, 2006/03/01 2006.
[91] D. Masih, H. Imai, T. Yokoi, J. N. Kondo, and T. Tatsumi, "Methanol conversion to lower olefins over RHO type zeolite," *Catalysis Communications,* vol. 37, pp. 1-4, 7/5/ 2013.
[92] A. K. Jamil, O. Muraza, M. Yoshioka, A. M. Al-Amer, Z. H. Yamani, and T. Yokoi, "Selective Production of Propylene from Methanol Conversion over Nanosized ZSM-22 Zeolites," *Industrial & Engineering Chemistry Research,* vol. 53, pp. 19498-19505, 2014/12/17 2014.
[93] Z. Liu, X. Dong, Y. Zhu, A.-H. Emwas, D. Zhang, Q. Tian, *et al.*, "Investigating the Influence of Mesoporosity in Zeolite Beta on Its Catalytic Performance for the Conversion of Methanol to Hydrocarbons," *ACS Catalysis,* vol. 5, pp. 5837-5845, 2015/10/02 2015.
[94] Q. Zhu, J. N. Kondo, T. Tatsumi, S. Inagaki, R. Ohnuma, Y. Kubota, *et al.*, "A Comparative Study of Methanol to Olefin over CHA and MTF Zeolites," *The Journal of Physical Chemistry C,* vol. 111, pp. 5409-5415, 2007/04/12 2007.
[95] J. H. Lee, M. B. Park, J. K. Lee, H.-K. Min, M. K. Song, and S. B. Hong, "Synthesis and Characterization of ERI-Type UZM-12 Zeolites and Their Methanol-to-Olefin Performance," *Journal of the American Chemical Society,* vol. 132, pp. 12971-12982, 2010/09/22 2010.
[96] I. Bull, A. Moini, and M. Rai, "Chabazite Zeolite Catalysts Having Low Silica to Alumina Ratios," ed: Google Patents, 2011.
[97] J. A. Hesek and R. C. Wilson, "Practical analysis of high-purity chemicals. X. Use of a microwave oven in in-process control," *Analytical Chemistry,* vol. 46, pp. 1160-1160, 1974/07/01 1974.
[98] P. Lidström, J. Tierney, B. Wathey, and J. Westman, "Microwave assisted organic synthesis—a review," *Tetrahedron,* vol. 57, pp. 9225-9283, 11/5/ 2001.
[99] R. Gedye, F. Smith, K. Westaway, H. Ali, L. Baldisera, L. Laberge, *et al.*, "The use of microwave ovens for rapid organic synthesis," *Tetrahedron Letters,* vol. 27, pp. 279-282, 1986/01/01 1986.
[100] P. Chu, F. G. Dwyer, and J. C. Vartuli, "Crystallization method employing microwave radiation," ed: Google Patents, 1988.

[101] A. Arafat, J. C. Jansen, A. R. Ebaid, and H. van Bekkum, "Microwave preparation of zeolite Y and ZSM-5," *Zeolites,* vol. 13, pp. 162-165, 1993/03/01 1993.
[102] M. Gharibeh, G. A. Tompsett, K. S. Yngvesson, and W. C. Conner, "Microwave Synthesis of Zeolites: Effect of Power Delivery," *The Journal of Physical Chemistry B,* vol. 113, pp. 8930-8940, 2009/07/02 2009.
[103] B. Panzarella, G. A. Tompsett, K. S. Yngvesson, and W. C. Conner, "Microwave Synthesis of Zeolites. 2. Effect of Vessel Size, Precursor Volume, and Irradiation Method," *The Journal of Physical Chemistry B,* vol. 111, pp. 12657-12667, 2007/11/01 2007.
[104] M. A. Sanhoob and O. Muraza, "Synthesis of silicalite-1 using fluoride media under microwave irradiation," *Microporous and Mesoporous Materials,* vol. 233, pp. 140-147, 10/1/ 2016.
[105] O. Muraza, I. A. Bakare, T. Tago, H. Konno, A.-l. Adedigba, A. M. Al-Amer, *et al.*, "Controlled and rapid growth of MTT zeolite crystals with low-aspect-ratio in a microwave reactor," *Chemical Engineering Journal,* vol. 226, pp. 367-376, 6/15/ 2013.
[106] O. Muraza, E. V. Rebrov, J. Chen, M. Putkonen, L. Niinistö, M. H. J. M. de Croon, *et al.*, "Microwave-assisted hydrothermal synthesis of zeolite Beta coatings on ALD-modified borosilicate glass for application in microstructured reactors," *Chemical Engineering Journal,* vol. 135, Supplement 1, pp. S117-S120, 1/15/ 2008.
[107] O. Muraza, A. Abdul-lateef, T. Tago, A. B. D. Nandiyanto, H. Konno, Y. Nakasaka, *et al.*, "Microwave-assisted hydrothermal synthesis of submicron ZSM-22 zeolites and their applications in light olefin production," *Microporous and Mesoporous Materials,* vol. 206, pp. 136-143, 4// 2015.
[108] M. M. Elamin, O. Muraza, Z. Malaibari, H. Ba, J.-M. Nhut, and C. Pham-Huu, "Microwave assisted growth of SAPO-34 on β-SiC foams for methanol dehydration to dimethyl ether," *Chemical Engineering Journal,* vol. 274, pp. 113-122, 8/15/ 2015.
[109] M. Sanhoob, O. Muraza, Z. H. Yamani, E. M. Al-Mutairi, T. Tago, B. Merzougui, *et al.*, "Synthesis of ZSM-12 (MTW) with different Al-source: Towards understanding the effects of crystallization parameters," *Microporous and Mesoporous Materials,* vol. 194, pp. 31-37, 2014/08/01/ 2014.
[110] U. Khalil and O. Muraza, "Microwave-assisted hydrothermal synthesis of mordenite zeolite: Optimization of synthesis parameters," *Microporous and Mesoporous Materials,* vol. 232, pp. 211-217, 2016/09/15/ 2016.
[111] M. A. Camblor, A. Mifsud, and J. Pérez-Pariente, "Influence of the synthesis conditions on the crystallization of zeolite Beta," *Zeolites,* vol. 11, pp. 792-797, 1991/11/01/ 1991.
[112] C. S. Cundy, B. M. Lowe, and D. M. Sinclair, "Direct measurements of the crystal growth rate and nucleation behaviour of silicalite, a zeolitic silica polymorph," *Journal of Crystal Growth,* vol. 100, pp. 189-202, 1990/02/01/ 1990.
[113] M. Niwa and N. Katada, "Measurements of acidic property of zeolites by temperature programmed desorption of ammonia," *Catalysis Surveys from Asia,* vol. 1, pp. 215-226, September 01 1997.

[114] Q. Zhu, M. Hinode, T. Yokoi, M. Yoshioka, J. N. Kondo, and T. Tatsumi, "Synthesis, characterization and catalytic studies of CHA zeotype materials containing boron and iron," *Catalysis Communications*, vol. 10, pp. 447-450, 1/25/ 2009.

Vitae

Name :Galal Atef Ahmed Nasser

Nationality :Yemen

Date of Birth :11/29/1988

Email :galal5522@gmail.com

Address :90th Street, Al-mansorah, Aden, Yemen

Academic Background : B.Sc. Chemical Engineering, (2009-2015),

KFUPM, Dhahran, Saudi Arabia.

M.S Chemical Engineering, (2015 - 2017),

KFUPM, Dhahran, Saudi Arabia.

Research Background :

- Development and characterization of **Nano-particles zeolites for Petrochemical and Refinery industries.**
- Fabrication of **Novel and Cost-Effective catalysts** for the conversion of **methanol to olefins;**
  The project is supported by **SABIC** through **CENT, KFUPM.**
- Modification and Characterization of Natural zeolites for n-hexane cracking to olefins and the conversion of DME to olefins.
- Designed an **Air-left Bioreactor** used for carbon dioxide capture by utilizing micro-green algae. The project was part of the undergraduate research supported by KFUPM.

Research Outcome :

- **Published papers**

1. **Galal Nasser**, Teguh Kurniawan , Koji Miyake , Ahmad Galadima , Yuichiro Hirota ,Norikazu Nishiyama , Oki Muraz. *Dimethyl ether to olefins over dealuminated mordenite (MOR) zeolites derived from natural minerals.* Journal of Natural Gas Science and Engineering, 2016. **28**(Supplement C): p. 566-571.
2. **Galal A. Nasser**, Teguh Kurniawan, Teruoki Tago, IdrisA.Bakare, TaichiTaniguchi, YutaNakasaka, Takao Masudac,Oki Muraza. *Cracking of n-hexane over hierarchical MOR zeolites derived from natural minerals.* Journal of the Taiwan Institute of Chemical Engineers, 2016. **61**(Supplement C): p. 20-25.
3. Idris A. Bakare, Oki Muraza, Taichi Taniguchi, Teruoki Tago, **Galal Nasser**, Zain H. Yamani, Takao Masuda. *Steam-assisted catalytic cracking of n-hexane over La-Modified MTT zeolite for selective propylene production.* Journal of Analytical and Applied Pyrolysis, 2015. **116**(Supplement C): p. 272-280.

- **Submitted Publications:**

1. **Galal A. Nasser**, Oki Muraza, Toshiki Nishitoba, Zuhair Malibari, Toshiyuki Yokoi. *Microwave-Assisted Hydrothermal Synthesis of Al-rich CHA Zeolite from Amorphous Aluminosilicate Gel in Presence of Seed*. Submitted to: **Crystal Growth & Design** Journal.

- **Work which are in progress:**

1. **Galal A. Nasser**, Oki Muraza, Toshiki Nishitoba, Zuhair Malibari, Toshiyuki Yokoi. *OSDA-free chabazite (CHA) zeolite synthesized from amorphous aluminosilicate gel in the presence of fluoride for selective methanol-to-olefins*. Will be submitted soon to: **Mesoporous Microporous Materials** Journal .
2. **Galal A. Nasser**, Oki Muraza, Toshiki Nishitoba, Zuhair Malibari, Toshiyuki Yokoi. *In-situ incorporation of transition and alkaline earth metals in the framework of OSDA-Free CHA zeolites for selective methanol-to-olefins.* In progress.

- **Submitted Publications:**

One patent from the MS thesis work is ongoing.